

**THE ROLE OF ENDOTHELIAL CELL INJURY AND REPAIR
IN DIABETIC RETINOPATHY**

By

Maria Tikhonenko

A DISSERTATION

**Submitted to
Michigan State University
In partial fulfillment of the requirements
for the degree of**

DOCTOR OF PHILOSOPHY

Physiology

2012

ABSTRACT

THE ROLE OF ENDOTHELIAL CELL INJURY AND REPAIR IN DIABETIC RETINOPATHY

By

Maria Tikhonenko

Diabetic retinopathy (DR) is one of the most threatening microvascular complications of diabetes. Despite extensive research, the mechanisms responsible for DR are unknown. In this dissertation, we fill this critical gap in knowledge by providing a better understanding of the vasodegenerative stage of DR. Our study reveals the fundamental mechanism of DR where diabetes simultaneously induces endothelial damage in the retinal vasculature and negatively affects endothelial progenitor cells (EPC) function, thus preventing efficient vascular repair in the retina. More importantly, we have separated these two factors and revealed that either preventing initial vascular damage or normalizing EPC-mediated repair improves the outcome of DR.

First, we studied the role of inflammation in DR. Although the exact mechanism leading to inflammatory conditions in the diabetic retina is not well resolved, it is likely to involve dyslipidemia and perturbation of fatty acid metabolism. We have demonstrated that reduced fatty acid remodeling results in the depletion of the n3 PUFA products and this translates into a pro-inflammatory state in the diabetic retina. This low-grade inflammatory state is likely to lead to premature death of endothelial cells in the retina.

Secondly, we addressed the hypothesis that diabetic animals cannot effectively regenerate the damaged vascular endothelium due to reduced numbers and function of circulating EPCs. In a rat model of diabetes, we found an altered circadian pattern of

EPC levels in the peripheral blood; likely due to their immobilization within the bone marrow (BM). Notably, the defect of EPC function was associated with BM neuropathy, thus allowing us to propose BM neuropathy as a mechanism for ineffective EPC release from the BM niche and ineffective vascular repair.

Importantly, dietary supplementation rich in n3 PUFAs improved the outcome of DR by both preventing inflammation in the retina and correcting EPC function. Feeding diabetic animals with n3 PUFA rich diet prevented increases in inflammatory cytokine levels, stimulated EPC migration and inhibited the loss of retinal capillaries.

Finally, to demonstrate a direct link between BM neuropathy and DR, we examined the effect of surgical BM denervation on the ability to repair retinal vasculature. The experiment was performed on non-diabetic rats, allowing us to study the direct effect of the denervation without other factors associated with diabetes. We did not find any signs of retinopathy in intact retinas of animals with surgically denervated BM. This finding suggests that a lack of regulated EPC release does not affect healthy vasculature. However, when coupled with retinal damage due to ischemia-reperfusion injury, animals with BM denervation developed more severe retinopathy than animals with healthy BM, demonstrating that the combination of endothelial damage and EPC dysfunction is required for the development of diabetic retinopathy.

In summary, both endothelial damage and EPC dysfunction are critical for the development of the vasodegenerative phase of DR. Preventing the initial inflammatory injury to retinal vasculature, stimulating EPC-mediated repair, or combining both approaches would lead to an effective therapy for DR.

ACKNOWLEDGEMENTS

I would like to take the opportunity to deeply thank everyone who contributed to my scientific work. First and foremost, I would like to thank my mentor Dr. Julia Busik, a leading researcher in Diabetic Retinopathy field, who kindly gave me the privilege to join her lab at Michigan State University in 2006 and supported my decision to pursue the PhD degree. Her enthusiasm and passion for diabetes research, continuous support of my progress and patience during my hard times had given me the strength to go through the graduate school. Dr. Busik is a wonderful advisor; she put a lot of effort in creating productive and positive atmosphere in the lab and I was extremely lucky to spend all those years under her guidance.

I greatly appreciate the help and support provided by my guidance committee. Many thanks to Dr. Karl Olson and who always had his door open for me. Dr. Olson has always given me a great advice which helped tremendously with my classes and research. My sincere thanks to Dr. Parameswaran, who always found time to give insightful comments for my work. My special thanks to Dr. McCabe and Dr. Perez for providing constructive discussion for my research. I greatly appreciate Dr. Esselman's help with writing my papers and advice on career choices.

I also thank all my co-workers: Svetlana Bozack, Todd Lydic, Madalina Opreanu, Kelly McSorley, Priyanka Pandey, Andrew Sochacki, Qi Wang and Matthew Faber. They all are wonderful people and it was a pleasure working with them. My special thanks to Svetlana Bozack, who is a skillful technician and exceptional person. Without her help with my animal models, all my projects would take very long time. Todd Lydic is a wonderful person, he has unique ability to cheer everyone up even at hardest of

times. It was great working with him. Thanks to Matt Faber who must have read my dissertation dozen times and corrected a lot of mistakes. Thanks to Andy Sochacki for all his help with Western Blots, thanks to Priyanka Pandey for all her work with denervation surgeries and thanks to Kelly McSorley for her help with lipid extraction and animal handling.

My sincere thanks go to out collaborators Dr. Maria Grant and all the members of her lab. We have a major paper published together and it would be impossible without their commitment. I express deep appreciation to Dr. Carrie Northcott for teaching us the catheterization surgery technique. I am also thankful to Dr. Miyan, who was so generous to teach me the denervation surgery technique. Thanks to Dr. Lily Yan for showing us how to isolate the SCN.

I am thankful to all wonderful MSU core facilities, including ULAR, Flow Cytometry (Louis King), quantitative RT-PCR (Jeff Landgraf) and especially to Histopathology Lab (Amy Porter, Kathy Joseph and Rick Rosebury).

Thanks to my two beautiful daughters, Anastasia and Katherine, for being the special part of my life. And last, but not least, I thank my dearest husband Sergey for giving me so much love and support during those years. He always knows how to motivate and inspire me.

TABLE OF CONTENTS

LIST OF TABLES.....	viii
LIST OF FIGURES.....	ix
LIST OF ABBREVIATIONS.....	xii
Chapter 1. Introduction	
1.1 Background and significance.....	1
1.2 Etiology of diabetic retinopathy.....	2
1.3 Inflammation in diabetic retinopathy.....	4
1.4 Diabetic dyslipidemia.....	6
1.5 Fatty acids and diabetic retinopathy.....	8
1.6 Elongases and Desaturases.....	15
1.7 Sphingolipids.....	16
1.8 Role of Endothelial Progenitor Cells in Diabetic Retinopathy.....	19
1.9 Circadian Function and Diabetes.....	23
1.10 Objective of the dissertation.....	28
Chapter 2. Remodeling of Retinal Fatty Acids in an Animal Model of Diabetes: a Decrease in Long-Chain Polyunsaturated Fatty Acids Is Associated With a Decrease in Fatty Acid Elongases Elovl2 and Elovl4	
2.1 Abstract.....	32
2.2 Introduction.....	33
2.3 Results.....	38
2.4 Discussion.....	52
2.5 Methods.....	56
Chapter 3. Diabetic Retinopathy is Associated with Bone Marrow Neuropathy and a Depressed Peripheral Clock	
3.1 Abstract.....	61
3.2 Introduction.....	62
3.3 Results and Discussion.....	63
3.4 Methods.....	97
Chapter 4. N3 fatty acids prevent diabetic retinopathy by inhibition of retinal vascular damage and enhanced endothelial progenitor cell reparative function	
4.1 Abstract.....	104
4.2 Introduction.....	105

4.3 Results.....	108
4.4 Discussion.....	126
4.5 Methods.....	130
Chapter 5. Direct Link between Diabetic Retinopathy and Bone Marrow Neuropathy	
5.1 Introduction.....	135
5.2 Results.....	137
5.3 Discussion.....	140
5.5 Methods.....	142
Chapter 6. Summary and future perspectives.....	144
References.....	147

LIST OF TABLES

Table 1.	Body weight gain and blood glucose concentrations of experimental animals.....	42
Table 2.	Blood plasma fatty acid profiles of control and diabetic animals.....	45
Table 3.	Liver fatty acid profiles of control and diabetic animals.....	46
Table 4.	Retinal fatty acid profiles of control and diabetic animals.....	47
Table 5.	Real-time qPCR primers.....	103

LIST OF FIGURES

Figure 1.	De novo lipogenesis and PUFA remodelling pathways.....	10
Figure 2.	Components of diabetic dyslipidemia.....	13
Figure 3.	Acid Sphingomyelinase is one of the key regulatory enzymes in sphingolipid metabolism.....	17
Figure 4.	Schematic illustration of the hematopoietic niche in the bone marrow.....	21
Figure 5.	The molecular feedback loops that control the circadian rhythms.....	26
Figure 6.	Schematic representation of the proposed mechanism.....	30
Figure 7.	Fatty acid structure.....	35
Figure 8.	Expression levels of elongases and desaturases in retinas and livers of control and diabetic animals.....	43
Figure 9.	Fatty acid analysis by RP-HPLC and comparative MS/MS analysis of GPCho lipids in control and diabetic animals at 3–6 weeks post-STZ injection.....	48
Figure 10.	Expression levels of inflammatory markers in retinas of control and diabetic animals.....	50
Figure 11.	Dramatic decrease in humerus bone marrow innervation in diabetic rats is associated with an increase in retinal acellular capillaries.....	70

Figure 12.	Denervation of the bone marrow precedes acellular capillaries formation in diabetic rats after 2 months of diabetes.....	70
Figure 13.	Rat thy-1+ cell characterization.....	76
Figure 14.	Diabetes decreases circadian release of EPCs.....	79
Figure 15.	Significant decrease in humerus bone marrow innervation in type 1 diabetic rats.....	81
Figure 16.	Type 1 diabetes reduced circadian release of EPC in the BBDP/Wor rat.....	83
Figure 17.	Characterization of thy-1+ EPC number and function in type 2 diabetic rats.....	85
Figure 18.	Increased plasma levels of NE in a type 2 diabetes model and decreased number of circulating CD3-positive cells in a type 2 model as compared with controls.....	87
Figure 19.	Clock gene expression analysis.....	89
Figure 20.	Quantitative PCR and Western blot analysis for clock genes in human retina.....	91
Figure 21.	Normal, but not diabetic, human EPCs, may participate in ocular vascular reendothelialization in diabetic mice.....	93
Figure 22.	Schematic representation of the proposed mechanism.....	95
Figure 23.	DHA-enriched fish oil diet prevents the formation of acellular capillaries in type 2 diabetes model.....	112
Figure 24.	DHA-enriched fish oil diet prevents increase in IL-1 β , IL-6, TNF α and ICAM gene expression in type 2 diabetes model.....	114

Figure 25.	DHA-enriched fish oil diet normalizes the ASM protein levels in the whole retinas of type 2 diabetic rats.....	116
Figure 26.	DHA-rich fish oil diet attenuates a decrease in the number of circulating EPCs and improves EPC colony formation in type 2 diabetes model.....	118
Figure 27.	The increase in ASM activity observed in diabetic EPCs is prevented by DHA-rich fish oil diet.....	120
Figure 28.	<i>In vitro</i> DHA pretreatment improves human CD34 ⁺ cell migration.....	122
Figure 29.	DHA-rich fish oil diet improves life span in type 2 diabetic rats.....	124
Figure 30.	Bone marrow denervation coupled with retina ischemia leads to increased vascular permeability.....	138

LIST OF ABBREVIATIONS

ANOVA	analysis of variance
BBZDR	Bio-breeding zucker diabetic rat
BM	bone marrow
BMAL1	Brain and muscle ARNT like 1
BSA	bovine serum albumin
CAM	cell adhesion molecule
CLOCK	circadian locomotor output cycles kaput
CPM	counts per minute
DHA	docosahexaenoic acid (22:6n3)
Dil-acLDL	Dil-labeled acetylated low-density lipoprotein
DR	diabetic retinopathy
Elovl	elongase
eNOS	endothelial nitric oxide synthase
EPA	eicosapentaenoic acid (20:5n3)
EPC	endothelial progenitor cell
FACS	Fluorescence-activated cell sorting
FITC	Fluorescein isothiocyanate
GPCho	phosphatidylcholine
HSC	hematopoietic stem cell
I/R	ischemia-reperfusion

ICAM-1	intercellular cell adhesion molecule -1
IL	interleukin
LDL	low density lipoprotein
LIMSA	Lipid Mass Spectrum Analysis
mg	milligram
ml	milliliter
mM	millimolar
MS	mass spectrometry
MUFA	monounsaturated fatty acid
NADPH	nicotinamide adenine dinucleotide phosphate
NE	norepinephrine
nESI-MS/MS	nano-electrospray ionization tandem mass spectrometry
NF200	neurofilament 200
NF-kB	nuclear-factor kappa B
PBS	Phosphate buffered saline
PCR	polymerase chain reaction
PUFAs	polyunsaturated fatty acids
RNA	ribonucleic acid
RORA	RAR-related orphan receptor A
RPE	R-Phycoerythrin
RP-HPLC	reverse-phase high pressure liquid chromatography
SCN	suprachiasmatic nucleus
SDF-1	stromal cell-derived factor-1

SDS	sodium dodecyl sulfate
SRA	saturated fatty acids
STZ	streptozotocin
TH	tyrosine hydroxylase
TNF	tumor necrosis factor
VEGF	vascular endothelial growth factor
VLCPUFA	very-long-chain polyunsaturated fatty acid
ZT	Zeitgeber time
$\Delta 5D$	$\Delta 5$ -desaturase
$\Delta 6D$	$\Delta 6$ -desaturase
$\Delta 9D$	$\Delta 9$ -desaturase
μ l	micro-liter

Chapter I

Introduction

1.1 Background and significance

Diabetes is a group of metabolic diseases classically defined by high blood sugar, either because the body does not produce insulin, or does not respond to the insulin that is produced. Recent estimates demonstrated that around 117 million people worldwide are suffering from diabetes mellitus and this number is predicted to increase to 300 million in 2025 [1]. The risk of death for a diabetic patient is two times higher than that of non-diabetic person. The cost of caring for diabetic patients in the US alone is more than one hundred billion dollars annually [2], emphasizing the socio-economic burden of this destructive disease.

There are two main types of diabetes. Type 1, also known as insulin-dependent or juvenile diabetes, is the result of a failure to produce insulin. Type 2 (or adult onset) diabetes results from cell resistance to insulin and may include insulin deficiency at later stage of the disease. Type 2 diabetic patients comprise over 85% of all diabetes cases. Both type 1 and type 2 diabetes patients may develop diabetic retinopathy (DR) and the risk increases proportionally with the duration of the disease. Type 1 diabetic patients are more likely to develop proliferative DR, while non-proliferative DR with macular edema is more common in Type 2 diabetes.

DR is a chronic sight-threatening microvascular disease that occurs in both type 1 and type 2 diabetes and affects about 80% of all patients who have had diabetes for 10 years [3]. DR in the form of macular edema and retinal neovascularization is the

leading cause of new cases of legal blindness among Americans 20 to 74 years of age [4]. In most severe cases, DR can lead to blindness. Disability resulting from blindness imposes enormous medical and social costs on both the health care system and the patient.

Very few therapies are available for patients with DR. Diabetes Control and Complications Trial (DCCT) has demonstrated that glycemic and blood pressure control may delay the onset of DR [5]. Scatter laser photocoagulation is highly invasive and does not reverse the pathology; however it remains the recommended treatment for patients with proliferative DR. Despite the progress in screening, blood glucose control and surgical intervention, the incidence of DR is rising and DR causes more than 12,000 new cases of blindness in the U.S. annually [6]. Although current therapy can improve some aspects of DR, no treatment is available to restore the damaged vasculature in the retina. The increasing incidence of DR with the evidence that vascular damage begins early on, emphasizes the need for new therapeutic strategies targeted against early microvascular lesions.

1.2 Etiology of diabetic retinopathy

Damage of the microvessels represents the key pathologic feature in DR [7], even though it is suggested that nonvascular retinal tissue is also damaged [8]. The progression of DR has two stages: the early vasodegenerative and the later proliferative stage. During the initial vasodegenerative stage, capillary components, such as pericytes and endothelial cells, die prematurely causing acellular capillaries formation [9]. Due to a lack of cellular support, weakness in the capillary wall is developed leading

to capillary aneurism (microaneurism), increased vascular permeability, lipid exudates, vascular non-perfusion and subsequent hypoxia of the retinal tissue [9].

The increase in vascular permeability as a result of breakdown of the blood-retinal barrier is an important early event on the development of DR, as it has been attributed to an increase in leukostasis, cytokines and growth factors in the retina [10, 11]. This increase in permeability occurs in patients with diabetes contributing to retinal edema and distortion of the central vision. In animal models, the permeability defect occurs as early as 7 days after onset of diabetes [12-14], preceding the death of vascular endothelial cells [15]. In the retina of diabetic animals, expression of the tight junction-associated protein occludin is decreased; this may increase paracellular permeability in the vascular endothelium [16]. The decrease in occludin was suggested to be a result of vascular endothelial growth factor (VEGF)-associated signaling [16].

In response to retinal non-perfusion in the proliferative stage of DR, local growth factors are secreted and pathologic intraocular vessels grow along the retina and in the vitreous [17]. The new abnormal blood vessels are fragile and leak blood in the center of the eye, blurring the vision.

The mechanisms underlying the initial pathological change in retinal microvessels which precede and stimulate the abnormal angiogenesis involves inflammation.

1.3 Inflammation in diabetic retinopathy

Historically, inflammation was first suggested to play a role in the pathology of DR when, in 1964, it was discovered that high doses of aspirin tended to lessen the severity of DR [18]. This notion was later confirmed in relevant dog models where aspirin prevented the classic histopathological features of DR such as acellular capillary development and intra-retinal hemorrhages [19]. Many of the molecular and functional characteristics of inflammation have been detected in diabetic retinas. There is a strong support of a concept that early DR is a low-grade inflammatory condition that involves upregulation of adhesion molecules in the vasculature followed by leukocyte adhesion and migration into the surrounding tissue [20]. Evidence for this notion was provided by the findings that the expression level of intracellular adhesion molecule-1 (ICAM-1) is increased in early diabetes and correlates with increase in number of leukocytes [21]; that the leukocytes actively adhere to the endothelium and transmigrate into the surrounding tissue in diabetic retina [21, 22]; and that the activation of leukocytes concurs with premature endothelial cell death and blood-retinal barrier breakdown [10].

In diabetes, abnormal leukocyte attachment to retinal microvessels occurs through the interaction of adhesion molecules, such as ICAM, with CD18 protein on monocytes and neutrophils [21]. Increased leukostasis in diabetes has been shown to be a factor in activation, apoptosis and premature death of retinal endothelial cells [10], leading to degenerated, non-perfused capillaries.

Several proinflammatory cytokines such as VEGF, tumor necrosis factor α (TNF α), interleukin (IL)-1 β and IL-6 were demonstrated to be increased at early stages of DR. VEGF is a growth factor and a proinflammatory molecule that plays a well-

recognized role in retina neovascularization and increased permeability [12, 23-25]. VEGF is produced by a variety of cell types in the retina such as ganglion cells, pericytes and Muller cells [26-28]. Increased intraocular levels of VEGF and the VEGF receptor were detected in diabetic retina [29], where it can induce ICAM expression on endothelial cells [30]. Anti-VEGF therapy has recently become a central point in the search for treatment of the advanced stages of DR and promising results have been shown [31-33].

TNF α has been implicated in diabetic microvascular complications including nephropathy [34] and retinopathy [35]. The levels of TNF α are increased in diabetic rats [35] and inhibition of TNF α by a drug etanercept was reported to inhibit retinal cell death in galactose-induced retinopathy [36].

Expression of IL-1 β is dramatically upregulated in retina in ischemia-reperfusion injury and other models of DR [37, 38]. Retinal endothelial cells have been shown to regenerate in response to treatment with IL-1 β *in vitro* or intravitreal injection of IL-1 β *in vivo*. Inhibition of caspase-1, the enzyme involved in the production of IL-1 β from its precursor, prevented the increase in IL-1 β and decreased diabetes-induced degeneration of retinal capillaries [38]. Long-term experiments have demonstrated that IL-1 β knock-out mice were protected from DR [38].

IL-6 is a powerful proinflammatory cytokine implicated in vascular inflammation in several pathologies including atherosclerosis and cancer [39, 40]. Patients with proliferative DR and macular edema have higher intravitreal IL-6 concentration as compared to controls [41] and levels of IL-6 are significantly associated with the severity of DR [42]. IL-6 has been shown to induce ICAM-1 and VEGF expression in models of

choroidal neovascularization. Blockage of the IL-6 receptor by antibodies or genetic IL-6 ablation led to the suppression of choroidal neovascularization [43]. Intravitreal injection of IL-6 induced an increase in leukocyte attachment to the endothelium in the retina [44].

Thus, new therapies that interfere with signaling pathways that promote inflammation would represent a significant advance in DR treatment. While the important role of inflammation in diabetic vascular complications is well accepted, the molecular steps leading to inflammation in the retina are not well resolved, but likely to involve hyperglycemia and dyslipidemia [45].

The effect of hyperglycemia in diabetes has been extensively studied and there is little doubt that hyperglycemia is a critical factor in the pathogenesis of DR [46]. However, whether glucose-lowering treatment alone is sufficient to prevent DR and other microvascular complications in diabetes remains a matter of debate. A number of recent studies demonstrated that dyslipidemia, another serious metabolic disorder in diabetes, plays major role in development of diabetic complications [45, 47-50].

1.4 Diabetic dyslipidemia

Diabetic dyslipidemia is the result of an imbalance in the regulation of lipid uptake and metabolism. Insulin is a major hormone in the control of carbohydrate, protein and lipid use. The action of insulin on adipocytes includes the activation of lipoprotein lipase and inhibition of hormone-sensitive lipase, the two rate-limiting enzymes for the fatty acid turnover in adipose tissue [51]. In the liver, the major organ

for fatty acid metabolism, insulin activates fatty acid desaturases and elongases, stimulates the conversion of fatty acid to triglycerides, which is followed by their secretion and transport to the blood as VLDL [52-54]. The lack of insulin action in diabetes induces imbalance in the regulation of lipid uptake, metabolism, release by adipocytes and clearance from circulation. This has a profound effect on the lipid levels and leads to dyslipidemia [51, 55]. A number of recent studies have demonstrated that dyslipidemia plays a key role in the development of diabetic complications [45, 49, 50].

Dyslipidemia is one of critical factors in the development of DR [56]. In type 2 diabetes, dyslipidemia is characterized by high triglycerides, high cholesterol and high free fatty acid content in the blood [57]. In type 1 diabetic patients receiving insulin therapy levels of triglycerides, cholesterol and free fatty acids are normal [58, 59]. However, the blood fatty acid profile is changed [60] with a marked decrease in the total amount of polyunsaturated fatty acids (PUFA) [61].

The DCCT study revealed that the severity of DR was associated with an increase in triglycerides levels and inversely associated with high-density lipoprotein-bound cholesterol [62]. The Early Treatment Diabetic Retinopathy Study has demonstrated that elevated serum lipid levels were associated with increase in retinal hard exudates in the macula and the severity of the vision loss in DR [50, 63]. The importance of treating dyslipidemia in diabetes has been highlighted by studies demonstrating that lowering cholesterol in type 2 diabetic patients leads to the reduction of vascular events and mortality [48]. Lowering lipid levels by dietary means or drug therapy led to the regression of hard exudates in the retina [64, 65]. In recent ACCORD

Eye study, combined cholesterol and triglyceride treatment with fenofibrate and simvastatin resulted in 40% reduction in the odds of retinopathy progression [66].

Importantly, it has been suggested that diets high in polyunsaturated fats may protect against retinopathy [67, 68].

1.5 Fatty acids and diabetic retinopathy

Fatty acid composition of the retina and other tissues depend on three factors: fatty acids and precursors uptake from the circulation, the local fatty acid metabolism through *de novo* lipogenesis from glucose and the PUFA remodeling through Sprecher pathway [69]. Hormones such as Insulin, triiodothyronine (T3) and glucocorticoids induce, while glucagon and epinephrine suppress *de novo* lipogenesis [70].

Sprecher pathway includes desaturation, elongation, mono-oxidation and peroxisomal β -oxidation (Fig. 1). These modifications can involve fatty acids generated *de novo* as well as fatty acids obtained from the diet.

Alteration of fatty acid metabolism in diabetes is an important part of diabetic dyslipidemia. Insulin controls fatty acid synthesis and remodeling by activating several critical desaturase [71-73] and elongase [52, 74, 75] enzymes. The lack of insulin action in diabetes may result in decreased fatty acid remodeling leading to accumulation of substrates and reduction of the products of Sprecher pathway.

N3 PUFAs have a unique ability to modulate various biological processes such as capillary structure, neovascularization and inflammation [76]. There are several pathways through which fatty acids could regulate inflammation. These include changes

in membrane fatty acid composition of the cells; alteration in membrane fluidity and receptor distribution in lipid rafts; production of oxidized bioactive lipids and regulation of transcription factors. These general mechanisms are not mutually exclusive and all may be involved.

We have previously shown that treatment of human retinal endothelial cells (HREC) with n3 PUFA inhibits adhesion molecule and cytokine expression induced by inflammatory agents [77-79]. Clinically, n3 PUFAs are widely applied to as an adjuvant immunosuppressant [79]. Numerous studies demonstrated positive role of n3 fatty acids in disorders with inflammatory background including heart disease [80], rheumatoid arthritis [81] and asthma [82].

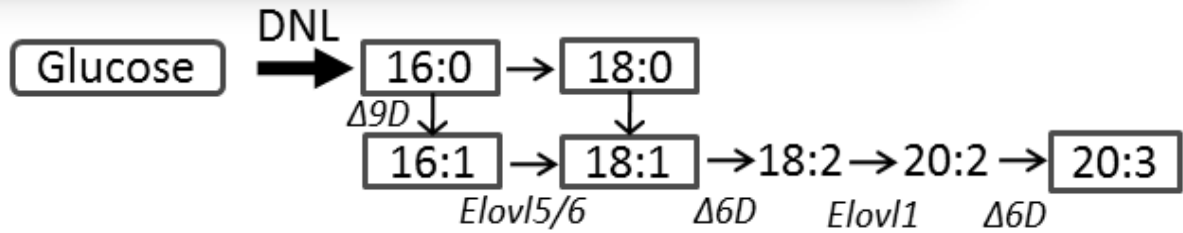
In general, n3 PUFA is described as anti-inflammatory [83, 84], while n6 PUFA is considered pro-inflammatory [85]. The relative amount of these PUFAs plays an important role in regulation of immunity. Diabetic dyslipidemia is characterized by a reduction of both membrane and serum levels of n3 PUFAs [86] which leads to a decrease in n3 to n6 fatty acid ratio and create a proinflammatory condition [87, 88].

Retina has a unique fatty acid profile enriched with long-chain PUFAs, especially the n3 PUFA DHA. DHA is the major structural lipid of microvessels and the outer segment membranes in photoreceptors [89-91]. In the retina, n3 PUFAs influence retinal gene expression, cell differentiation and survival. There is consistent evidence that suggests a protective role of n3 PUFAs against ischemia and inflammation-associated pathology in both vascular and neural retina [76].

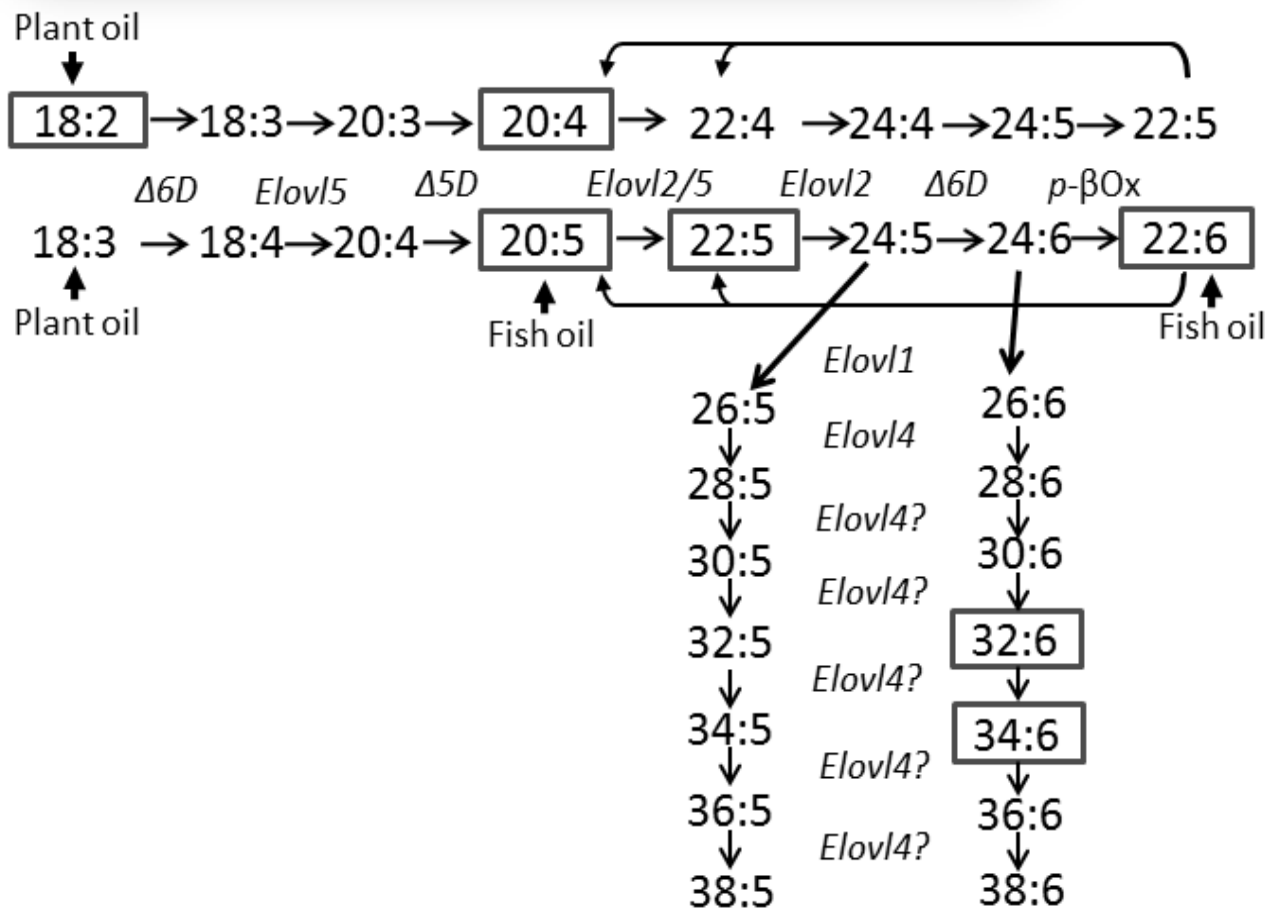
Figure 1: De novo lipogenesis and PUFA remodelling pathways. Fatty acids are synthesized from glucose through de novo lipogenesis or converted from dietary palmitic16:0, oleic18:1n9, linoleic18:2n6, and α -linolenic18:3n3 acids to long-chain unsaturated fatty acids in vivo by a series of desaturation (Δ 5-desaturase [Δ 5D], Δ 6-desaturase [Δ 6D], or Δ 9-desaturase [Δ 9D]) and elongation (Elovl1–7) reactions. Fatty acids that accumulate in animal and human tissues are in solid boxes. Dietary linoleic18:2n6 and α -linolenic18:3n3 acids are obtained from plants, and EPA (eicosapentaenoic acid 20:5n3) and DHA (22:6n3) are rich in fish oil. A recent study demonstrated that Elovl4 is necessary for synthesis of C26 and C28 VLCPUFAs from 24:5n3 and 24:6n3 fatty acid precursors and suggests that Elovl4 is also required for synthesis of >C28 VLCPUFAs. There is no interconversion between n3, n6, and n9 fatty acids in animals.

Figure 1 (cont'd)

De Novo Lipogenesis and MUFA Synthesis



Sprecher Pathway for PUFA Synthesis



Recent study in the retinopathy of prematurity mouse model has shown that increasing n3 PUFAs levels in the body by dietary or genetic means inhibits inflammation in the retina and has a beneficial effect on retinal microvessel pathology [68]. Our previous work on human retinal HREC supported the important role of n3 DHA as an anti-inflammatory agent acting to suppress the cellular response to cytokines in HRECs [77].

Therefore, perturbation of lipid metabolism in diabetes with a subsequent decrease in n3 PUFAs levels can promote cytokine-induced ICAM expression, leukocyte adhesion and have a significant impact on retinal health and disease (Fig. 2).

Figure 2: Components of diabetic dyslipidemia. Diabetic dyslipidemia is characterized by increased levels of triglycerides, cholesterol, esterified and non-esterified fatty acids. Modification of the PUFA profile with an increase in the n6 to n3 ratio is a very important feature of diabetic dyslipidemia. N6 fatty acids are considered to be proinflammatory, while n3 are believed to be anti-inflammatory. The change of the n6 to n3 ratio in the diabetic retina shifts the balance towards a proinflammatory state.

Figure 2 (cont'd)

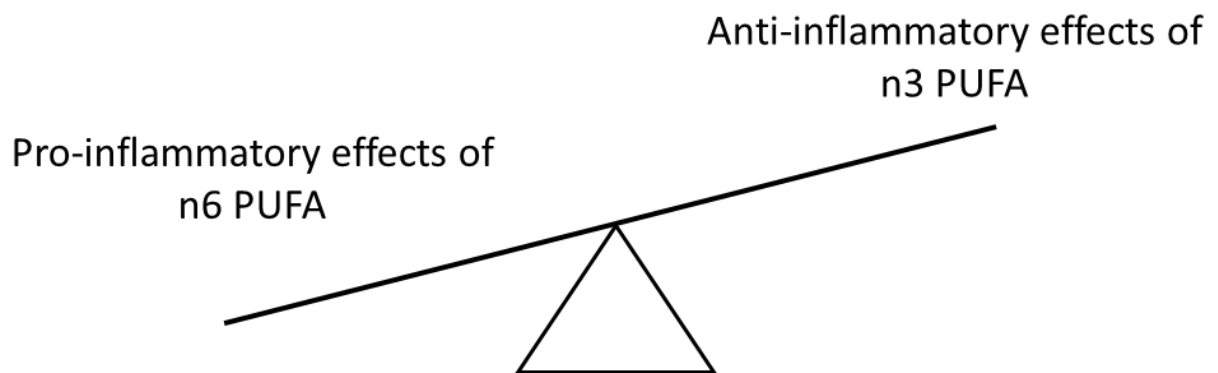
Diabetic dyslipidemia

↑ Triglycerides

↑ Cholesterol

↑ Esterified and non-esterified fatty acids

↑ N6 PUFAs/ N3 PUFAs ratio



1.6 Elongases and Desaturases

Saturated fatty acids (SFA), monounsaturated fatty acids (MUFA) and PUFAs are synthesized from dietary precursors (glucose, palmitic, oleic, α -linoleic, EPA, DHA) through a series of desaturation reactions performed by desaturases ($\Delta 5$, $\Delta 6$, $\Delta 9$) and elongation reactions performed by elongases (Elovl1-7).

Desaturases catalyze oxygen-dependent dehydrogenation of lipids. $\Delta 5$ and $\Delta 6$ desaturases carry out the rate-limiting step in fatty acid metabolism. Insulin activates while glucagon inhibits the expression of $\Delta 5$, $\Delta 6$ and $\Delta 9$ desaturases [72, 92]. In diabetes, the lack of insulin inhibits $\Delta 5$ and $\Delta 6$ desaturases in the liver, adrenal glands and testes. Insulin treatment restores the activity of both desaturases to normal levels [72].

Fatty acid elongation involves four enzymes and requires NADPH, malonyl-CoA and fatty acyl-CoA as substrates. Elongases perform condensation, the first rate-limiting step of the reaction. Seven fatty acid elongase subtypes (Elovl1-7) have been described. Elongases demonstrate differential substrate specificity and tissue distribution [93, 94]. For example, Elovl1, 2, 3, 5, and 6 are expressed in the liver and Elovl1, 5 and 6, but not Elovl2 are expressed in the heart [95]. Function of elongases is regulated by various factors such as stage of development, disease, hormones and diet [95].

Elovl6 together with $\Delta 9$ desaturase produce 18-carbon MUFA such as oleic acid (18:1n9). Elovl2 and Elovl5 together with $\Delta 5$ and $\Delta 6$ desaturases produce the end product of n3 and n6 pathways arachidonic and docosahexaenoic acid (DHA) [95].

In the recent work by Agbaga *et al.*, the Sprecher pathway has been extended to include very long chain PUFAs (VLCPUFA), up to 38 carbon fatty acids (Fig. 1) [96]. Results of this study let to suggest Elovl4 to be the critical enzyme in formation of VLCPUFA.

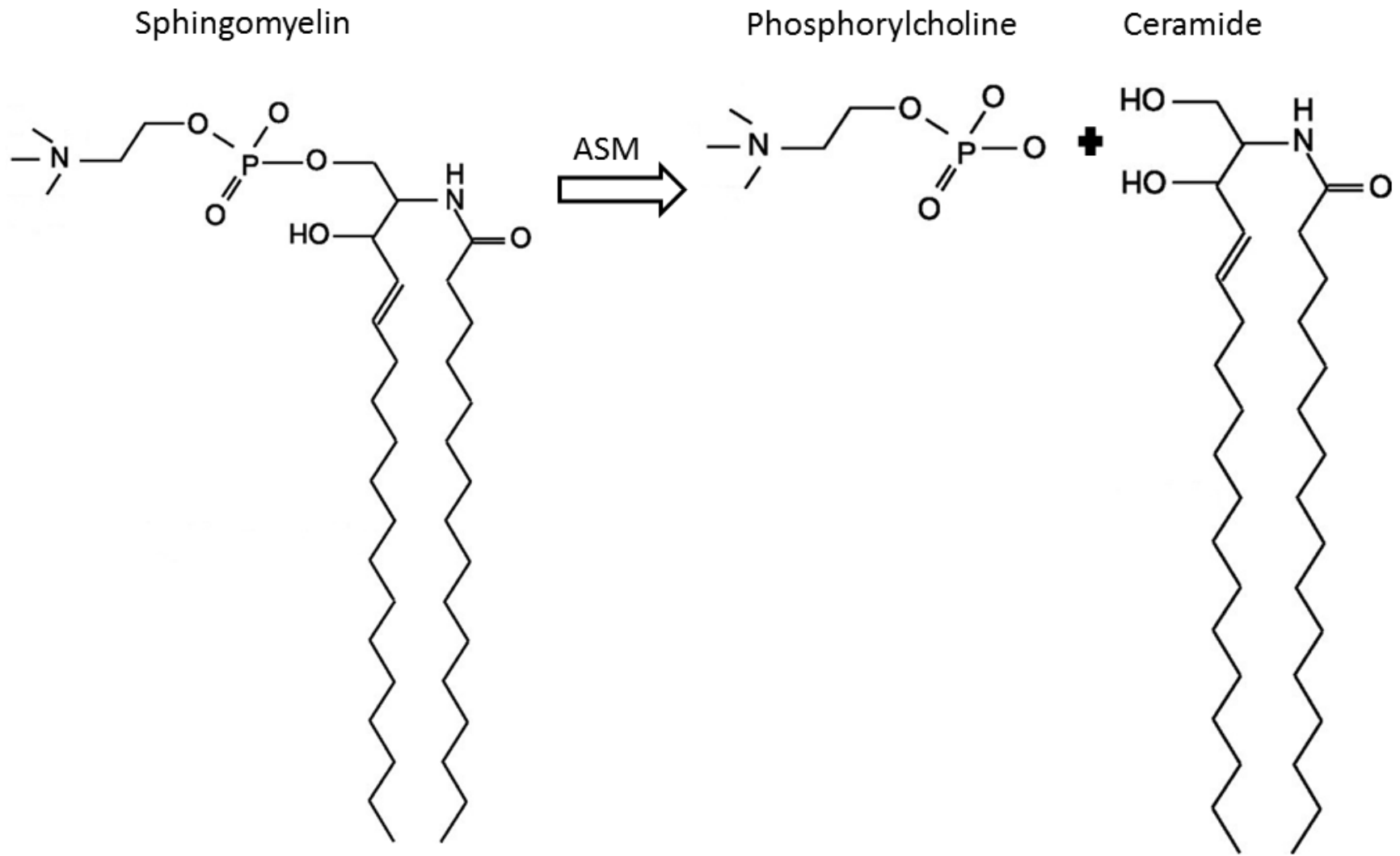
1.7 Sphingolipids

Sphingolipids are an essential component of a cell plasma membrane, where they are usually abundant in the outer leaflet. Cholesterol and sphingolipids form caveolae/lipid raft structures [97], which serve as platforms for protein assemblies and play an important role in regulating vascular permeability [98], lipid trafficking [99] and especially signal transduction [100]. Ceramide is the simplest of the sphingolipids and can be generated by catabolism of sphingomyelin by sphingomyelinases or by *de novo* production. Ceramides are known to have pro-apoptotic and proinflammatory effects: hydrolysis of sphingomyelin into ceramide facilitates receptor clustering and stimulates transduction of inflammatory signals.

Sphingomyelinases are important early responders in inflammatory cytokine signaling. Acid sphingomyelinase (ASM) plays a critical role in ceramide-mediated signal transduction [101]. This process involves translocation of ASM from the intracellular compartment into the outer leaflet of cell membrane, localization in caveolar microdomains and hydrolysis of sphingomyelin into ceramide [102] (Fig.3).

Figure 3: Acid Sphingomyelinase is one of the key regulatory enzymes in sphingolipid metabolism. It induces sphingomyelin hydrolysis to generate ceramide, the pro-inflammatory and pro-apoptotic messenger.

Figure 3 (cont'd)



This ceramide production initiates membrane reorganization and stimulates merging of lipid microdomains leading to protein-protein interactions, receptor dimerization and downstream signaling of several receptors such as IL-1 β and TNF- α , known to mediate pathological changes typically associated with DR [97, 103].

We have previously demonstrated in a primary human retinal endothelial cell model that ASM was activated in diabetic cells. DHA suppresses cytokine-induced inflammatory signaling and the activation of the cells [77]. This effect was mediated, at least in part, through a reduction in ASM activity and expression [104]. Inhibition of ASM through genetic manipulation in type 1 diabetic animal model prevented inflammatory cytokine production, retinal capillary loss and neovascularization [105].

1.8 Role of Endothelial Progenitor Cells in Diabetic Retinopathy

Traditionally, microvascular repair was described as a result of mature endothelial cells proliferation. However, there is a growing body of evidence that cells defined as endothelial progenitor cells (EPCs) play a critical role in endothelial repair and maintenance, including in the retinal vasculature [106-108].

The reliable characterization of endothelial progenitors has generated some confusion within the field of regenerative medicine. To this point, unique surface markers that permit to specifically identify EPC were not identified [109]. A recent study[110] and a review by Schatteman *et al.*[111] have suggested that despite phenotypic overlap between various progenitor cell types, the endothelial phenotype can best be characterized by three features: eNOS expression, colony formation and integration into tube-like structures formed by endothelial cells. It is suggested that

these criteria might be the best *in vitro* method of confirming the endothelial phenotype. This simplified interpretation is important, as it recognizes the importance of the identification of EPCs based on their ability to acquire the functional properties of endothelial cells. In our studies, rat EPCs were identified as Thy-1 positive, CD3, CD4, CD8-negative cells and human EPCs were identified as CD34 positive cells. As we demonstrated, cells isolated in this study displayed all three of these features.

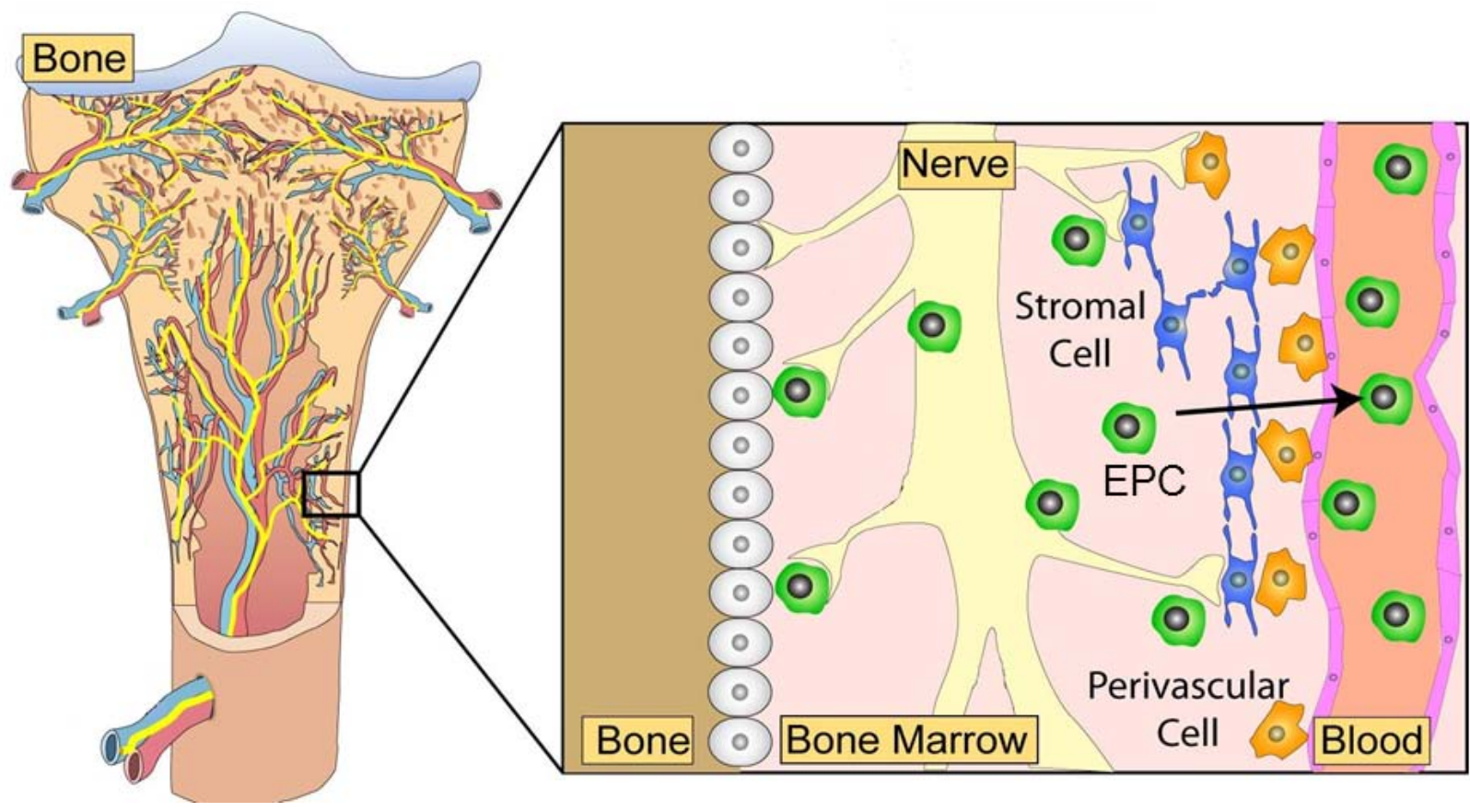
EPCs and other bone marrow (BM)-derived cells mobilization is suggested to occur as a result of activation of sympathetic nerve fibers in BM and decrease in the local levels of stromal derived factor-1[112-114] (Fig. 4). However, there is a discrepancy among studies describing the effect of sympathectomy on cell release from the BM: it was shown to affect cell mobilization [115], or have no clear effect [116].

EPCs arising from the BM are recruited to areas of vascular repair where they incorporate into injured capillary walls and differentiate into endothelial cells to replace diseased endothelium [106]. Additionally, EPCs contribute to vascular repair through the paracrine release of pro-angiogenic growth factors, promoting the proliferation of mature endothelial cells [117]. The mobilization of EPC from the BM and homing to the site of injury occurs in response to specific angiogenic stimuli. Specifically, it has been reported that chemokines such as stromal-derived factor 1 (SDF-1) and VEGF induce the release of EPC from the BM [118, 119]. It was suggested that that the mechanism of mobilization involves activation of matrix metalloproteinase-9, which alters EPCs interactions with BM stromal cells and thus allows them to disengage [120].

Figure 4: Schematic illustration of the hematopoietic niche in the bone marrow. The bone marrow is a reservoir of EPC. The bone marrow is fed with nerves that follow the blood vessels. Those nerve fibers are believed to interact with stromal cells and progenitor cells and in turn regulate the progenitor cells migration and release from the bone marrow. With permission from Dr. Maria Grant.

For interpretation of the references to color in this and all other figures, the reader is referred to the electronic version of this dissertation.

Figure 4 (cont'd)



Nevertheless, in diabetes the mobilization of EPCs is dramatically reduced [121-123] suggesting that in diabetes, EPCs have decreased migratory properties. Inhibition of EPC reparative function in the presence of consistent ischemia may lead to the loss of microvascular repair in diabetes and development of acellular capillaries [106, 124-127].

Correction of EPC dysfunction could treat early stages of vasodegeneration by enhancing vessel repair, preventing ischemia and progression to late stages of DR. It has been shown that EPC function can be strongly affected by circadian oscillations [112].

1.9 Circadian Function and Diabetes

Circadian rhythmicity provides adaptation to daily variations of light, temperature, food availability and other living conditions [128]. The circadian rhythms regulate multiple physiological processes including sleep-awake cycle, feeding behavior, control of body temperature, cardiovascular, endocrine, gastrointestinal, hepatic and renal function. The rhythms are generated by an endogenous oscillator composed of a central clock in the suprachiasmatic nucleus (SCN) and numerous peripheral clocks in peripheral tissues [129].

The SCN oscillations are entrained by the external light/dark signals and the SCN synchronizes the peripheral clocks in peripheral organs. In the SCN and peripheral tissues, circadian rhythm is generated by conserved autoregulatory molecular feedback loops composed of the products of the clock genes. These products form a self-

sustaining cascade with 24hr periodicity. Period genes (*Per1*, *Per2*) and Cryptochrome genes (*Cry1*, *Cry2*), *Rev-ERB* and *RORA* comprise the negative loop, while *Clock* and *BMAL1* genes comprise the positive loop of regulation [130]. The clock-controlled genes coordinate downstream cascades. At least 20% of tissue transcripts are under circadian control [131]. It is important to understand that the synchronization of metabolic functions with each other is as important as their synchronization with the environmental cycles [132]. Dysregulation of the expression of clock genes leads to disorders including abnormal sleep cycle, premature aging, metabolic syndrome, and obesity [133].

Particularly relevant to diabetes is the observation that *Bmal-1* and *Clock* directly regulate glucose homeostasis [134]. *Per2* gene knock-outs demonstrate impaired endothelial function and a shortened lifespan. Moreover, EPC-mediated repair is impaired in *Per2* mutant mice. Type 2 diabetic mice are hypertensive and have a disrupted heart rate circadian rhythm which is associated with dampened oscillations of *Bmal1* in vasculature [135].

Circadian regulation plays vital role in the mobilization of hematopoietic stem cells from the BM. First study suggesting that release of the cells from the BM can be regulated by circadian rhythms was published in 1950 [136]. Recent elegant study carried out by Mendez-Ferrer revealed that the release of EPCs is regulated by signals about light/dark cycle coming from SCN [112] (Fig. 5). In mice, there was definite peak of EPC release which occurred during the light phase, the rest period for nocturnal animals [112]. Activation of sympathetic nerve fibers in the BM results in a decrease of local SDF-1 levels, promoting EPC mobilization [112-114]. Thus, circadian progenitor cell release is regulated at the SCN level (clock genes expression), the BM

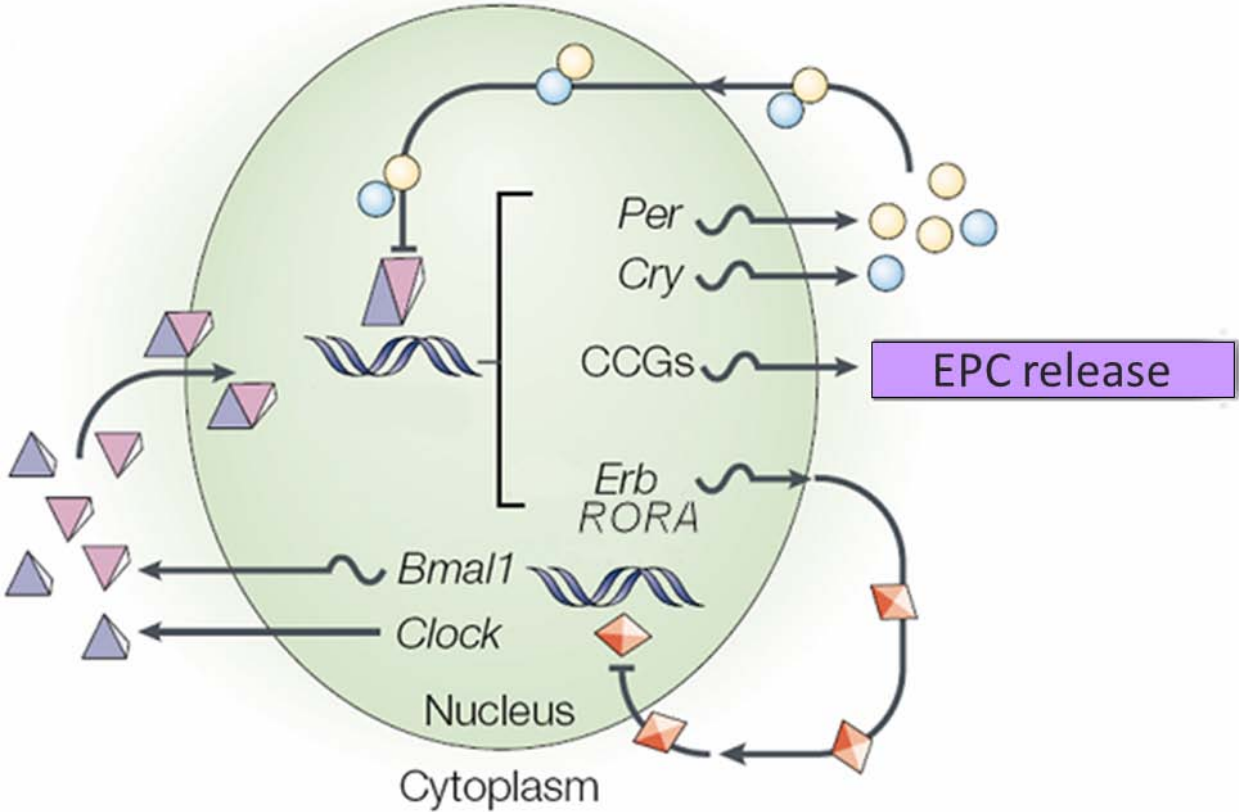
(sympathetic innervation, local clock genes expression) and the EPCs ability to receive SDF-1 signals and migrate in response. Several studies have demonstrated that diabetic patients have a decreased number of circulating EPCs [122, 123] and that EPC migration and repair capacity is severely reduced in diabetes [125, 137-140]. The circadian rhythm of EPCs in diabetes was not previously described.

Interestingly, prior work has found that in obese diabetic mice clock gene expression is attenuated in adipose tissue and the liver [141]. Additional studies in which mice were subjected to a high-fat diet inducing metabolic syndrome resulted in attenuated clock genes expression in the adipose tissue. However, this study did not show any changes in clock gene expression in the SCN, suggesting that a high-fat diet and obesity affects peripheral, but not central clocks [134].

Figure 5: The molecular feedback loops that control the circadian rhythms.

Three interlocking streams of rhythmic gene expression control circadian timing in suprachiasmatic nuclei and peripheral tissues. Early in circadian day, Clock/Bmal heterodimers bind to E-box and activates expression of Per/Cry. When Per/Cry heterodimers bind to E-box and activates expression of Per/Cry. When Per/Cry complexes accumulate by the late circadian day, Per/Cry complexes inhibit the binding of Clock/Bmal1 heterodimer to the E-boxes. When Per/Cry levels decline, the next circadian cycle of expression is initiated. Erb and RORA work through disinhibition by activating Bmal1 expression. Number of clock-control genes (CCG) is regulated through E-boxes and can affect the release of progenitor cells from the bone marrow. Modified from Hastings *et al.*, 2003 [130].

Figure 5 (cont'd)



1.10 Objective of the dissertation

The individual steps leading to DR are not well known, but likely involve the complex interplay between diabetes-induced microvascular damage and impaired EPC function synergistically leading to vasodegeneration in the retina.

In this dissertation, we test the following central hypothesis: in diabetes, a decrease in n3 PUFA levels promotes inflammation in the retina causing damage of the vascular endothelial cells. The reduction in the availability of circulating EPCs inhibits the repair of injured capillaries. Therefore, inhibiting the initial inflammatory injury or stimulating EPC-mediated repair prevents diabetic retinopathy. (Fig. 6)

Chapter II describes diabetes-induced changes in retinal fatty acid metabolism and its connection to the inflammatory profile in the retina.

Chapter III demonstrates the dramatic reduction of nerve endings in the diabetic BM accompanied by a decreased number of EPCs in circulation and an increased number of acellular capillaries in the retina.

Chapter IV investigates beneficial effect of DHA-rich diet on retinal vascular health through inhibition of retinal inflammation and correction of EPC number and function.

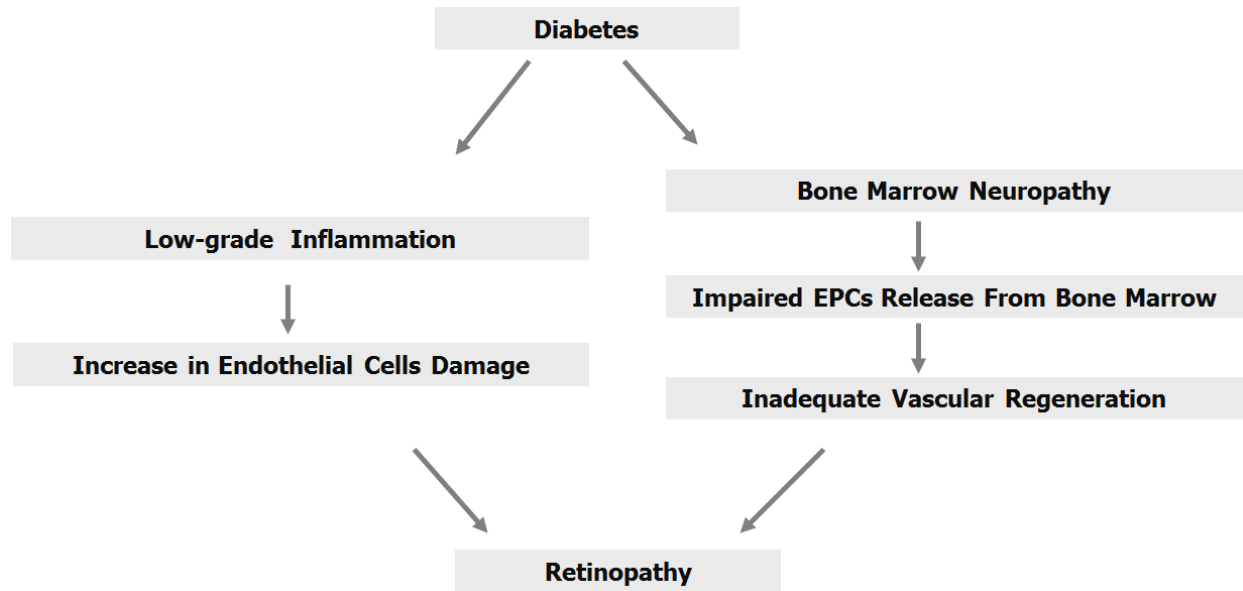
Chapter V examines the effect of surgical BM denervation on vascular retina health in order to determine direct link between BM denervation and lack of repair in the retina.

Chapter VI summarizes all described data and outlines future studies.

The results of this work provide an important mechanistic understanding of retinal vascular pathology in diabetes and may promote the development of novel safe and non-invasive therapeutic strategies for treatment of DR.

Figure 6: Schematic representation of the proposed mechanism. In diabetes, both increased endothelial cell damage and inadequate vascular regeneration have to coincide to initiate the development of DR. Preventing damage in endothelial cells and/or stimulating EPC release and repair function could prevent and treat the disease.

Figure 6 (cont'd)



Chapter II

Remodeling of Retinal Fatty Acids in an Animal Model of Diabetes: a Decrease in Long-Chain Polyunsaturated Fatty Acids Is Associated With a Decrease in Fatty Acid Elongases Elovl2 and Elovl4

This chapter is the edited version of a research article that was published in *Diabetes*, Volume 59, Issue 1 (219-227), 2009.

Authors: Tikhonenko, M., Lydic, T. A., Wang, Y., Chen, W. Opreanu, M., Sochacki, A., McSorley, K. M., Renis, R. L., Kern, T., Jump, D. B., Reid, G. E. and Busik, J.V.

2.1 Abstract

The results of the Diabetes Control and Complications Trial/Epidemiology of Diabetes Interventions and Complications cohort study revealed a strong association between dyslipidemia and the development of DR. However, there are no experimental data on retinal fatty acid metabolism in diabetes. This study determined retinal-specific fatty acid metabolism in control and diabetic animals.

Tissue gene and protein expression profiles were determined by quantitative RT-PCR and Western blot in control and streptozotocin-induced diabetic rats at 3–6 weeks of diabetes. Fatty acid profiles were assessed by reverse-phase high-performance liquid chromatography, and phospholipid analysis was performed by nano-electrospray ionization tandem mass spectrometry.

We found a dramatic difference between retinal and liver elongase and desaturase profiles with high elongase and low desaturase gene expression in the retina compared with liver. Elov14, an elongase expressed in the retina but not in the liver, showed the greatest expression level among retinal elongases, followed by Elov12, Elov11, and Elov16. Importantly, early-stage diabetes induced a marked decrease in retinal expression levels of Elov14, Elov12, and Elov16. Diabetes-induced downregulation of retinal elongases translated into a significant decrease in total retinal docosahexaenoic acid, as well as decreased incorporation of very-long-chain PUFAs, particularly 32:6n3, into retinal phosphatidylcholine. This decrease in n3 PUFAs was coupled with inflammatory status in diabetic retina, reflected by an increase in gene expression of proinflammatory markers interleukin-6, vascular endothelial growth factor, and intercellular adhesion molecule-1.

This is the first comprehensive study demonstrating diabetes-induced changes in retinal fatty acid metabolism. Normalization of retinal fatty acid levels by dietary means or/and modulating expression of elongases could represent a potential therapeutic target for diabetes-induced retinal inflammation.

2.2 Introduction

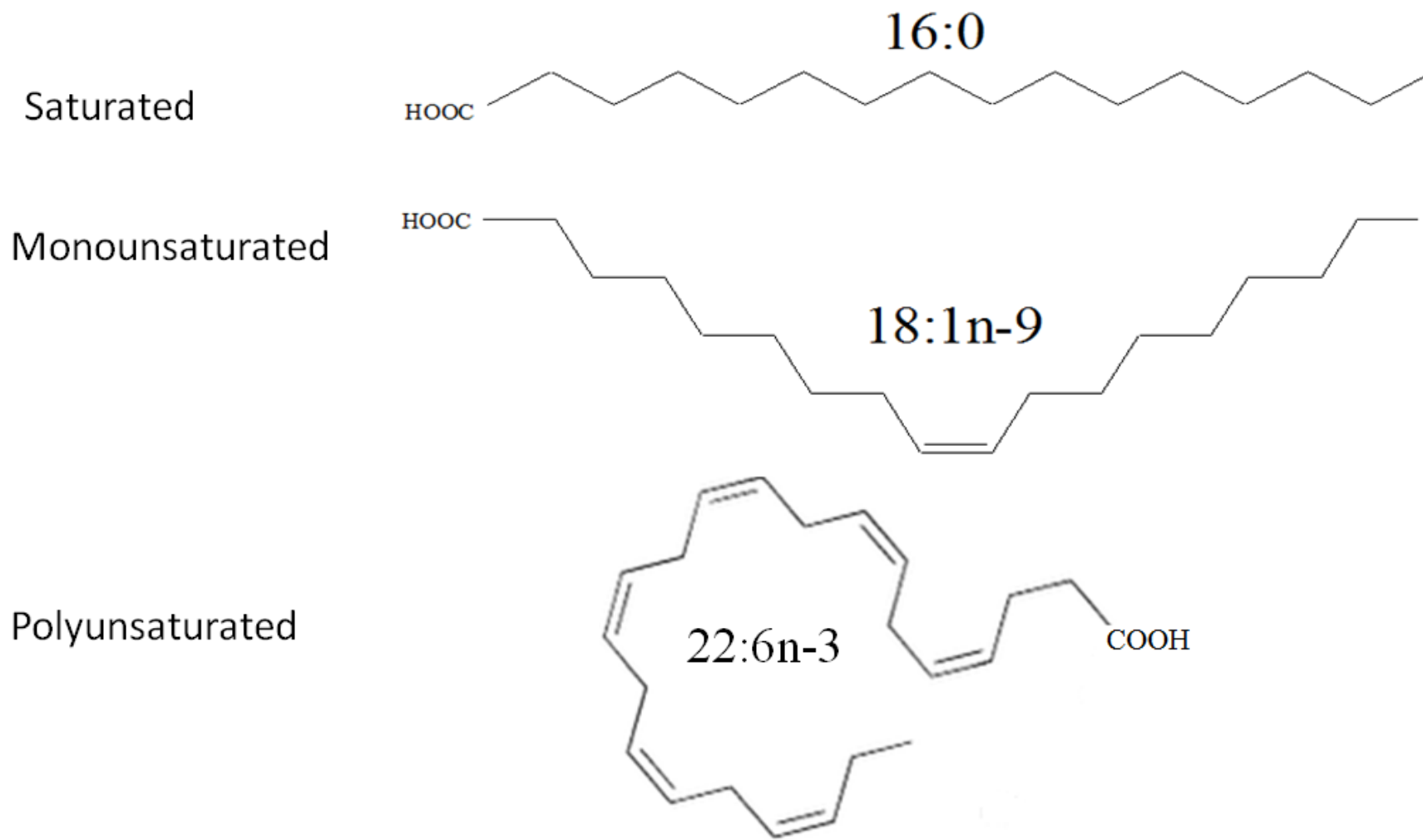
Early DR has been suggested to be a low-grade chronic inflammatory disease [20, 21, 142] with a number of inflammatory markers, such as VEGF [143, 144], ICAM-1 [145, 146], TNF- α [35], and IL-6 [147], shown to be upregulated in the diabetic retina. The individual molecular steps leading to inflammation in the retina are not well resolved but likely involve hyperglycemia and dyslipidemia associated with diabetes.

Dyslipidemia is a major metabolic disorder of diabetes, and the Diabetes Control and Complications Trial/Epidemiology of Diabetes Interventions and Complications cohort study revealed that dyslipidemia was significantly associated with the development of DR [62]. Diabetic dyslipidemia is the result of an imbalance in the complex regulation of lipid uptake, metabolism, release by adipocytes, and clearance from circulation [51, 55]. Fatty acid metabolism perturbation in diabetes is an important part of diabetic dyslipidemia [148].

To understand the effects of diabetes on plasma and tissue fatty acid composition, two metabolic routes have to be considered: de novo lipogenesis and PUFA remodeling Sprecher pathway [69]. Saturated fatty acids (SRAs), monounsaturated fatty acids (MUFAs), and PUFAs (Fig. 7) are synthesized from dietary precursors (glucose, palmitic 16:0, oleic 18:1n9, linoleic 18:2n6, α -linolenic 18:3n3, EPA 20:5n3, and DHA 22:6n3 through a series of desaturation (Δ 5-desaturase [Δ 5D], Δ 6-desaturase [Δ 6D], or Δ 9-desaturase [Δ 9D]) and elongation (Elovl1–7) reactions. In the recent work by Agbaga et al. [96], the Sprecher pathway was expanded to include very-long-chain PUFAs (VLCPUFAs), up to 38 carbon fatty acids, in which elongation of shorter-chain fatty acids precursors is performed by Elovl4 (Fig. 1). Elovl4 has very limited tissue specificity. It is highly expressed in the retina [149], thymus, and skin [150], as well as at lesser levels in the brain [150, 151] and testis [151]. Elovl4 is not expressed in the liver [150, 151].

Figure 7: Fatty acid structure. Example of chemical structure of saturated (16:0, palmitic), monounsaturated (18:1 n9, oleic) and polyunsaturated fatty acid (22:6n3, docosahexaenoic).

Figure 7 (cont'd)



In human retina, Elovl4 was shown to be primarily expressed in the inner segment of photoreceptors extending to photoreceptor cell bodies in the outer nuclear layer [152]. Moderate labeling was also observed in the ganglion cells [152]. Elovl4 has received much attention recently, as an autosomal-dominant Stargardt-like macular dystrophy was linked to several dominant-negative mutations in Elovl4 [152-154]. The role of VLCPUFAs produced by Elovl4 is not known, but because of their localization in retinal outer-segment membranes and their ability to span both leaflets of the lipid bilayer, they are suggested to play a role in stabilizing cellular membranes with high curvature, such as the rims of photoreceptor disks [96]. Fatty acid desaturase enzymes are known to be inhibited in diabetes [72, 155, 156], and there is emerging information suggesting that certain elongases might also be affected [52]. Thus, diabetes may result in reduced fatty acid remodeling and, consequently, lead to an accumulation of the substrates and depletion of the products. The elongases Elovl2 and Elovl6 are ubiquitously expressed in most tissues; however, retina expresses Elovl2 at a very high level. Elovl2 is involved in several steps of DHA (22:6n3) biosynthesis [157]. Retina has a unique fatty acid profile with one of the highest levels of long-chain PUFAs, especially DHA, in the body [89]. We have previously demonstrated that DHA has a pronounced anti-inflammatory effect on cytokine-induced activation of the nuclear factor (NF)- κ B pathway and adhesion molecule expression in HRECs [77]. Thus, perturbation of lipid metabolism in diabetes with a subsequent decrease in DHA could create proinflammatory conditions in the retina, potentially contributing to the development of DR. The effect of diabetes on retinal fatty acid elongases and desaturases and

diabetes-induced changes in retinal fatty acid remodeling has not been analyzed and represents one of the goals of this study.

2.3 Results

Body weight gain and blood glucose concentration of experimental animals. As presented in Table 1, body weight gain was significantly slower in diabetic animals compared with control animals. Blood glucose levels were almost five times higher in diabetic animals compared with controls. As this was a short-term diabetes study, A1C levels were not measured.

Elongase and desaturase expression level in control and diabetic animals. The gene expression levels of elongases and desaturases in control retinas were determined by quantitative RT-PCR and compared with the levels found in the livers of the same animals. Retinal-specific elongase, Elov14, had the highest expression level among all the elongases in the retina and was not expressed in the liver. Retinas also had high levels of Elov12 expression (Fig. 8A). Livers exhibited higher levels of Elov15 and Δ 5-, Δ 6-, and Δ 9-desaturases than retina (Fig. 8A), and the liver profile of all elongases and desaturases agreed with our previous study [52].

In the liver, diabetes induced a 25% decrease in Elov12 and a 33% decrease in Elov16 expression, as well as an 85% decrease in Δ 9-desaturase (Fig. 8B) compared with controls. In the retina, diabetes induced a 40% reduction in Elov14 and 50% reduction in Elov12 expression levels (Fig. 8C). There was no significant effect of diabetes on the retinal desaturases (Fig. 8C). A decrease in Elov14 protein level was confirmed by Western blot, as shown in Fig. 8D.

Blood plasma fatty acid profiles of control and diabetic animals. The control and diabetic blood plasma fatty acid profiles 3 weeks after STZ injection are presented in Table 2. There was a tendency toward higher total fatty acids level in diabetic versus control blood plasma. We observed changes in the plasma fatty acid profile consistent with inhibition of fatty acid remodeling in diabetes that leads to a lower end product-to-precursor fatty acid ratio. There was a decrease in two major end products of the PUFA synthesis pathway, arachidonic 20:4n6 acid and DHA, relative to their precursors, linoleic 18:2n6 and α -linolenic 18:3n3 acid, respectively (Table 2). As a result of these changes, we observed a decrease in unsaturation index (the number of double bonds per fatty acyl residue) and a decrease in long-chain-to-short-chain PUFA ratio in diabetic versus control animals (Table 2).

Liver fatty acid profiles of control and diabetic animals. The control and diabetic liver fatty acid profiles 3 weeks after STZ injection are presented in Table 3. There was an increase in the linoleic acid 18:2n6 level in the livers of diabetic versus control animals that led to a decrease in long-chain-to-short-chain PUFA ratio (Table 3). There were no other significant changes in liver fatty acid profiles in diabetic versus control animals. The liver unsaturation index and PUFA synthesis pathway end product-to-precursor ratios did not change in diabetic versus control animals (Table 3).

Retinal fatty acid profiles of control and diabetic animals. Retina has a unique fatty acid profile, with the highest content of long-chain PUFAs in the body. In agreement with other studies, retinal profiles were very rich in DHA and arachidonic 20:4n6 acid (Table 4). The levels of linoleic 18:2n6 and α -linolenic 18:3n3 acids in the retina were very low; thus we did not calculate the PUFA synthesis pathway end

product-to-precursor ratios. Importantly, the retinas of diabetic animals had 28% less DHA compared with controls. As a result, we observed a decrease in unsaturation index, a decrease in long-chain-to-short-chain PUFA ratio, and a decrease in the n3-to-n6 PUFA ratio in the retinas of diabetic versus control animals (Table 4). Representative reverse-phase high pressure liquid chromatography (RP-HPLC) chromatograms of saponified fatty acids from control and diabetic retina are presented in Fig. 9A.

Retinal and erythrocyte phospholipid profiles of control and diabetic animals. In agreement with saponified fatty acid profile data, nESI-MS/MS analysis of the retina lipid extracts of diabetic animals (n = 3) showed a significant (up to 34%) decrease in the abundance of glycerophospholipids containing DHA compared with the control animals (n = 3). For example, compare the abundance of the GPCho(18:0/22:6) and GPCho(22:6/22:6) lipids in the ratiometric analysis shown in Fig. 9B. Similar decreases in the abundances of DHA containing lipids were also observed for glycerophosphoethanolamine and glycerophosphoserine lipids (data not shown). In contrast, an increase (37%) in the abundance of the linoleic 18:2n6 acid-containing GPCho(16:0/18:2) lipid was observed for the same samples as shown in Fig. 9B. In addition to known fatty acids identified by HPLC analysis, nESI-MS/MS analysis revealed several VLCPUFAs, primarily 32:6n3 and 34:6n3, esterified to GPCho in the retina. Interestingly, GPCho(32:6/22:6) was significantly decreased (24%) in diabetic retinas compared with controls, and there was a nonsignificant decrease (9%) of GPCho(34:6/22:6).

In erythrocyte lipid extracts, an increase in the abundance of linoleic 18:2n6 acid-containing lipids, namely GPCho(16:0/18:2) and GPCho(18:0/18:2), was observed

between the diabetic and control samples, consistent with the changes in retina lipids, as shown in Fig. 9C. Erythrocytes had very low levels of DHA-containing phospholipid species, and there was no effect of diabetes on these species. There was no detectable GPCho(32:6/22:6) or GPCho(34:6/22:6) in the erythrocytes or in liver and blood plasma (data not shown).

Inflammatory marker expression in control and diabetic retinas. As n3 PUFAs are known to have anti-inflammatory properties, we hypothesized that a decrease in n3 PUFAs would be associated with a proinflammatory state in diabetic retinas. As shown in Fig. 10, diabetic retinas had increased expression levels of several inflammatory markers including ICAM-1, cytokines (IL-6), and growth factors (VEGF).

Table 1

Body weight gain and blood glucose concentrations of experimental animals

	<i>n</i>	Weight gain (g/day)	Blood glucose (mmol/l)
Control animals	4	4.05 ± 0.65	4.33 ± 0.29
Diabetic animals	7	2.32 ± 0.89	20.80 ± 1.16

Data are means ± SD.

Figure 8: Expression levels of elongases and desaturases in retinas and livers of control and diabetic animals. Total RNA was extracted from retinas and livers of normal control (n = 4) and STZ-induced diabetic animals (n = 5) after 3–6 weeks of diabetes and analysed by real-time PCR for elongases 1–7 (E1–7) and Δ 5-, Δ 6-, and Δ 9-desaturase (D5D, D6D, and D9D) expression level.

A comparison of the expression levels in retina (□) and liver (■) of normal control animals is presented in A.

Diabetes-induced changes in liver elongase and desaturase expression levels are presented in B (□, control; ■, diabetes).

Diabetes-induced changes in retinal expression levels are presented in C (□, control; ■, diabetes).

A Western blot of diabetes-induced changes in retina Elovl4 protein level (lanes 1–4 control, lanes 5–8 diabetic), and quantification by ratiometric comparison to tubulin, are presented in D (□, control; ■, diabetes).

Data are presented as means \pm SD of five independent experiments.

* = Statistical significance at $P < 0.05$.

Figure 8 (cont'd)

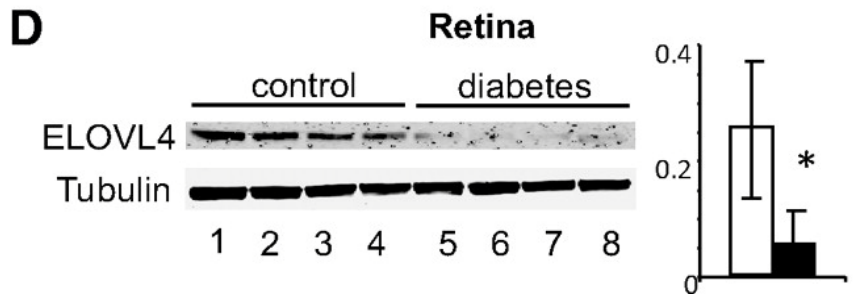
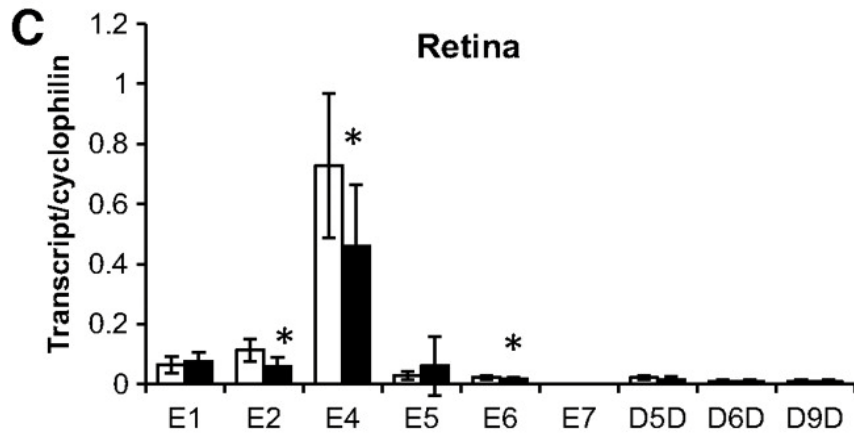
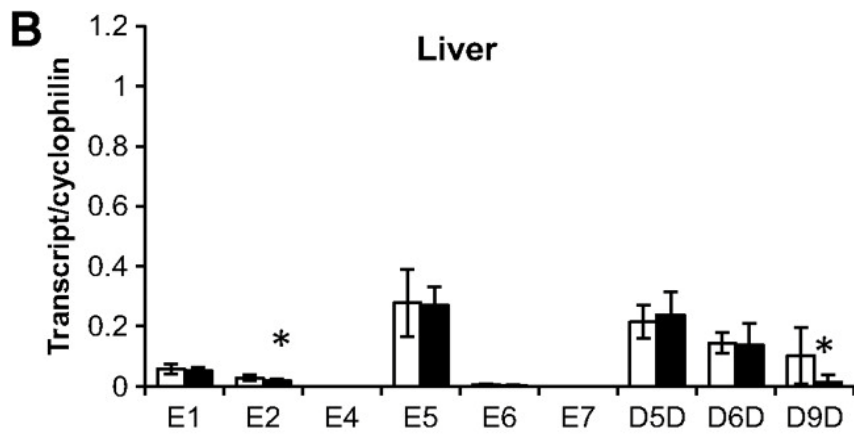
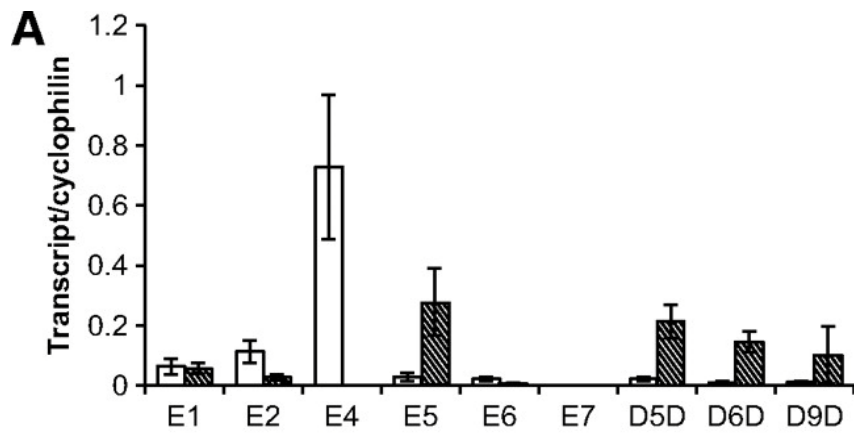


Table 2Blood plasma fatty acid profiles of control ($n = 4$) and diabetic ($n = 7$) animals

Fatty acids	Blood plasma			<i>P</i>
	Control animals	Diabetic animals	Difference	
Total (nmol/mg protein)	2,262.55 ± 639.64	3,286.54 ± 766.69		0.0972
Mole % of total fatty acids				
16:0 (palmitic)	2.19 ± 1.17	3.70 ± 0.46	↑	0.0362*
18:0 (stearic)	2.25 ± 0.34	2.08 ± 0.40		0.5639
18:1n9 (oleic)	12.65 ± 1.03	13.43 ± 1.74		0.5126
18:2n6 (linoleic)	54.12 ± 2.31	57.44 ± 2.62		0.1207
18:3n3 (α-linolenic)	1.93 ± 0.32	2.71 ± 0.36	↑	0.0214*
18:3n6 (γ-linolenic)	0.31 ± 0.13	0.51 ± 0.37		0.4028
20:3n6 (dihomo-γ-linolenic)	0.84 ± 0.12	0.87 ± 1.15		0.9631
20:3n9 (mead)	0.52 ± 0.32	0.35 ± 0.30		0.4636
20:4n6 (arachidonic)	21.29 ± 2.70	15.90 ± 1.95	↓	0.0161*
20:5n3 (eicosapentaenoic)	0.53 ± 0.08	0.51 ± 0.03		0.7449
22:5n3 (docosapentaenoic)	0.84 ± 0.22	0.54 ± 0.04	↓	0.0235*
22:6n3 (docosaheptaenoic)	2.78 ± 0.23	1.72 ± 0.25	↓	0.0010*
Fatty acid ratios				
Unsaturation index	61.58 ± 18.05	38.91 ± 5.56	↓	0.0342*
LCPUFAs/SCPUFAs†	0.48 ± 0.06	0.33 ± 0.05	↓	0.0107*
20:4n6/18:2n6	0.40 ± 0.07	0.28 ± 0.04	↓	0.0232*
22:6n3/18:3n3	1.46 ± 0.17	0.64 ± 0.13	↓	0.0002*

Data are means ± SD. * $P < 0.05$. †Long-chain PUFAs/short-chain PUFAs.

Table 3Liver fatty acid profiles of control ($n = 4$) and diabetic ($n = 7$) animals

Fatty acids	Liver		Difference	<i>P</i>
	Control animals	Diabetic animals		
Total (nmol/mg protein)	1,762.82 ± 480.50	1,357.85 ± 241.19		0.1,542
Mole % of total fatty acids				
16:0 (palmitic)	26.73 ± 8.18	17.55 ± 3.25		0.0518
18:0 (stearic)	11.25 ± 3.74	12.64 ± 3.55		0.9706
18:1n9 (oleic)	3.11 ± 1.03	3.39 ± 1.04		0.4785
18:2n6 (linoleic)	33.14 ± 5.34	39.90 ± 2.71	↑	0.0161*
18:3n3 (α-linolenic)	0.49 ± 0.11	0.59 ± 0.11		0.2101
18:3n6 (γ-linolenic)	0.13 ± 0.14	0.09 ± 0.04		0.2173
20:3n6 (dihomo-γ-linolenic)	0.34 ± 0.04	0.43 ± 0.15		0.3942
20:3n9 (mead)	0.62 ± 0.24	0.51 ± 0.14		0.9340
20:4n6 (arachidonic)	19.87 ± 4.43	21.37 ± 2.50		0.4581
20:5n3 (eicosapentaenoic)	0.15 ± 0.03	0.15 ± 0.05		0.7777
22:5n3 (docosapentaenoic)	0.57 ± 0.15	0.44 ± 0.07		0.2388
22:6n3 (docosahexaenoic)	3.60 ± 0.92	2.94 ± 0.35		0.2294
Fatty acid ratios				
Unsaturation index	5.05 ± 1.82	6.56 ± 1.31		0.0911
LCPUFA/SCPUFA†	0.74 ± 0.07	0.64 ± 0.02	↓	0.0123*
20:4n6/18:2n6	0.60 ± 0.07	0.53 ± 0.03		0.1211
22:6n3/18:3n3	7.74 ± 2.96	5.11 ± 1.05		0.0979

Data are means ± SD. * $P < 0.05$. †Long-chain PUFAs/short-chain PUFAs.

Table 4Retinal fatty acid profiles of control ($n = 4$) and diabetic ($n = 7$) animals

Fatty acids	Retina		Difference	<i>P</i>
	Control animals	Diabetic animals		
Total (nmol/mg protein)	488.96 ± 17.64	460.32 ± 27.82		0.43
n3 fatty acids	225.1 ± 4.23	166.34 ± 20.66	↓	0.0495*
n6 fatty acids	38.67 ± 4.71	40.59 ± 3.9		0.7693
Mole % of total fatty acids				
16:0 (palmitic)	15.51 ± 0.8	18.32 ± 1.67		0.2046
18:0 (stearic)	18.61 ± 0.97	21.98 ± 2.		0.2046
18:1n9 (oleic)	10.58 ± 0.2	12.9 ± 0.77	↑	0.0441*
18:2n6 (linoleic)	0.44 ± 0.06	0.88 ± 0.05	↑	0.0051*
18:3n3 (α-linolenic)	0.24 ± 0.06	0.17 ± 0.02		0.3556
20:3n6 (dihomo-γ-linolenic)	0.11 ± 0.02	0.04 ± 0.01		0.0819
20:3n9 (mead)	0.97 ± 0.06	1.09 ± 0.2		0.6103
20:4n6 (arachidonic)	7.33 ± 0.75	7.9 ± 0.64		0.6004
20:5n3 (eicosapentaenoic)	0.04 ± 0.02	0.01 ± 0.01		0.2910
22:5n3 (docosapentaenoic)	0.47 ± 0.08	0.28 ± 0.05		0.1129
22:6n3 (docosahexaenoic)	45.37 ± 1.32	35.47 ± 2.71	↓	0.0305*
Fatty acid ratios				
Unsaturation index	20.77 ± 1.63	14.9 ± 2.57		0.1259
LCPUFA/SCPUFA†	80.39 ± 4.86	42.53 ± 3.94	↓	0.0038*
% n3 fatty acids of total	46.12 ± 1.41	35.93 ± 2.77	↓	0.0306*

Data are means ± SD. * $P < 0.05$. †Long-chain PUFAs/short-chain PUFAs.

Figure 9: Fatty acid analysis by RP-HPLC and comparative MS/MS analysis of GPCho lipids in control (n = 3) and diabetic (n = 3) animals at 3–6 weeks post-STZ injection.

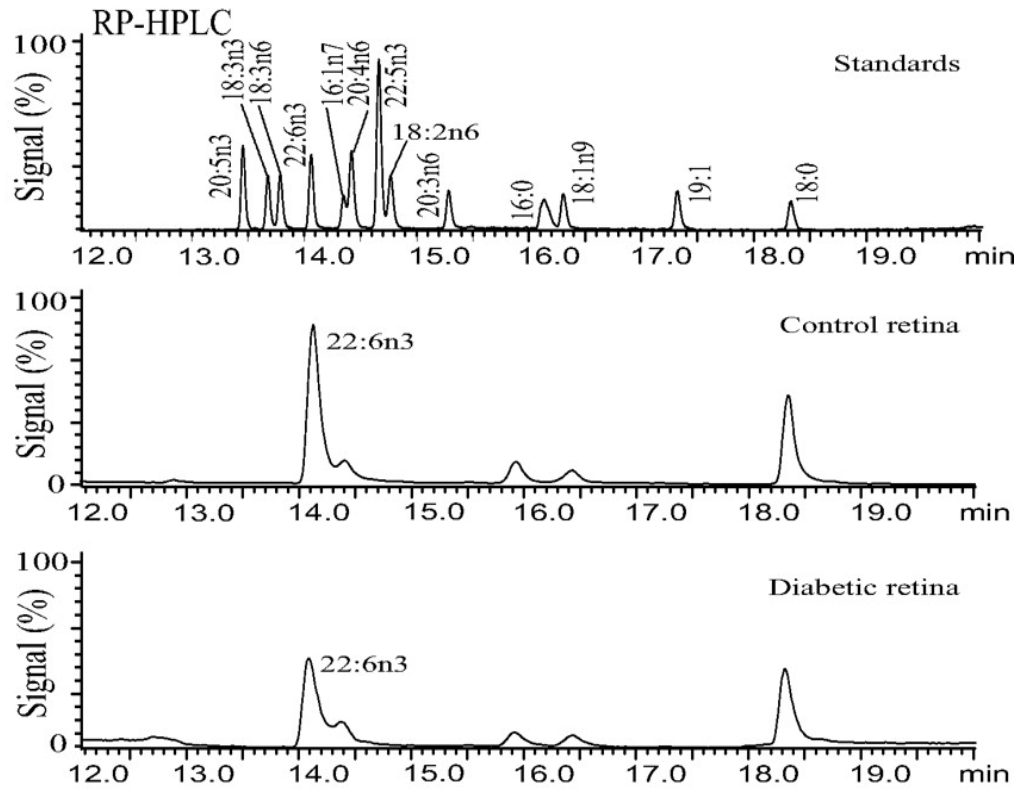
A: Identification and quantification of diabetes-induced changes in total retina saponified fatty acids. Top: RP-HPLC chromatogram of a mixture of authentic fatty acid standards. Middle: Control retina saponified fatty acids. Bottom: Diabetic retina saponified fatty acids.

B: Ratiometric analysis of changes in GPCho lipid abundance (Abund.) between control (□) and diabetic (■) retina. GPCho species were detected by nESI-MS/MS using PI m/z 184 and further characterized as described in research design and methods.

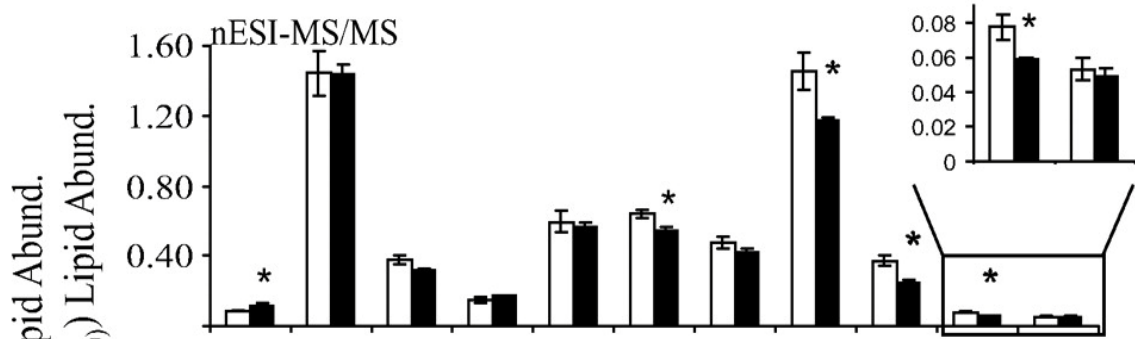
C: Ratiometric analysis of changes in GPCho lipid abundance between control and diabetic erythrocytes. Data are presented as means ± SD. *Statistical significance at P < 0.05.

Figure 9 (cont'd)

A



B



C

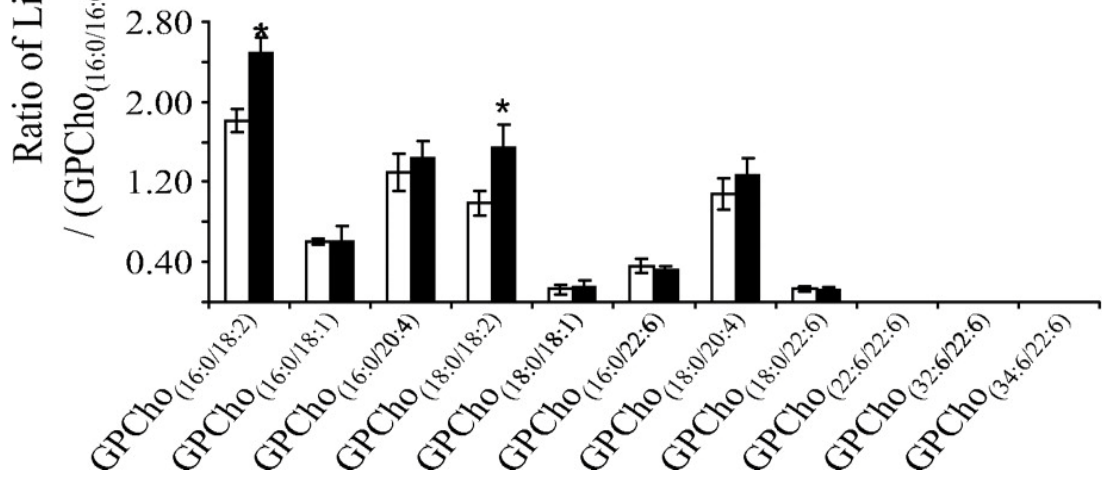
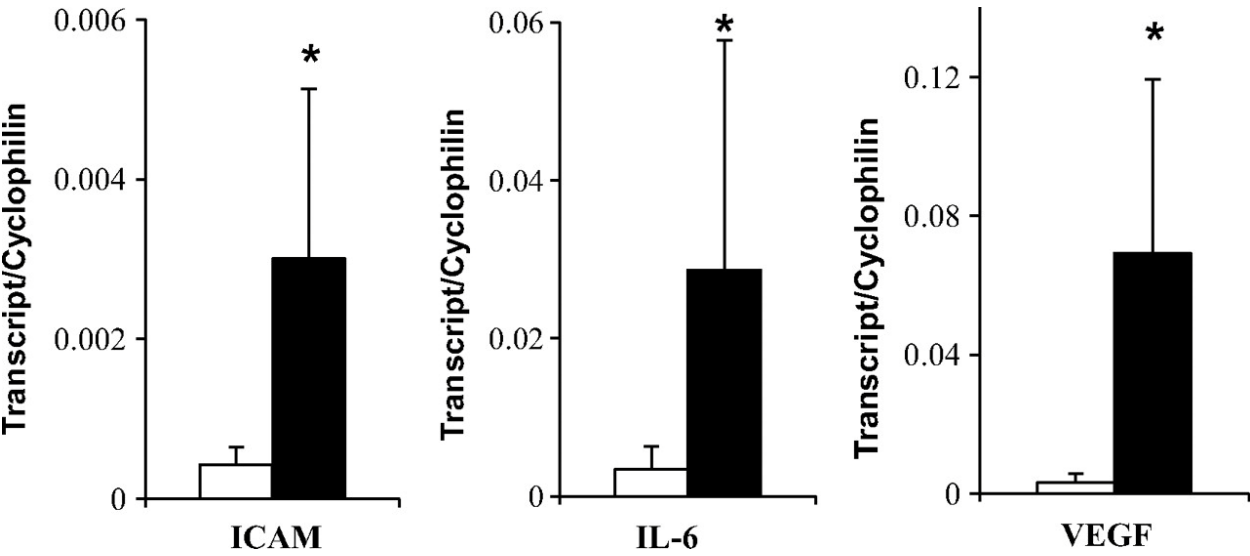


Figure 10: Expression levels of inflammatory markers in retinas of control (□, n = 7) and diabetic (■, n = 7) animals. Total RNA was extracted from retinas of control and diabetic animals after 3–6 weeks of diabetes and analysed by real-time PCR. Diabetes-induced changes in retinal ICAM-1, IL-6, and VEGF expression are shown. Data are presented as means ± SD of at least four independent experiments.

*Statistical significance at $P < 0.05$.

Figure 10 (cont'd)



2.4 Discussion

The association of dyslipidemia with the development of DR has been underscored by the Diabetes Control and Complications Trial/Epidemiology of Diabetes Interventions and Complications cohort study [35]. Despite this evidence, the experimental data on diabetes-induced changes in lipid profile and lipid metabolism in the retina are not available. This is the first comprehensive study to analyze retinal-specific fatty acid profiles and metabolism and to compare them to liver and blood plasma in control and diabetic animals.

In this study utilizing STZ-induced diabetic rats, we found a decreased level of DHA, the major retinal long-chain PUFA, in diabetic retina. This finding confirmed earlier studies showing a decrease in the relative percentage of DHA in the diabetic retina [158, 159]. In addition to DHA, VLCPUFAs including 32:6n3 and 34:6n3 were detected as substituents of retina GPCho. VLCPUFAs were not detected in lipid classes other than GPCho and were only detected in retina. Three weeks of diabetes reduced retinal levels of 32:6n3-GPCho compared with controls. As a result of these changes, the diabetic retina had a lower unsaturation index and lower long-chain-to-short-chain PUFA ratio. Moreover, there was a shift toward n3 PUFA-deficient, n6 PUFA-rich, profile in the diabetic retina.

In general, n6 PUFAs induce, while n3 PUFAs inhibit, inflammation, and the relative amount of these PUFAs plays an important role in the regulation of immunity [160]. Our previous studies indicated that treatment of a cell type affected by DR, HRECs, with n6 PUFA leads to a lipoxygenase-dependent increase in ICAM-1/vascular cell adhesion molecule-1 expression [85]. Conversely, we have demonstrated that DHA

inhibited cytokine-induced activation of the NF- κ B signaling pathway and adhesion molecule expression in HRECs [77]. Thus, a decrease in the n3-to-n6 PUFA ratio in the diabetic retina observed in this study would create proinflammatory conditions potentially contributing to the development of DR. Indeed, previous studies demonstrated an upregulation in a number of inflammatory markers in the retina early in diabetes: VEGF [143, 144], ICAM-1 [145, 146], TNF- α [35], and IL-6 [147]. ICAM-mediated leukostasis was detected within 1 week of diabetes in rats [10, 30]. VEGF was shown to increase ICAM expression in retinas of nondiabetic mice [161], and vitreal VEGF levels were found to be correlated with that of IL-6 and severity of DR in diabetic patients [42].

In this study, we chose a cytokine (IL-6), a growth factor (VEGF), and an ICAM-1 as readout of inflammatory status in the retinas of diabetic animals with decreased n3/n6 PUFAs. mRNA levels of all three markers were elevated in diabetic retinas compared with controls.

Importantly, diabetes induced the most pronounced changes in the retinal fatty acid profile, whereas liver fatty acid profile was only slightly affected, indicating that the disruption of retinal fatty acid metabolism in diabetes might not simply be a result of altered liver metabolism. Moreover, VLCPUFA-containing phospholipids detected in the retina were not present in the liver or erythrocyte total lipids. The fatty acid profile in a particular peripheral tissue depends on two factors: 1) the profile in circulation due to the diet and liver metabolism and 2) the ability of a local tissue to remodel fatty acids. Retina has a unique fatty acid profile characterized by one of the highest levels of DHA in the body and by the presence of VLCPUFAs [89, 162]. While the expression level of

retinal desaturases was relatively low compared with retinal elongases, it has been reported that retina can synthesize DHA from α -linolenic 18:3n3 acid and EPA 20:5n3 [163]. Although retina may obtain additional DHA by uptake from the circulation, changes in the retinal fatty acid profiles of diabetic animals did not mirror changes observed in liver and plasma fatty acid profiles. Thus, a retina-specific decrease in DHA in diabetes is likely to be due to changes in retinal fatty acid metabolism.

To determine the effect of diabetes on retinal fatty acid metabolism, we analyzed the level of fatty acid elongase and desaturase gene expression in control and diabetic animals. Retinas had a very high expression level of the retinal-specific elongase, Elov14, as well as high expression levels of long-chain PUFA elongase Elov12. Δ 5-, Δ 6-, and Δ 9-desaturase levels were low compared with the liver expression levels. The high levels of Elov14 and Elov12 and low levels of desaturases suggest that the retina is preferentially involved in production of very-long-chain fatty acids and exhibits a low level of de novo lipogenesis. The retinal elongase expression profile that we observed likely explains the high level of long-chain PUFAs in the retina compared with liver and blood plasma levels. Elov12 elongates C20–22 fatty acids [93, 94, 164]. Elov14 was recently shown to be involved in VLCPUFA synthesis with substrate specificity for C26–36 fatty acids [96]. The role of VLCPUFAs is not known. Because of their specific presence in tissues with high membrane curvature and their ability to span both leaflets of the lipid bilayer, VLCPUFAs are suggested to play the role of an anchor stabilizing high curvature cellular membranes [96]. In the retina, VLCPUFAs are mainly present in the rod outer-segment membrane [96], where they are suggested to play a role in stabilizing the rims of photoreceptor disks. This specific localization might explain low

abundance of VLCPUFAs in the total retinal lipids extracted in this study. At the same time, specific localization suggests that VLCPUFAs might play an important role in photoreceptor function. This study provides the first direct evidence that a significant decrease in Elov14 in diabetic retina is indeed associated with a decrease in VLCPUFA (i.e., 32:6n3) synthesis. Despite lower abundance, the diabetes-induced decrease in 32:6n3 containing GPCho (24%) was similar to the decrease in DHA22:6n3 containing GPChos (15–34%). Elov14 protein expression in diabetic retina was inhibited to a higher degree (73%) compared with mRNA expression (40%), suggesting control of Elov14 expression at both the transcriptional and translational levels. Although decrease of VLCPUFAs is most likely to arise from Elov14 loss, another plausible explanation could be that this reduction was due to reduction in VLCPUFA precursor lipids, EPA 20:5n3, and/or DHA. This possibility can be tested in the future by determining whether downregulation of VLCPUFAs in diabetes persists in animals supplemented with high-EPA/DHA diet.

Another possibility could be that high level of reactive oxygen species in diabetic retina leads to degradation of a highly oxidation-prone DHA molecule. Previous studies using the same STZ-induced diabetic model of similar duration, however, did not find oxidized DHA products in diabetic retina [165].

Several Elov14 gene mutations have been recently identified in pathogenesis of another retinal disease, Stargardt-like macular dystrophy [152-154]. Stargardt-like macular dystrophy is an autosomal-dominant disorder due to a dominant-negative effect of the mutated Elov14 on wild-type protein [152]. As Elov14 is highly expressed in the photoreceptors [152, 154], it is not surprising that mutant Elov14 transgenic mice are

characterized by lipofuscin accumulation, abnormal electrophysiology, and photoreceptor degeneration [153]. Although photoreceptors are not the primary site of DR, several abnormalities in neural retina have been associated with the development of DR [166, 167]. The decrease in Elov14 observed in this study would not be expected to have as dramatic an effect on photoreceptor viability as the dominant-negative mutation in Elov14. However, the reduction in Elov14 in diabetic retina could be responsible for more subtle changes in photoreceptor/retinal pigment epithelium cell function that could lead to metabolic changes in the whole retina and eventually contribute to the pathology characteristic of DR.

In conclusion, a decrease in the expression level of retinal fatty acid elongases Elov12 and Elov14 and concomitant decrease in the major n3 PUFA, DHA (22:6n3), as well as the VLCPUFA 32:6n3, results in an increased n6-to-n3 PUFA ratio in the diabetic retina that likely creates a proinflammatory state contributing to the development of DR. Increasing the gene expression of fatty acid elongases in the retina represents a potential therapeutic strategy for modulating fatty acid metabolism and altering the pathogenesis of DR.

2.5 Methods

Reagents. High-performance liquid chromatography (HPLC)-grade acetonitrile, acetic acid, methanol, chloroform, streptozotocin (STZ), and commonly used chemicals and reagents were from Sigma-Aldrich Chemical (St. Louis, MO).

Animals and induction of STZ-induced diabetes. Male Sprague-Dawley rats weighing 237–283 g were made diabetic with a single intraperitoneal injection of 65 mg

STZ per kg body wt. Body weight gains and blood glucose for the control and STZ-induced diabetic groups were monitored biweekly. At 3–6 weeks after STZ injection, the animals were killed and blood plasma, liver, and retina were recovered for analyses of fatty acid profiles and/or fatty acid elongase and desaturase expression levels. To isolate the retina, the optic nerve was cut out; the eye was opened; the coronary, cornea, and lens were discarded; and the retina was separated from choroid, washed in PBS, and frozen. Rats were maintained on Harlan-Teklad laboratory diet (no. 8,640) and water ad libitum. The fatty acid composition of the diet was analyzed by reverse-phase HPLC (RP-HPLC, see below) and found to be 16:0, 20.0%; 18:0, 1.8%; 18:1n9, 21.9%; 18:2n6, 50.8%; 18:3n3, 5.6%; 18:3n6, 0.1%; 20:4n6, 0.1%; 20:5n3, 0.4%; 22:5n3, 0.1%; and 22:6n3, 0.3%. Animal protocol was approved by the Michigan State University Institutional Animal Care and Use Committee. All experiments followed the guidelines set forth by the Association for Research in Vision and Ophthalmology Resolution on Treatment of Animals in Research.

RNA and protein isolation. Rat tissues were homogenized in Trizol reagent (Invitrogen), and RNA was isolated according to manufacturer instructions. After adding chloroform, the upper aqueous phase was separated and RNA was precipitated with isopropyl alcohol, washed with 75% ethanol, and redissolved in RNase-free water. Proteins from the same samples were isolated by washing in Tris buffer (30 mmol/l Tris-HCl, pH 6.8, with 0.1% SDS) followed by concentration on Amicon-15 (Millipore) centrifugal filters. After concentration, protease/phosphatase inhibitor cocktail was added and samples were frozen until further analysis.

Real-time qRT-PCR. Transcript-specific primers were designed using Primer3 software (available at <http://frodo.wi.mit.edu/primer3/>). First-strand cDNA was synthesized using the SuperScript II RNase H Reverse Transcriptase (Invitrogen, Carlsband, CA), and PCRs were performed in triplicate as previously described (25). Transcripts of interest were normalized to the abundance of cyclophilin mRNA. Rat gene-specific primers used in this study were Elovl4: GAAGTGGATGAAAGACCGAGA (sense) and GCGTTGTATGATCCCATGAA (antisense); Elovl7: TGGCGTTCAGCGATCTTAC and GATGATGGTTTGTGGCAGAG; IL-6: CCAGGAAATTTGCCTATTGA and GCTCTGAATGACTCTGGCTTT; VEGF A: GCTCTCTTGGGTGCACTGG and CACCACTTCATGGGCTTTCT; and ICAM-1: CCACCATCACTGTGTATTCGTT and ACGGAGCAGCACTACTGAGA. All other primers for rat elongases and desaturases were described previously [52].

Western blotting. Protein concentration was determined by a Qubit fluorometer (Invitrogen), according to manufacturer's instructions, and equivalent amounts of protein were loaded on the SDS-polyacrylamide (10%) minigels for SDS-PAGE separation. The separated proteins were electrophoretically transferred to a nitrocellulose membrane (Bio-Rad, Hercules, CA), blocked for 30 min at room temperature, and probed with primary rabbit anti-Elovl4 (Abcam) and mouse anti- α tubulin (Sigma) antibody followed by fluorescent secondary antibody (Invitrogen). The blots were analyzed by the Licor Odyssey scanner and quantitated using Licor Odyssey software.

Total lipid extraction. Total lipids from retina, blood plasma, and liver were extracted with chloroform-methanol (2:1, vol/vol), normalized to tissue weight, dried, and resuspended as previously described [168]. Acidification of total lipid extracts was

omitted, as low pH has been demonstrated to destroy acid-labile plasmalogen lipids [169], which are abundant in neural tissues. No significant decrease of recovery of abundant lipid classes was observed in the absence of pH modification [168]. Blood plasma lipids were normalized to protein, as measured by Qubit assay. Erythrocyte total lipids were extracted from 100 mg of packed cells by a modified Rose and Oklander method [170]. Briefly, lysed cells were combined with 6.8 ml of 80% 2-propanol, vortexed, and incubated for 1 h on ice with occasional mixing. Lipids were extracted twice by addition of 3.2 ml of 100% chloroform and 1-h incubation on ice, with phase separation after each chloroform addition achieved by centrifugation at 2,000g for 30 min. Acidification of the extraction mixture was omitted, as it was found that low pH destroys acid-labile plasmalogen lipids [169], which are abundant in neural tissues. No significant decrease of recovery of abundant lipid classes was observed in the absence of pH modification [168]. Pooled lipid extracts were dried, resuspended, and stored as described above.

Lipid analysis by nano-electrospray ionization tandem mass spectrometry. Lipid extracts were introduced to a triple-quadrupole mass spectrometer (Thermo Scientific model TSQ Quantum Ultra, San Jose, CA) for nano-electrospray ionization tandem mass spectrometry (nESI-MS/MS) analysis of lipid species as previously described [168]. Identification of phospholipid species by precursor ion and neutral loss scan mode MS/MS was performed according to published methods [168, 171]. Assignment of phosphatidylcholine (GPCCho) acyl substituents was achieved by negative ion mode analysis of corresponding GPCCho $[M+Cl]^-$ ions byproduct ion scan mode MS/MS, as well as by precursor ion scanning for m/z corresponding to specific

deprotonated fatty acyl ions. Peak finding and correction for ^{13}C isotope effects was performed using the Lipid Mass Spectrum Analysis (LIMSA) software version 1.0 peak model fit algorithm [172]. Quantitative analysis of the relative changes in GPCho lipid abundances between control and diabetic samples was achieved by normalization of the peak area of each detected GPCho m/z to that of the GPCho(16:0/16:0) lipid present in each of the samples, after correction for ^{13}C isotope contributions.

Tissue fatty acid analysis by RP-HPLC. An aliquot of total lipids from tissues and blood fractions was saponified (0.4 N KOH in 80% methanol, 50°C for 1 h). Saponified fatty acids were acidified and extracted with diethyl ether (according to Wang et al. [52]) and stored in methanol containing 1 mmol/l butylated hydroxytoluene. Saponified free fatty acids were fractionated and quantitated by RP-HPLC using a YMC J-Sphere (ODS-H80) column and a sigmoidal gradient starting at 86.5% acetonitrile + acetic acid (0.1%) and ending at 100% acetonitrile + acetic acid (0.1%) over 50 min with a flow rate of 1.0 ml/min using a Waters 600 controller. Fatty acids were introduced to the HPLC by injection in methanol and detected using ultraviolet absorbance and evaporative light scatter as previously described [52]. Authentic fatty acid standards (Nu-Chek Prep) were used to generate calibration curves for verification and quantification of fatty acids.

Statistical analysis. Data are expressed as the means \pm SD. Student's t test was used for comparing data obtained from independent samples. Significance was established at $P < 0.05$.

Chapter III

Diabetic Retinopathy is Associated with Bone Marrow Neuropathy and a Depressed Peripheral Clock

This chapter is the edited version of a research article that was published in Journal of Experimental Medicine, volume 206, Issue 13 (2897-2906), 2009.

Authors: Tikhonenko, M., Busik, J.V., Bhatwadekar, A., Opreanu, M., Yakubova, N., Caballero, S., Player, D., Nakagawa, T., Afzal, A., Kielczewski, J., Sochacki, A., Hasty, S., Li Calzi, S., Kim, S., Duclas, S. K., Segal, M. S., Guberski, D. L., Esselman, W. J., Boulton, M. E., Grant, M. B.

3.1 Abstract

The present epidemic of diabetes is resulting in a worldwide increase in cardiovascular and microvascular complications including retinopathy. Current thinking has focused on local influences in the retina as being responsible for development of this diabetic complication. However, the contribution of circulating cells in maintenance, repair, and dysfunction of the vasculature is now becoming appreciated. Diabetic individuals have fewer EPCs in their circulation and these cells have diminished migratory potential, which contributes to their decreased reparative capacity. Using a rat model of type 2 diabetes, we show that the decrease in EPC release from diabetic BM is caused by BM neuropathy and that these changes precede the development of DR. In rats that had diabetes for 4 months, we observed a dramatic reduction in the number of nerve terminal endings in the BM. Denervation was accompanied by increased

numbers of EPCs within the BM but decreased numbers in circulation. Furthermore, denervation was accompanied by a loss of circadian release of EPCs and a marked reduction in clock gene expression in the retina and in EPCs themselves. This reduction in the circadian peak of EPC release led to diminished reparative capacity, resulting in the development of acellular retinal capillaries. Thus, for the first time, DR is related to neuropathy of the BM. This novel finding shows that BM denervation represents a new therapeutic target for treatment of diabetic vascular complications.

3.2 Introduction

Endothelial dysfunction is central to the development of diabetic macro- and microvascular complications, and it is these complications that contribute to the major morbidity and mortality for diabetic patients. BM-derived progenitor cells play a critical role in endothelial repair [106, 107]. EPCs arising from the BM circulate in the bloodstream and home to areas of injury to orchestrate vascular repair [106]. Recently, it was determined that the release of all BM-derived cells occurs in a distinct circadian pattern [112]. The SCN in the central nervous system initiates this and other circadian rhythms as well as synchronizing peripheral clocks in organs and tissues. Circadian rhythms occur via autoregulatory transcriptional-translational feedback loops consisting of a defined set of clock genes. Pathological clock gene expression leads to diverse pathophysiological disorders including metabolic syndrome, obesity, premature aging, and abnormal sleep cycle [133]. The physiological relevance of a disturbed circadian rhythm in diabetes is indicated by the observation that myocardial dysfunction, acute coronary syndrome, sudden cardiac death, and ischemic stroke occur with peak

incidence in nondiabetics in the early morning, yet in diabetic patients the peak is at night [173-177]. Interestingly, db/db mice, a model of type 2 diabetes, have disrupted circadian variation of blood pressure, heart rate, and locomotor activity, each associated with dampened oscillations of peripheral clock genes [135].

Mobilization of EPC from the BM occurs after activation of peripheral noradrenergic neurons and release of norepinephrine (NE), which suppresses osteoblast activity [112, 178]. This results in a local decrease in SDF-1 and subsequent EPC mobilization from the BM [179]. Diabetic neuropathy is a common complication of both type 1 and type 2 diabetes [180, 181]. We reasoned that diabetes-associated peripheral and/or autonomic neuropathy would reduce BM innervation and thus reduce hematopoietic stem cell (HSC)/EPC release from the BM. Decrease in circulating EPCs would reduce repair of injured retinal vessels in diabetic animals and lead to development of acellular capillaries, the hallmark feature of irreversible DR.

3.3 Results and Discussion

Bio-Breeding Zucker diabetic rat (BBZDR)/Wor rats after 4 months of diabetes were used and compared with their age-matched nondiabetic BBDR littermates.

To explore the role of the sympathetic nervous system in the release of EPCs in diabetes, we first undertook an analysis of BM histology and determined 24-hour cycles of circulating NE levels. Histological examination of the BM in rats with 4 months of diabetes revealed a marked 50% reduction in the number of nerve endings as determined by neurofilament 200 (NF200) staining and increased BM lipid deposition compared with age-matched controls (Fig. 11, A–F). Tyrosine hydroxylase (TH) staining

showed positive nerve processes running along blood vessels in the BM of controls (Fig. 11, C and C') but was very rarely found in diabetic animals (76% reduction) (Fig. 11, D and D'), demonstrating a defect in sympathetic innervation. As shown in Fig. 11, 4 months of diabetes resulted in the appearance of increased numbers of acellular capillaries within the retina (Fig. 11, J and K) compared with age-matched controls (Fig. 11, I and K). We observed that denervation of the BM preceded the development of this retinal pathology because at 2 months of diabetes, the rats did not have any retinal histopathological changes (Fig. 12 C) but already showed early signs of denervation (Fig. 12, A and B).

In these studies, we characterized the progenitor population based on surface expression of thy-1 and CD133 [182], endothelial nitric oxide synthase expression [110], and the ability of these cells to incorporate into capillary tubes in vitro [183] (Fig. 13). To determine whether denervation of BM affected circadian EPC release in type 2 diabetes, peripheral blood EPCs were enumerated by flow cytometry analysis every 2 hours in diabetic rats and compared with age-matched controls. Control rats showed a dramatic peak of circulating EPCs between ZT-1 and ZT-5 (Fig. 14 A), where ZT-0 is the beginning of the light cycle and ZT-12 is the end of it. In contrast, diabetic animals exhibited a marked reduction in the amplitude and a broader peak in the number of circulating EPCs between ZT-21 and ZT-7. There number of EPC at ZT-3 was more than 2 times lower in diabetic animals compared to control. Moreover, the controls demonstrated a dramatic drop to baseline EPC numbers immediately after the ZT-3 peak. In contrast, diabetic rats lost this abrupt drop. The total number of EPC was significantly lower in the type 2 diabetic animals as compared to control.

To answer a question regarding whether the loss of nerve endings was only specific to type 2 diabetes, we studied the BM of type 1 diabetic rats after 6 weeks of diabetes. TH staining showed positive nerve fibers running along blood vessels in the BM of controls. We observed 37% a significant decrease in the number of nerve fiber in the BM of type 1 diabetic rats as compared to age-matched controls (Fig.15), demonstrating a defect in sympathetic innervation. This observation strongly suggests that BM neuropathy is a common complication of both types of diabetes. Although various peripheral sensorimotor and autonomic neuropathies have been extensively described [180, 181], we were first to demonstrate neuropathy of the BM in diabetes.

To determine if the loss of nerve fibers in the BM affected circadian EPC release in diabetes, we looked at circadian pattern of EPC levels in type 1 diabetes model. Peripheral blood EPCs were enumerated by flow cytometry analysis for samples collected every 2 hours in type 1 diabetic rats and compared with age-matched controls. The total number of EPCs in blood was consistently lower in type 1 diabetic animals compared with control animals. Type 1 diabetic animals exhibited a significant reduction in the peak at ZT-3 as compared to controls (Fig. 16). However, in both control and diabetes, the peak of EPC occurred at the same time at ZT-3. This data suggests that in diabetes, the phase of the circadian rhythm does not shift, but the quantity of the response is lower.

We interpreted the persistent elevation of EPCs until ZT-7 in type 2 diabetes animals as reduced release and also diminished clearance of these cells from the blood. This reduced clearance was likely the result of a diminished ability of EPCs to

migrate into tissues from the circulation and is in keeping with the profound migratory defect of these cells observed in diabetes [137] (Fig. 17).

To further explore this possibility, we generated chimeric mice that underwent transplantation with BM HSCs from *gfp* homozygous transgenic mice and then were stably engrafted for 4 months. Retinal flat mounts were prepared from animals euthanized at either ZT-5 (peak of rest phase in mice) or ZT-13 (trough of EPC release in circulation). In agreement with *thy-1* enumeration data in healthy rats (Fig. 14 A), many more *gfp*⁺ cells were present in the retinal circulation at the peak release for mice, ZT-5, as compared with ZT-13 (Fig. 14, B–D).

We thus postulated that in diabetes, the EPCs were trapped within the diabetic BM as a result of a lack of sympathetic innervation and reduced NE release. To test this, we examined the BM in the same rats that underwent 24-h blood sampling for EPC enumeration. These diabetic rats with decreased peripheral blood EPCs showed a marked elevation in the number of BM EPCs compared with controls (Fig. 17 A). In addition, diabetic BM EPCs showed a reduction in colony formation ability (Fig. 17, B–D) and proliferation (Fig. 17 F). Both blood and BM EPCs had a reduced migration to VEGF (Fig. 17 E) compared with age-matched controls.

We reasoned that circulating NE levels in these diabetic animals with peripheral neuropathy and retinopathy may be altered and therefore measured NE levels in the blood of these rats. Control rats had two distinct peaks of plasma NE levels, one at ZT-1 and one at ZT-13 (Fig. 18 A). Interestingly, in diabetic animals, the first NE peak at ZT-1 was considerably higher and broader than in controls, showing a compensatory adrenal

response, whereas the second peak at ZT-13 was absent, supporting the concept of sympathetic dysfunction in these rats.

These experiments demonstrate that type 2 diabetes is associated with a reduction in circadian release of EPCs from the BM. Because circadian rhythm is under tight control of not only the central clock, the SCN, but also peripheral clocks, we next examined whether clock gene expression in the SCN, retina, BM, and peripheral blood EPCs was altered in diabetes. At peak release of EPCs, animals were sacrificed and their SCN brain regions, retinas, BM, and peripheral blood harvested for messenger RNA (mRNA) extraction. Clock genes (*Clock*, *Bmal1*, *Per-1*, *Per-2*, *CRY-1*, *CRY-2*, *ERB*, and *RORA*) were quantified by real-time PCR in these tissues and cells. Rats with diabetes demonstrated a significant decrease ($P < 0.05$) in expression of these clock genes in the retina and in *thy-1*⁺ cells isolated from both blood and BM (Fig. 19, A–C). Protein studies revealed reduction in Bmal expression in diabetic rats as compared with controls (Fig. 19 E). This dramatic reduction in both the positive and negative arms of circadian gene regulators would lead to dampened oscillations and lower and broader peaks, which is the pattern we observed in the circulating EPCs in diabetic rats compared with age-matched controls. Healthy rats, in contrast, demonstrated a higher narrower peak than the diabetic rats. Although expression of clock genes was reduced in the SCN regions of diabetic rats, the difference from controls was not significant (Fig. 19 D). This lack of change suggests that diabetes is associated with dysfunction of the peripheral rather than the central clock. The mRNA and protein expression of clock genes in control and diabetic human retina (Fig. 20) is in agreement with the alterations of clock gene expression found in the diabetic rat model.

The potential to form new blood vessels and repair damaged vessels depends on the EPCs' ability to both leave the BM and to migrate toward the site of angiogenesis. In this study, we observed that type 2 diabetic rats demonstrate the hallmark feature of DR, acellular capillaries within the retina, at the precise time when there is denervation of the BM and a reduction in peripheral clock gene expression. We confirmed here that normal, but not diabetic, EPC participate in ocular vascular reendothelialization in diabetic mice (Fig. 21).

The resultant acellular capillaries seen at 4 months of diabetes appear to be caused, in part, by the loss of proper EPC reparative function and by failure of circadian EPC release secondary to diabetes-associated denervation of the BM (Fig. 22). In the presence of innervation, as observed in control rats, there was normal retinal histology and a robust circadian release of EPC from the BM. We report that by 4 months of diabetes in our model of type 2 diabetes, there is inherent sympathetic denervation that can alter circadian release of EPC from the BM. Our data supports that the loss of circadian EPC release results in inadequate levels of cells in the circulation at the optimal time of repair (rest phase) and that this defect, in addition to defects of EPC function (reduced proliferation and migration), contributes to the development of DR.

Circadian dysfunction itself can have profound effects on the diabetic state. Prior work has shown that mice with a specific clock gene mutation demonstrate impaired endothelial function, including decreased tube formation and faster senescence and impaired EPC-mediated repair [184]. Other clock genes have been shown to directly regulate glucose homeostasis, and their inactivation suppresses diurnal variation in glucose and triglycerides along with reduced gluconeogenesis [134].

Our novel findings would indicate that restoration of sympathetic innervation to the diabetic BM should result in physiological EPC egress from the BM and improved retinal vascular repair [177]. Moreover, strategies to normalize peripheral clock gene expression may be a novel way to both treat and prevent the development of diabetic macro- and microvascular complications by circumventing sympathetic nervous system dysfunction.

Figure 11: Dramatic decrease in humerus bone marrow innervation in diabetic rats is associated with an increase in retinal acellular capillaries.

(A and B) NF200-positive nerve processes (arrowheads) are visible in bone marrow of control rats (A and A') but significantly decreased in diabetic rats (B and B').

(C and D) TH-positive nerve processes running along blood vessels (arrows) were present in the bone marrow of controls (C and C') but very rare in diabetic animals (D and D').

(E and G) No staining was found in negative controls treated only with secondary antibody. Bars: (A–D) 20 μ M; (A'–D', E, and G) 5 μ M.

(F and H) Quantification of the NF200 and TH data are shown in F and H, respectively. Diaphysis of the humerus bone from control (n = 4) and diabetic (n = 3) animals were assessed. At least 10 fields per humerus were analysed on duplicate slides from each bone by three independent individuals. The experiment was repeated on two independent sets of animals.

* = P < 0.05.

(I and J) Retinal vasculature from control (I) and diabetic (J) animals was prepared using trypsin digestion and stained with hematoxylin and periodic acid–Schiff. Dramatically increased number of acellular capillaries (black arrows) was observed in retinal vasculature isolated from diabetic animals (I) compared with control (J). (K) Quantification of I and J.

Bars, 10 μ M. The data represent mean \pm SD of three independent sets of animals, with nine control and nine diabetic animals total. At least eight fields per retina were counted in duplicates by two independent investigators. *** = P < 0.001.

Figure 11 (cont'd)

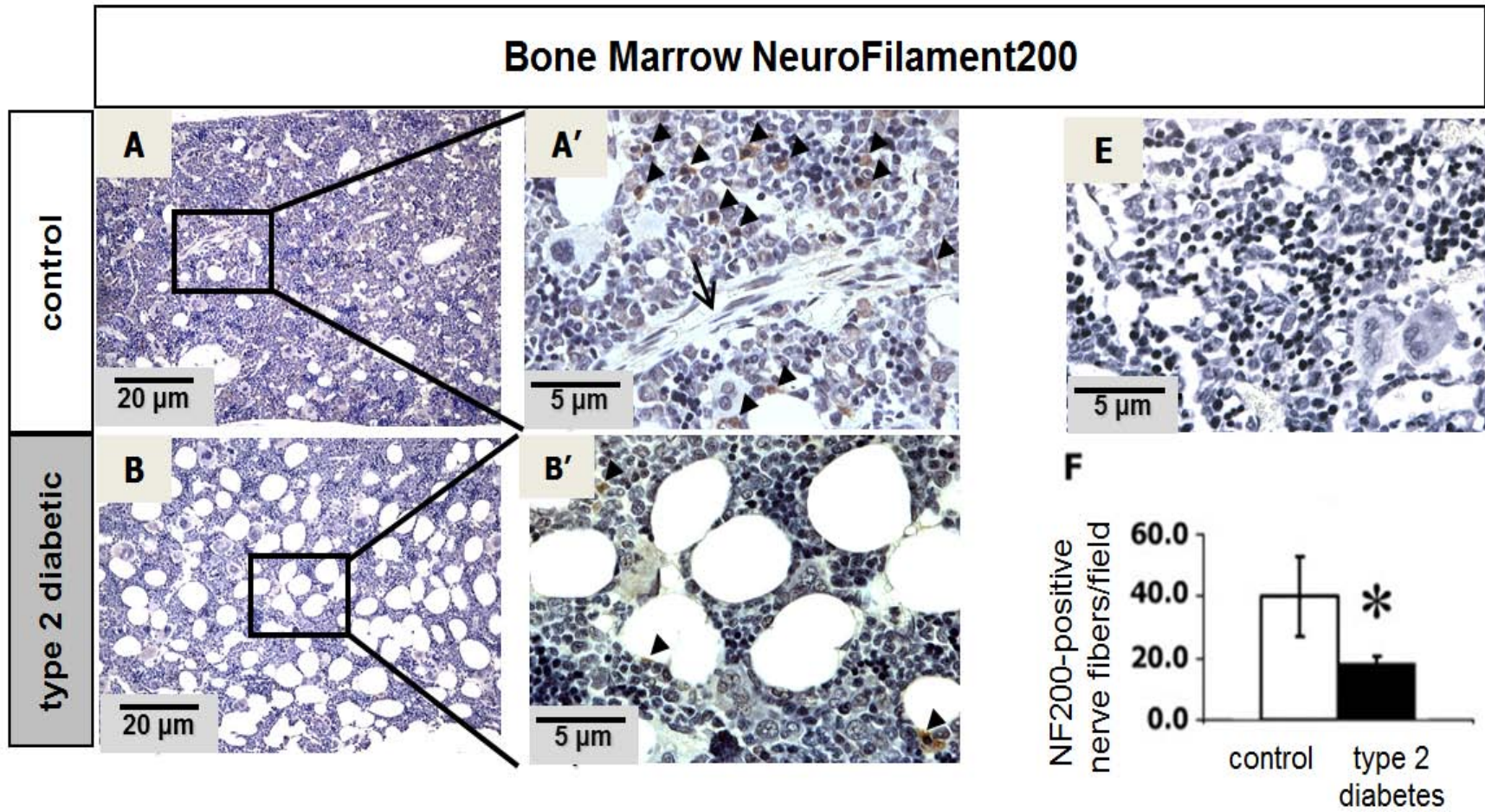


Figure 11 (cont'd)

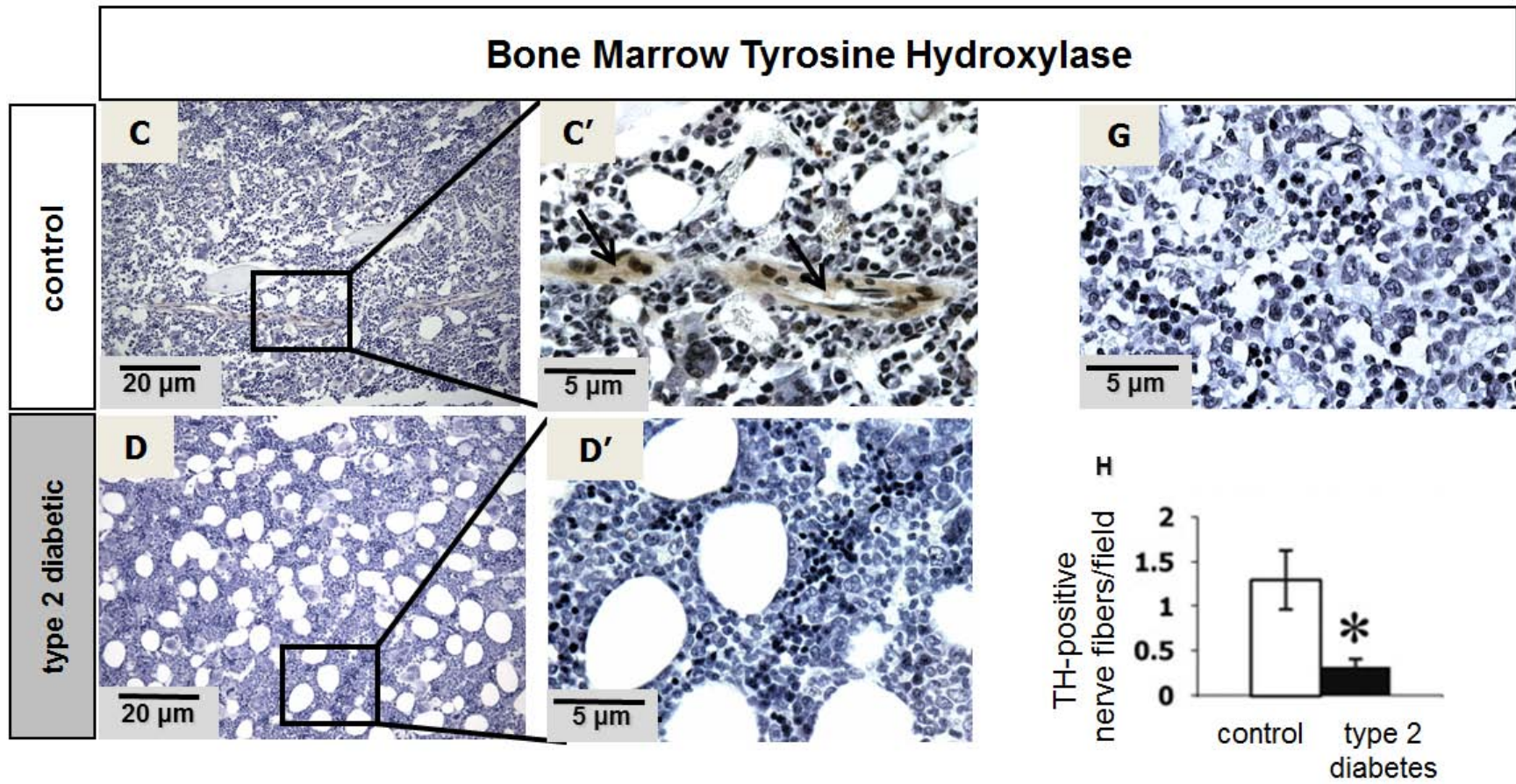


Figure 11 (cont'd)

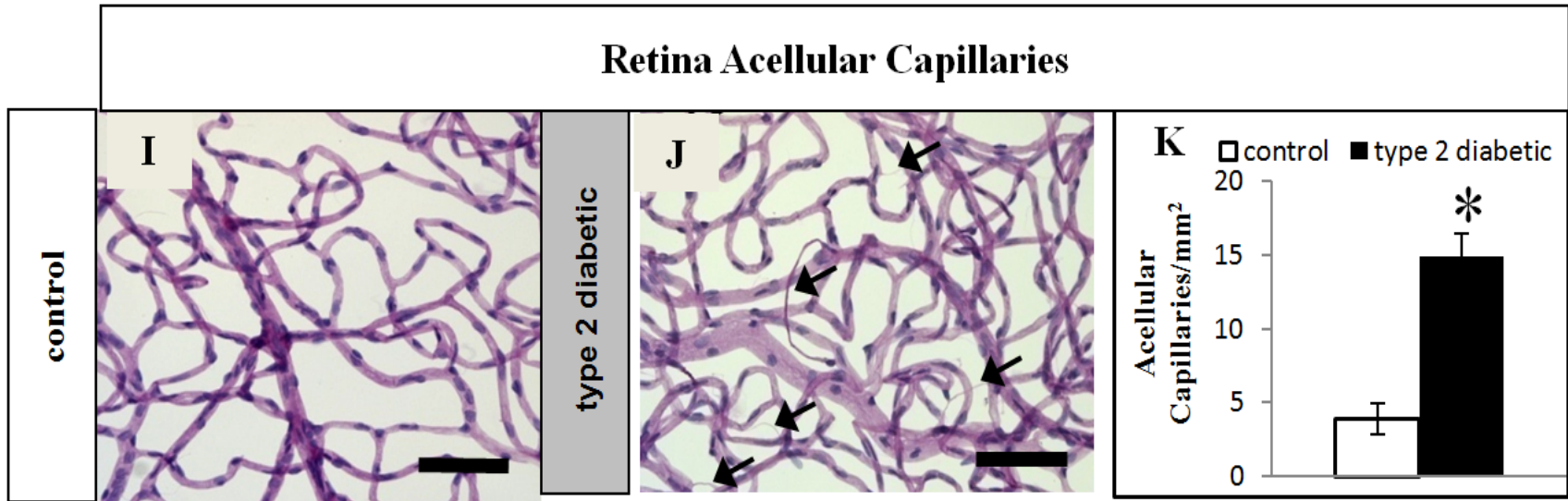


Figure 12: Denervation of the bone marrow precedes acellular capillaries formation in diabetic rats after 2 months of diabetes.

(A and B) TH-positive nerve processes running along blood vessel (arrow) were present in diabetic bone marrow at 2 months of diabetes (A and A') but were significantly decreased compared with controls (B). At least 10 fields were analysed on duplicate slides from each bone by three independent individuals. Bars: (A) 20 μm ; (A') 5 μm . *, $P < 0.05$. The experiment was repeated on two independent sets of animals. Data are presented as the mean \pm SD of four control and three diabetic (A and B) rats.

(C) On the contrary, the number of acellular capillaries was not changed. Data in C are presented as the mean of two independent sets of animals, with six control and six diabetic rats total. At least eight fields per retina were counted in duplicates by two independent investigators. *, $P < 0.05$.

Figure 12 (cont'd)

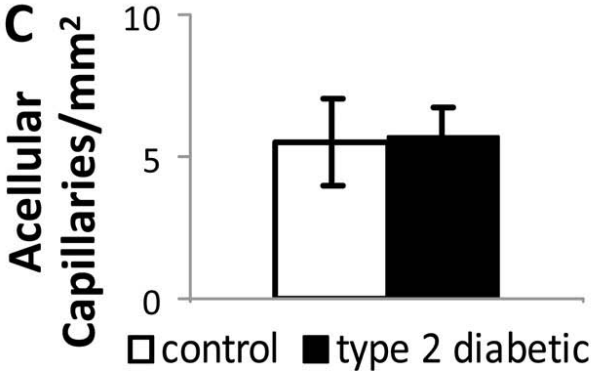
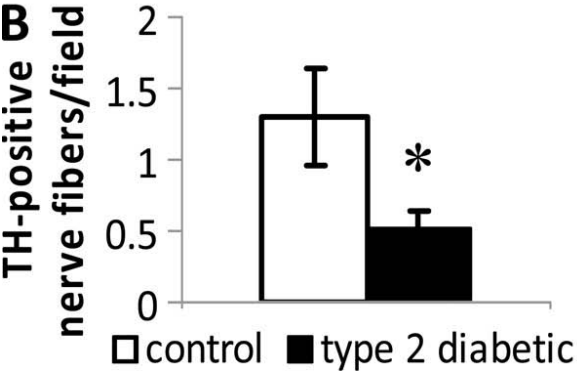
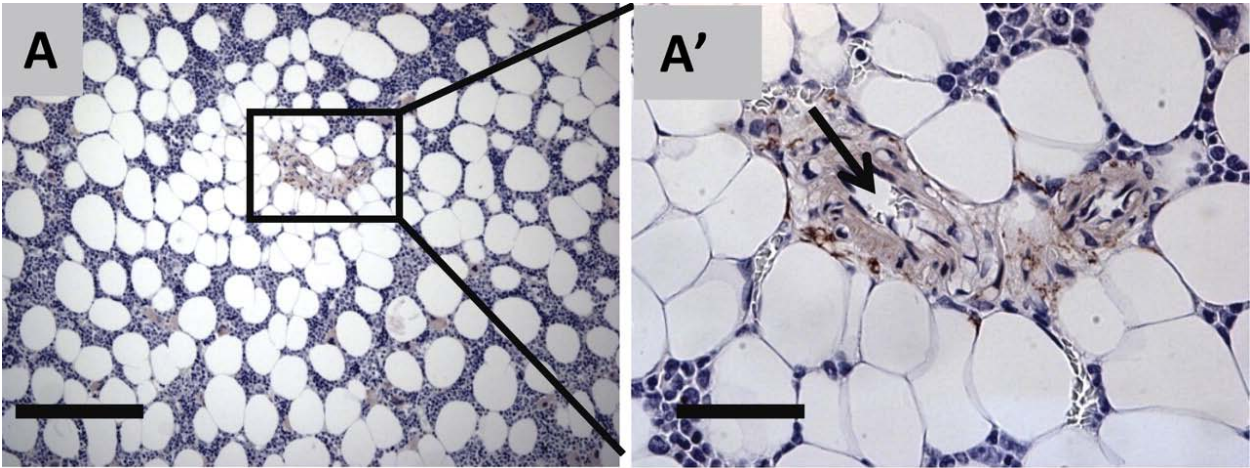


Figure 13: Rat thy-1+ cell characterization. Thy-1+ cells isolated from rat bone marrow were analysed by FACS for progenitor marker expression.

(A–C) Isolated cells express CD133 (A), Thy-1 (B), and VEGFR-2 (C). The red line represents the samples incubated with respective antibody. The black line in the representative histogram plot corresponds to the samples incubated with the appropriate isotope control antibodies.

(D) Thy-1+ progenitors express endothelial nitric oxide synthase (green) as detected by immunofluorescence with nuclei stained with DAPI (blue). Bar, 10 μ M.

(E and F) Cells in culture form colonies (E) and incorporate Dil-acLDL (red; F). Thy-1+ cells incorporate into capillary tubes with human retinal endothelial cells.

(G) Fluorescently labelled Thy-1 cells (red) incorporating into HRECs. (H) Phase contrast image of same region as in G.

(I) Merged phase contrast and fluorescence images of Thy-1+ cells (red) participating in tube formation. Bar, 100 μ M. Flow cytometry data are represented as percentage of cells expressing respective marker for rats (n = 3).

Images are representative of n = 4 of individual experiments.

Figure 13 (cont'd)

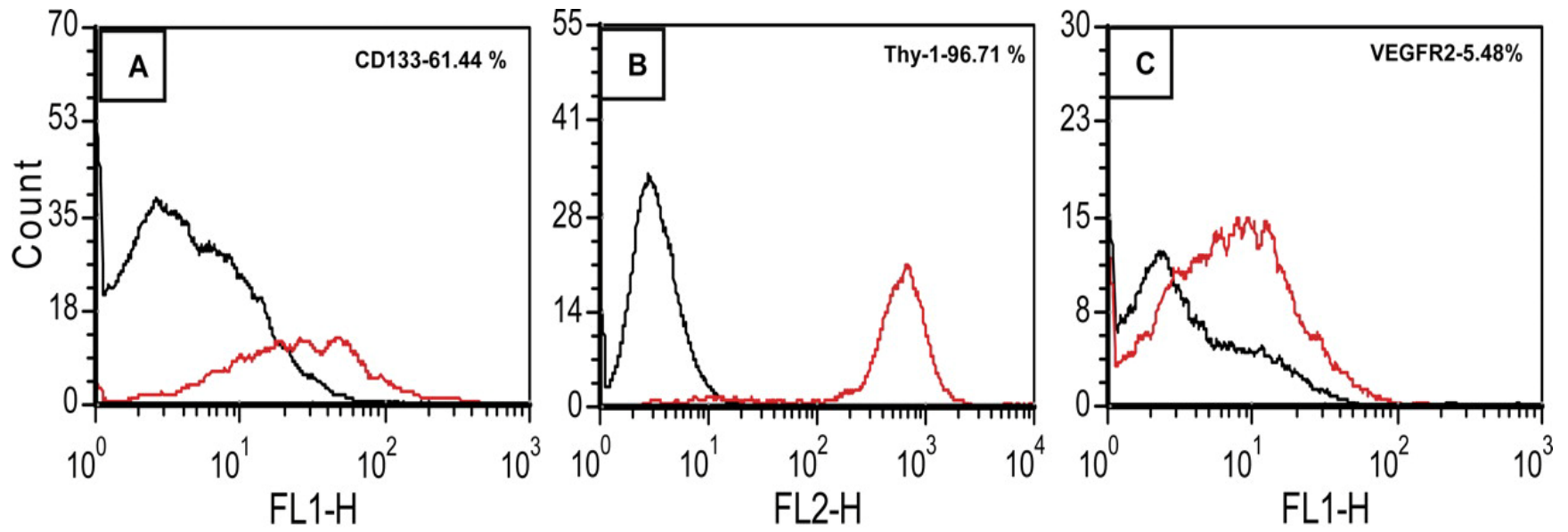


Figure 13 (cont'd)

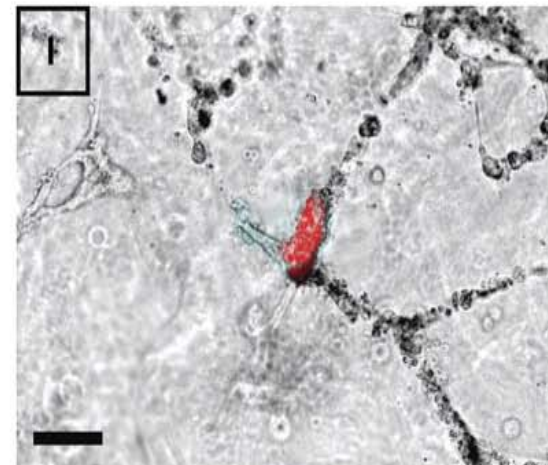
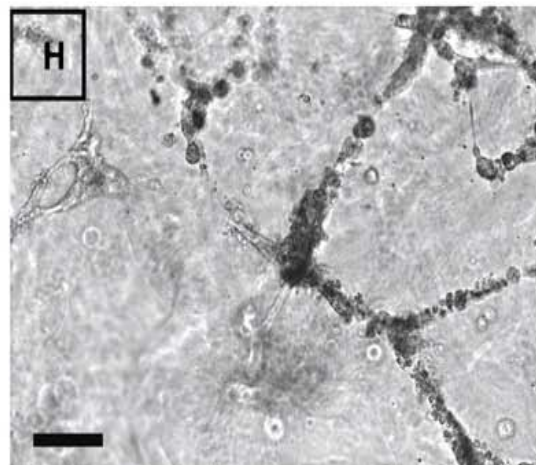
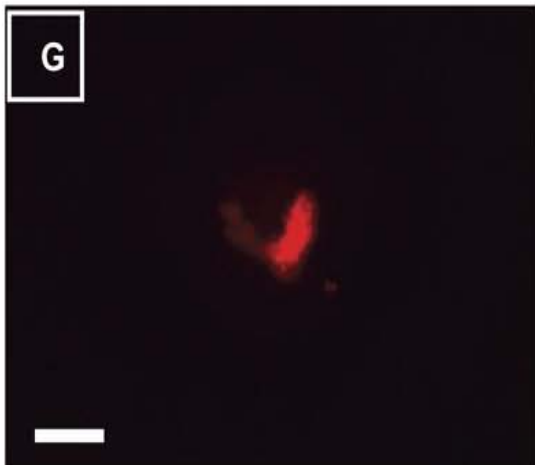
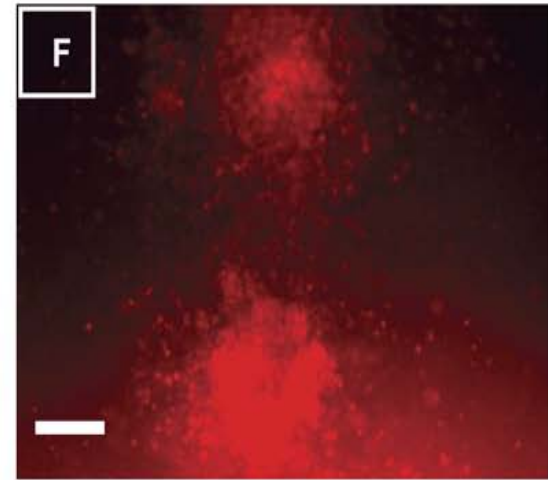
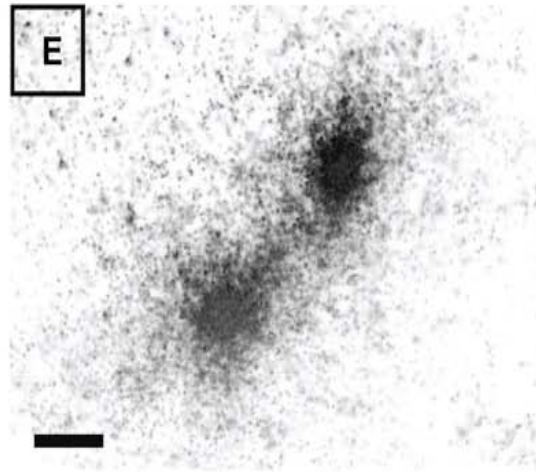
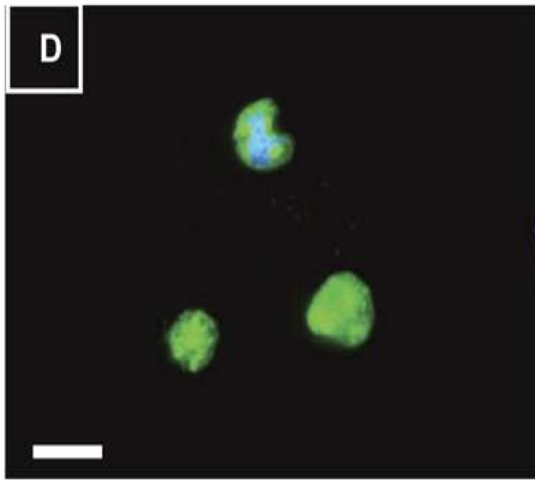


Figure 14: Diabetes decreases circadian release of EPCs. (A) Control (n = 4) and diabetic (n = 3) rats were maintained on a 12/12 h light/dark cycle (lights on at ZT-0, lights off at ZT-12). 100 μ l of blood was taken every 2 h and analyzed for the number of EPCs by flow cytometry. EPCs were determined as number of thy-1+CD3-CD4-CD8- cells per μ l of blood. There is a clear peak in the EPC number at ZT-3 in control animals (red line). However, the response is blunted in Type 2 (blue line) diabetic animals. The number of EPCs in blood was consistently lower in type 2 diabetic animals compared with control animals. The data represent the mean \pm SD. The experiment was performed on two independent sets of animals, with 12 repetitions per animal. Statistical analysis was performed using two-way analysis of variance (ANOVA) for diabetes and time effect (***, P < 0.0001) and Bonferroni post-test to compare replicates by row (*, P < 0.05; ***, P < 0.001).

(B) Circadian variation in the number of bone marrow-derived cells in the retinal circulation of mice. Retinal flat mounts from gfp+ chimeric control mice show increased numbers of bone marrow-derived circulating cells (green) in the retinal capillaries at ZT-5 (B and B') as compared with ZT-13 (C and C'). 10 fields per retina were evaluated and both retinas per mouse were analysed. Magnification is 4 \times in B and C and 20 \times in B' and C'. Bars: (B and C) 100 μ m; (B' and C') 10 μ m.

(D) Quantification of gfp+ cells shows an increase in green fluorescence in retinal capillaries at ZT-5 as compared with ZT-13 (n = 4; ***, P < 0.001). The data represents mean \pm SE. The experiment was performed on three independent sets of animals, with the total number of mice per time point equal to nine.

Figure 14 (cont'd)

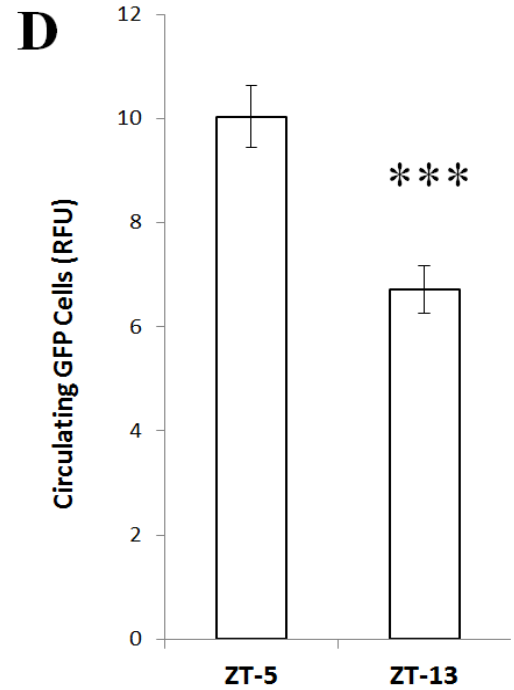
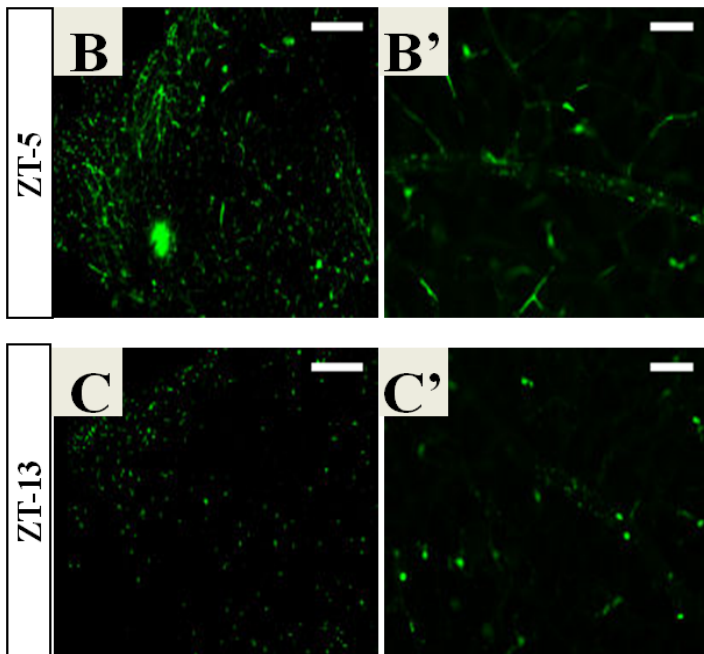
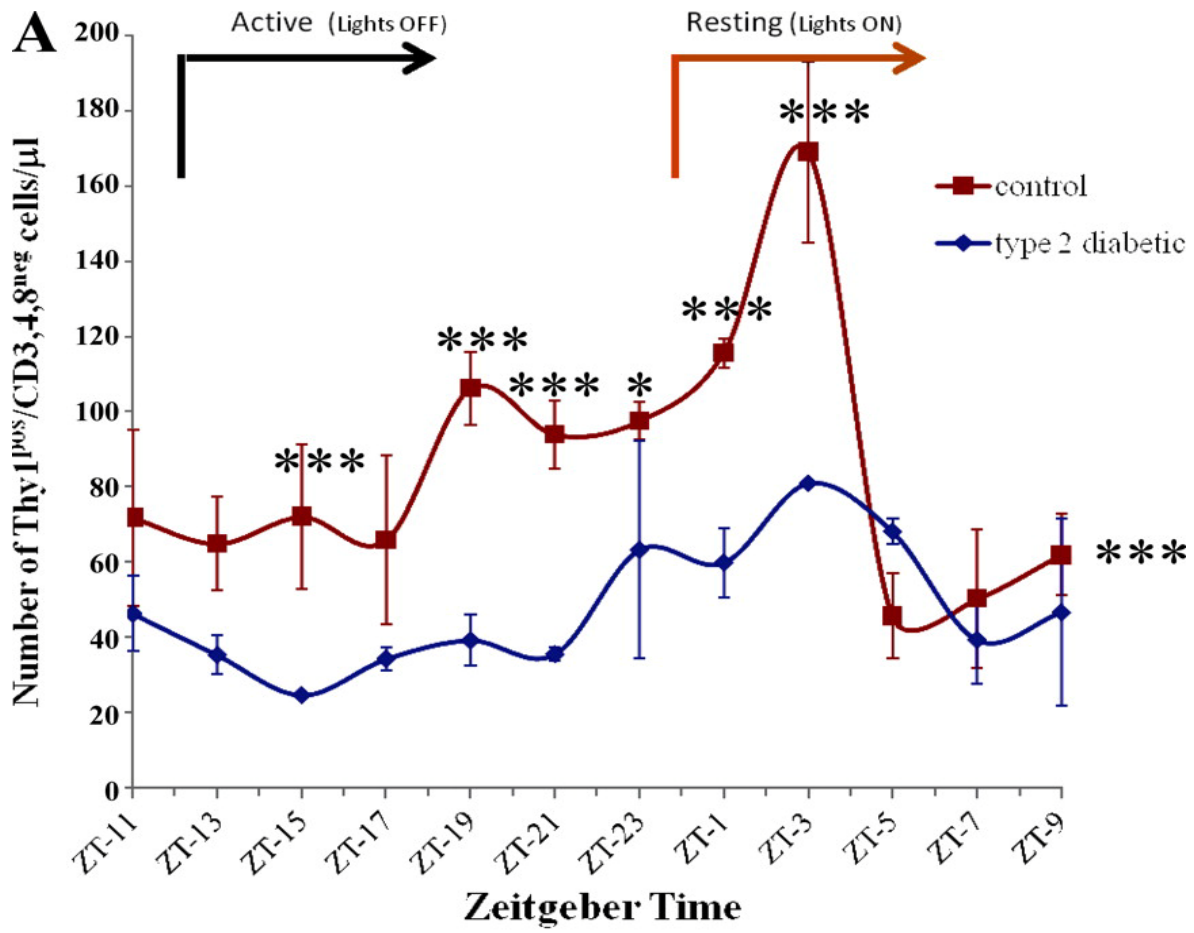


Figure 15: Significant decrease in humerus bone marrow innervation in type 1 diabetic rats. STZ-induced type 1 diabetic rats were used. Tyrosine hydroxylase-positive nerve processes running along blood vessels were present in the bone marrow of controls (A and A') but were rare in diabetic animals (B and B').

(C) Quantification of the data. Diaphysis of the femoral bone from control (n = 17) and diabetic (n = 18) animals were assessed. At least 10 fields per humerus were analysed on duplicate slides from each bone by three independent individuals.

* = $P < 0.05$. The experiment was repeated on two independent sets of animals.

Figure 15 (cont'd)

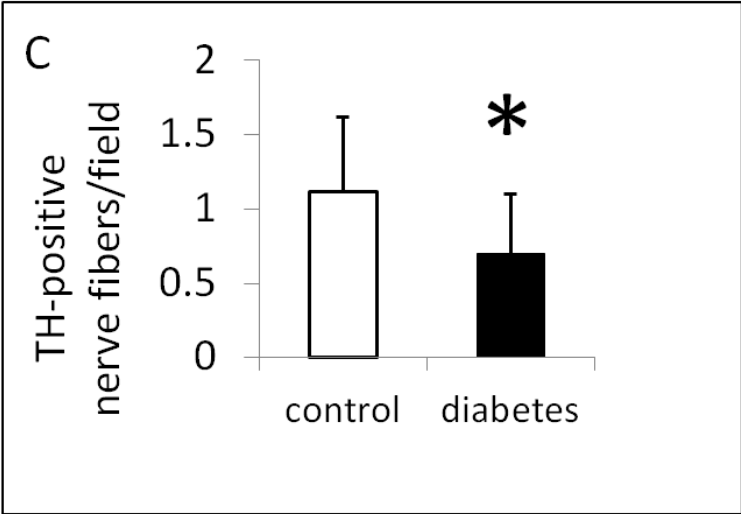
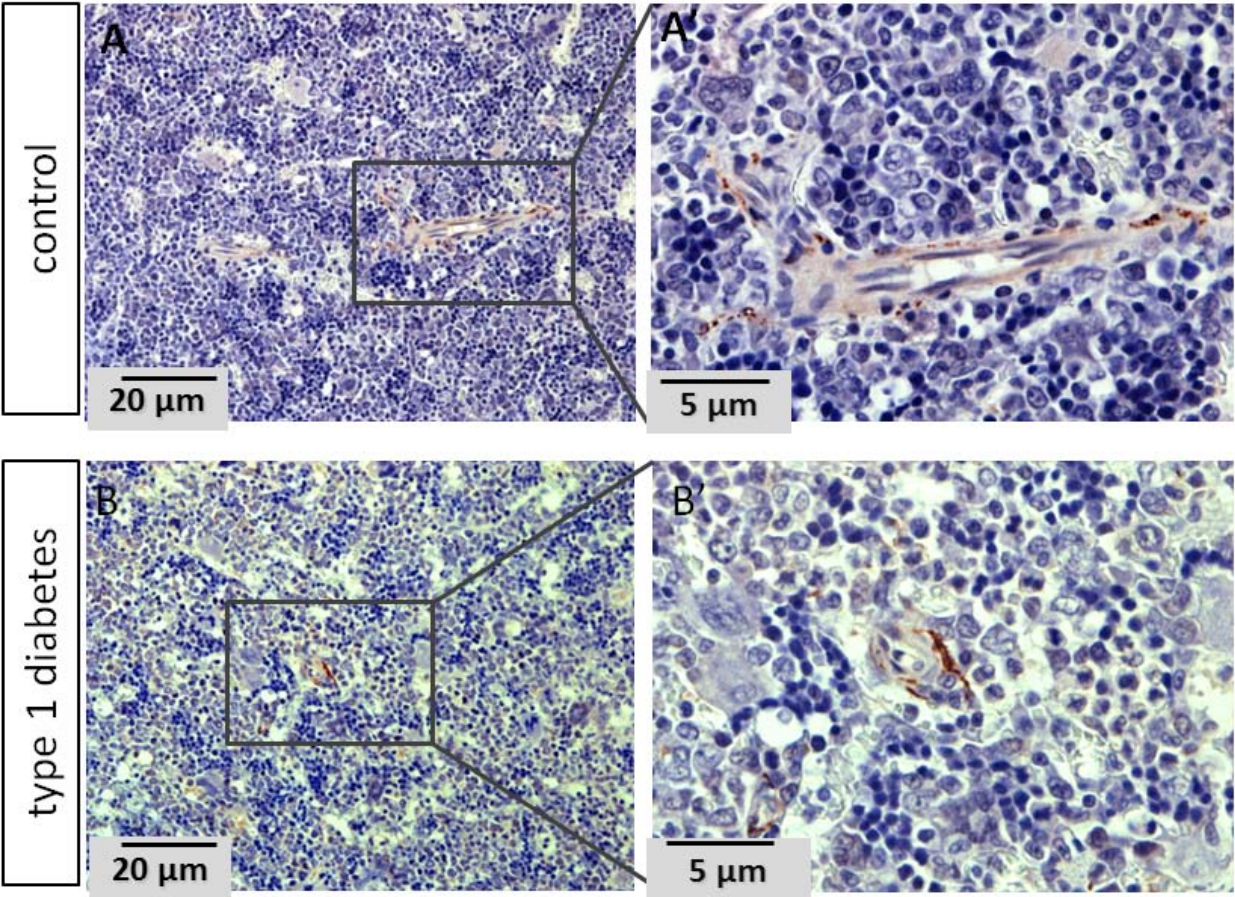


Figure 16: Type 1 diabetes reduced circadian release of EPC in the BBDP/Wor rat. Control (n = 4) and diabetic (n = 3) rats were maintained on a 12/12 h light/dark cycle (lights on at ZT-0, lights off at ZT-12). 100 μ l of blood was taken every 2 hours and analysed for the number of EPCs by flow cytometry. EPCs were determined as number of thy-1+ CD3+ CD4+ CD8+ cells per microliter of blood. The number of EPCs was normalized to the baseline (ZT-5) for both groups. There is a clear peak in the EPCs number at ZT-3 in control animals (red). However, the response is blunted in type 1 diabetic animals (green). The number of EPCs in blood was consistently lower in type 1 diabetic animals compared with control animals.

* =P < 0.05,

** = P < 0.01.

Figure 16 (cont'd)

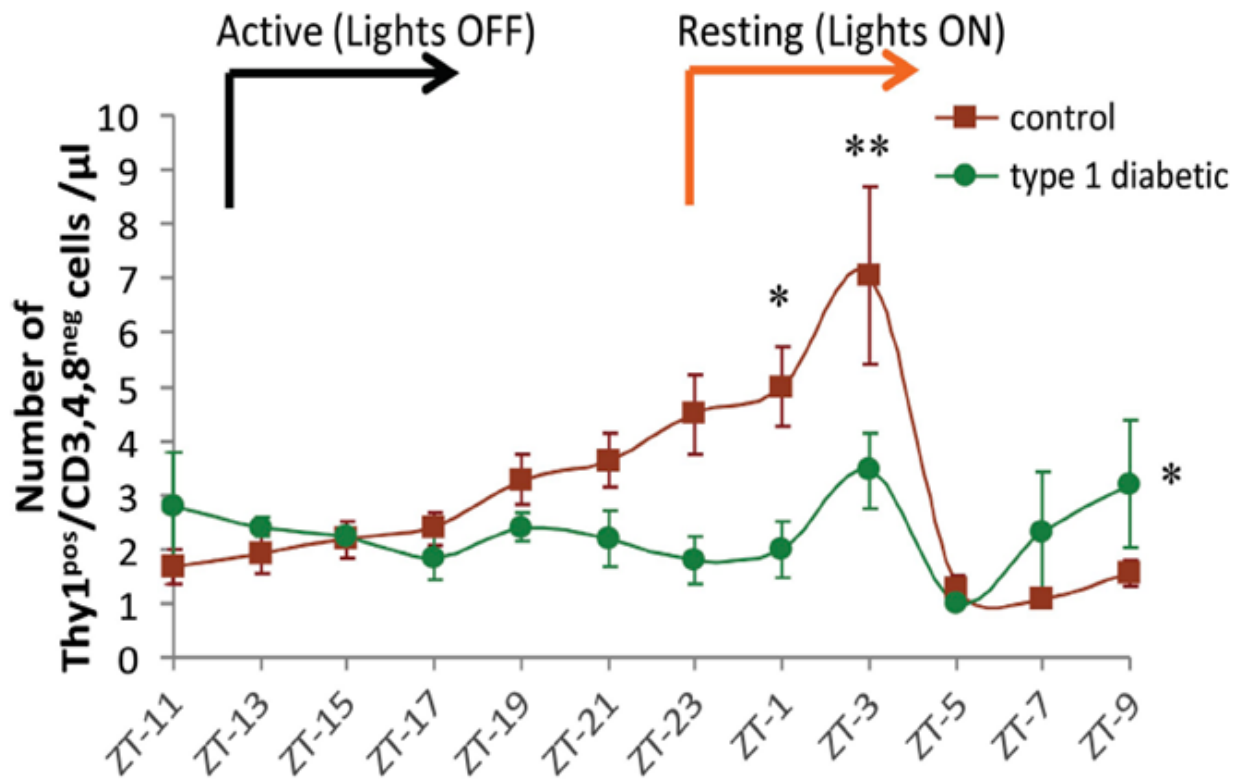


Figure 17: Characterization of thy-1+ EPC number and function in type 2 diabetic rats.

(A) Diabetic rats (n = 3; black) with decreased peripheral blood EPCs showed a marked increase in the number of bone marrow EPCs compared with controls (n = 6; white).

(B) Diabetic bone marrow (black) showed a reduction in CFU compared with healthy controls (white). (C and D) Typical colony formation observed from explanted control (C) and diabetic EPCs (D). Bars, 100 μ M.

(E) Both blood and bone marrow EPCs of diabetic origin (black) demonstrate reduced migration to VEGF compared with control (white).

(F) Diabetic bone marrow EPCs (black) show reduced proliferation compared with control cells (white). The data represent the mean \pm SE of minimum of four separate experiments. *, P < 0.05.

Figure 17 (cont'd)

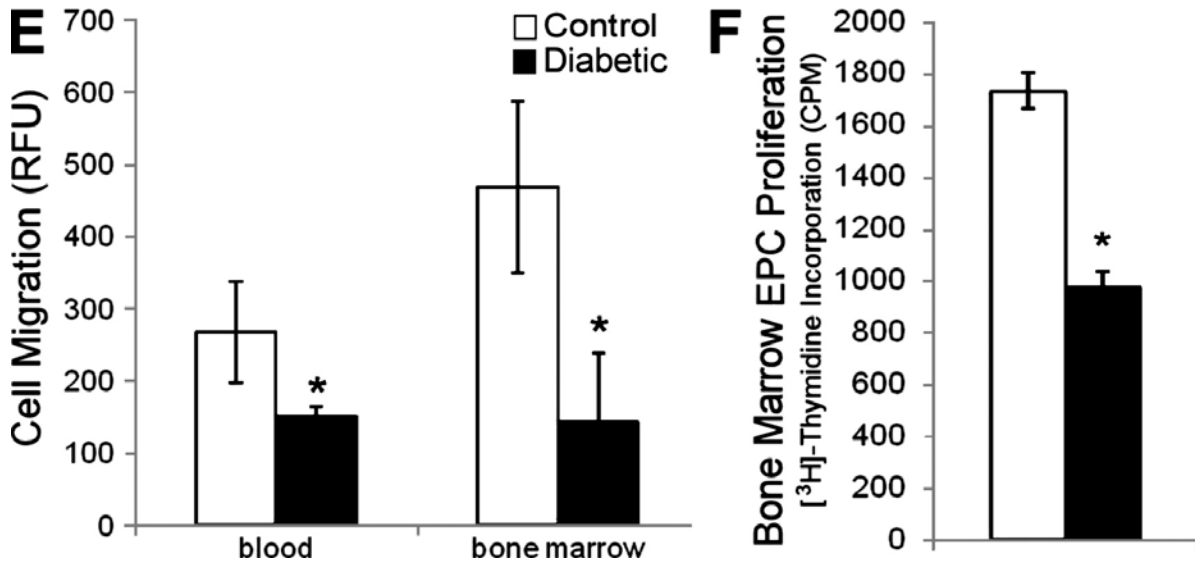
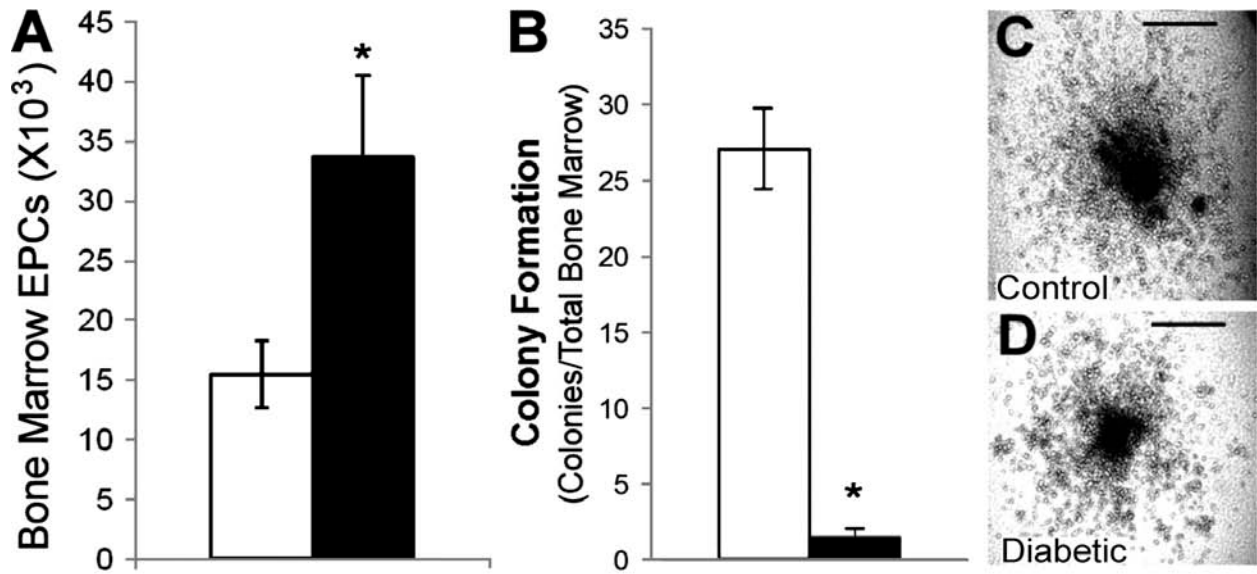


Figure 18: Increased plasma levels of NE in a type 2 diabetes model and decreased number of circulating CD3-positive cells in a type 2 model as compared with controls.

(A) Plasma NE levels in diabetic rats. Blood was analysed for plasma NE level by competitive ELISA kit. Control rats (red) demonstrate two distinct peaks at the beginning of the active and resting phases. In type 2 diabetic rats (blue) there is complete loss of the active phase peak and there is a dramatic increase in the amplitude and widening of the resting phase peak (red).

(B) Diabetes decreased circadian release of CD3+ cells. The blood was analysed for the number of CD3+ per microliter of blood by flow cytometry. There is a clear peak in the CD3+ cells number at ZT-3 in control animals (red). However, the response is blunted in Type 2 (blue) diabetic animals. The number of CD3+ in blood was consistently lower in type 2 diabetic animals compared with control animals.

Data are presented the mean \pm SD of four control and three diabetic rats. Statistical analysis was performed using two-way ANOVA for diabetes and time effect and Bonferroni post-test to compare replicates by row. *, $P < 0.05$; **, $P < 0.01$; ***, $P < 0.001$.

Figure 18 (cont'd)

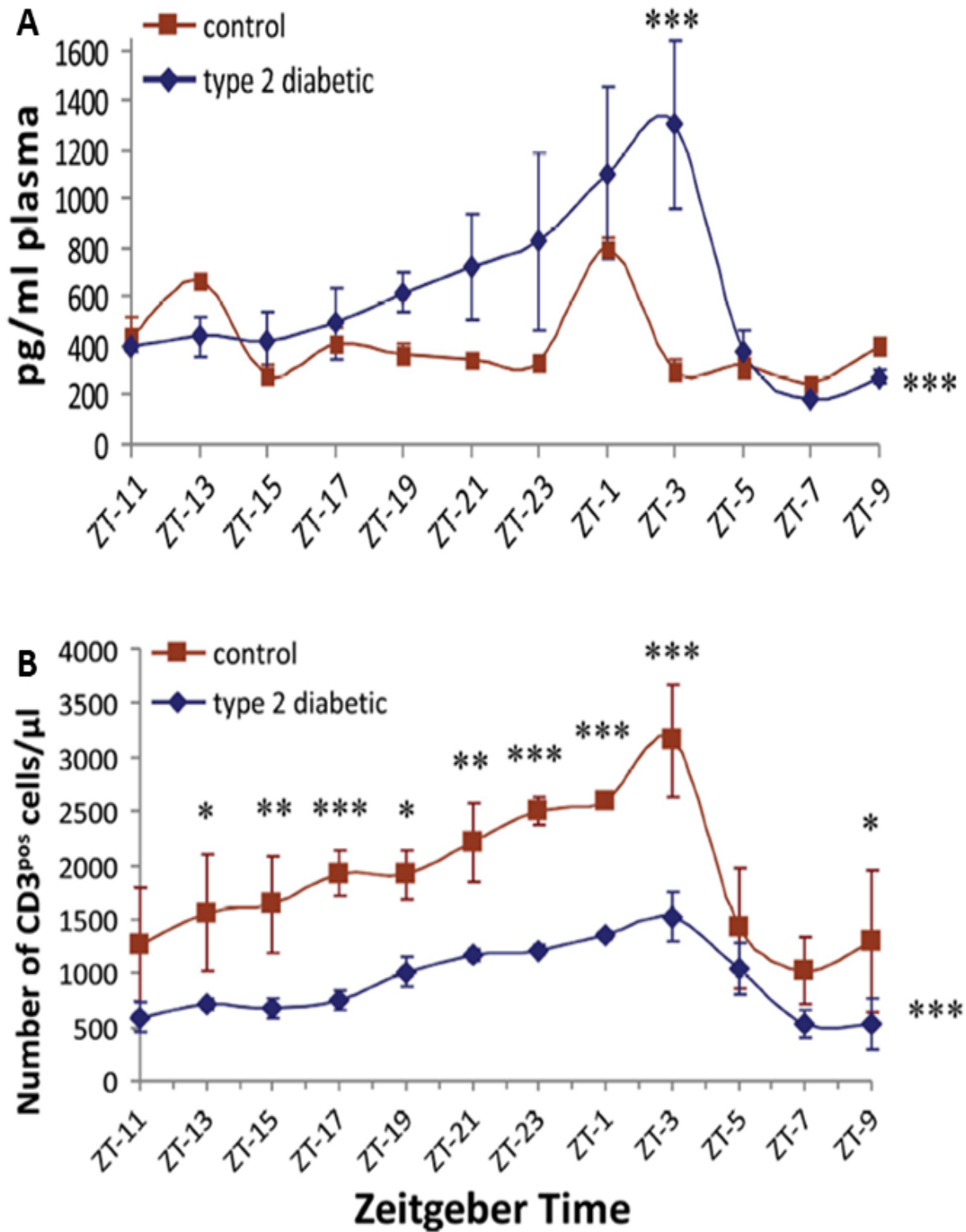


Figure 19: Clock gene expression analysis. Rats used in the circadian rhythm study were sacrificed during the peak time of EPC release, ZT1–5, 24 h after blood collection. (A–D) RNA extracted from total retina (A), peripheral blood thy-1+ (B), bone marrow thy-1+ populations (C) and SCN (D) were analysed for the clock genes Clock, Bmal1, Per1, Per2, CRY1, CRY2, ERB, and RORA. Clock genes demonstrate reduced expression in the diabetic retinas and thy-1+ cells. In the bone marrow fraction, Bmal1 and Per2 were significantly reduced in diabetic animals. Although changes in SCN were not significant, means for all clock genes were lower in diabetes. The mRNA expression levels were normalized to cyclophilin and expressed as fold change over control animals.

(E) Western blotting from the retina demonstrated reduction of BMAL in diabetes. The quantitative PCR data are presented as the mean \pm SE and the Western blotting represents a mean \pm SD of four control and three diabetic animals. The experiment was performed on two independent sets of animals with triplicate measurements for quantitative PCR and duplicate Western blots. *, $P < 0.05$ compared with control.

Figure 19 (cont'd)

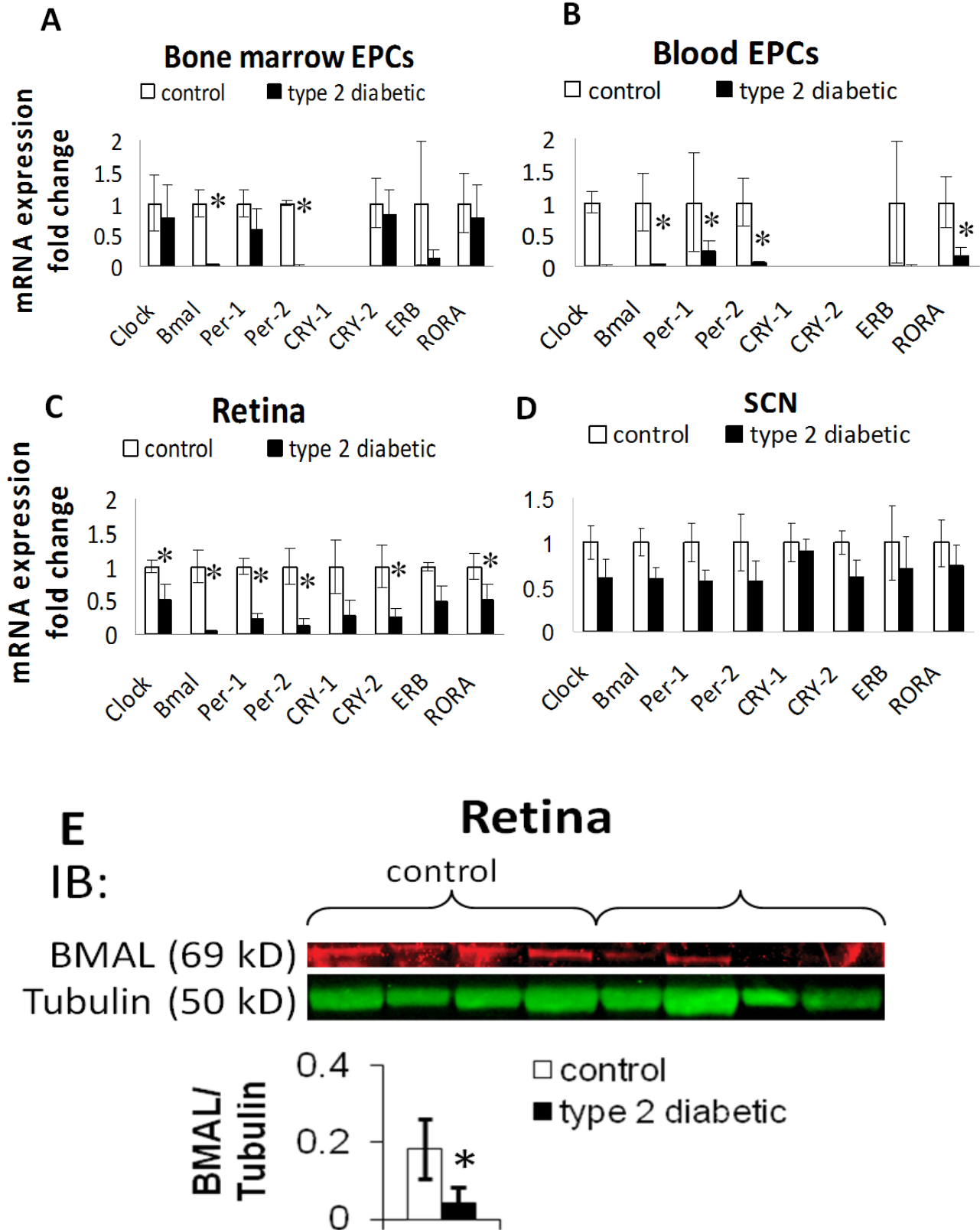


Figure 20: Quantitative PCR and Western blot analysis for clock genes in human retina. Retinas were isolated 24 h postmortem, flash frozen, and stored at -80°C until use.

(A) The RNA extracted was analyzed for the clock genes *Clock*, *Bmal1*, *Per1*, *Per2*, *CRY1*, *CRY2*, *ERB*, and *RORA*. Clock genes demonstrate altered expression in the diabetic retinas. The mRNA expression levels were normalized to cyclophilin and expressed as fold change over controls.

(B and C) Western blot analysis from the retina demonstrated down-regulation of Clock in diabetes. Quantitative PCR data are presented as mean \pm SD of eight control and eight diabetic patients. Western blot data represents the mean \pm SD of four control and four diabetic patients.

*, $P < 0.05$; **, $P < 0.01$ compared with control.

Figure 20 (cont'd)

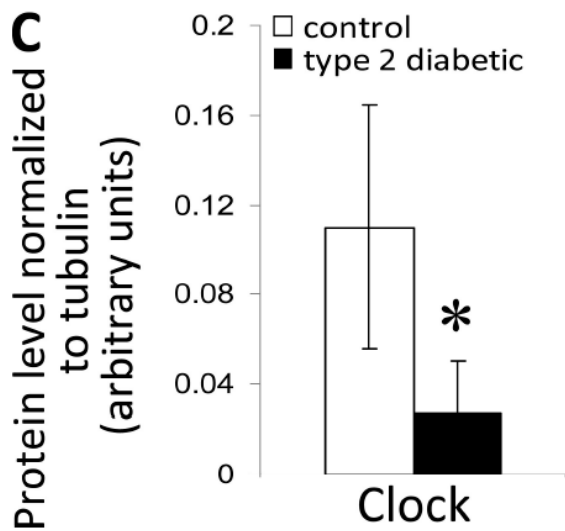
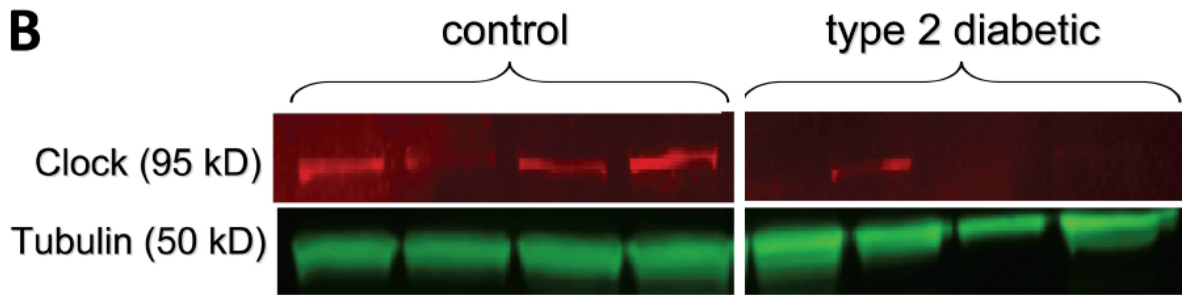
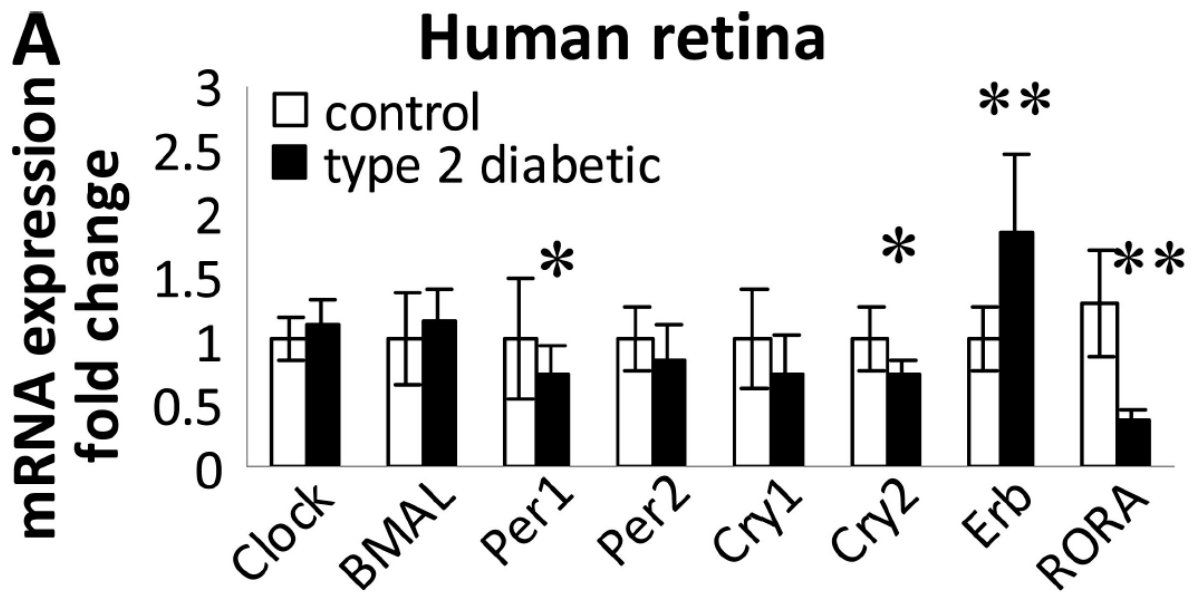


Figure 21: Normal, but not diabetic, human EPCs, may participate in ocular vascular reendothelialization in diabetic mice.

(A) Typical retina (inset, red) from a diabetic mouse that received diabetic human EPC. Note that the human EPCs form clumps (inset, green) and do not associate with the vessels. (B) Widespread incorporation of normal human EPC s into areas of damaged vasculature of this STZ diabetic mouse.

Figure 21 (cont'd)

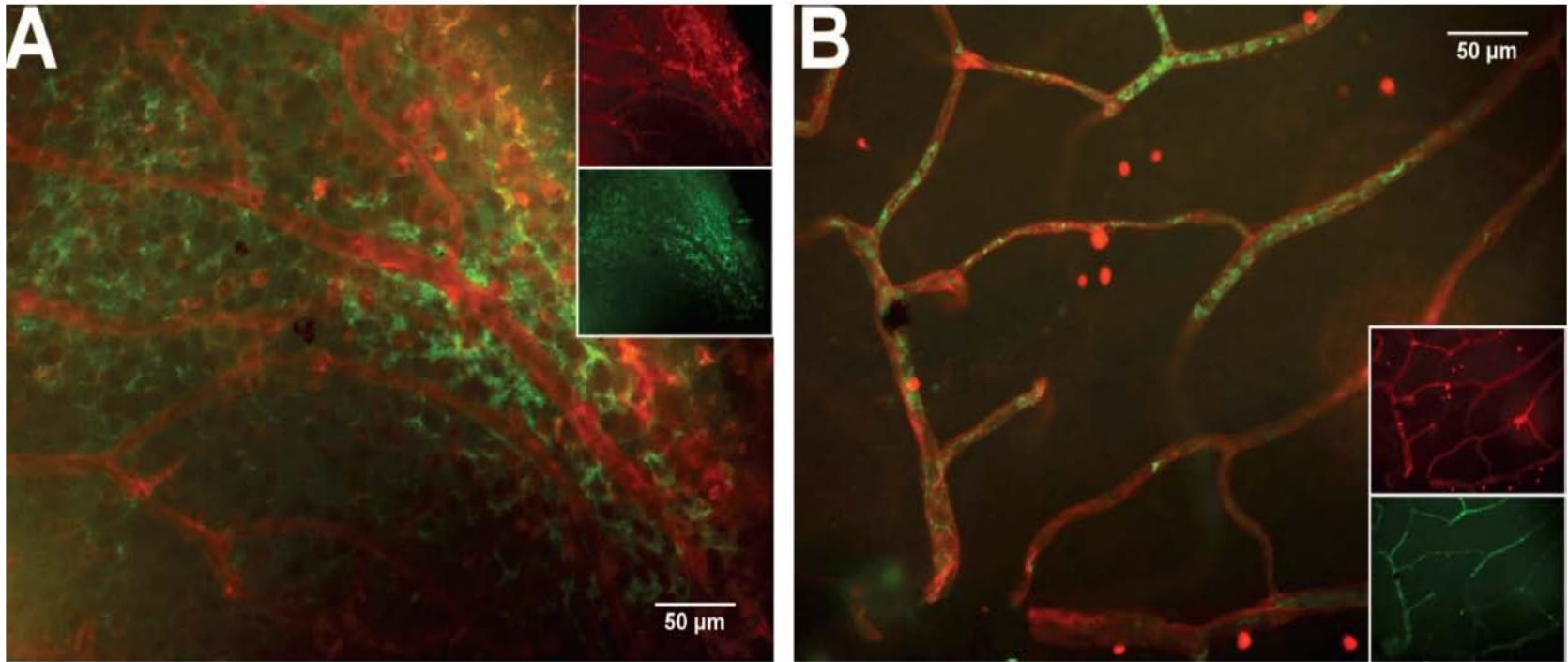
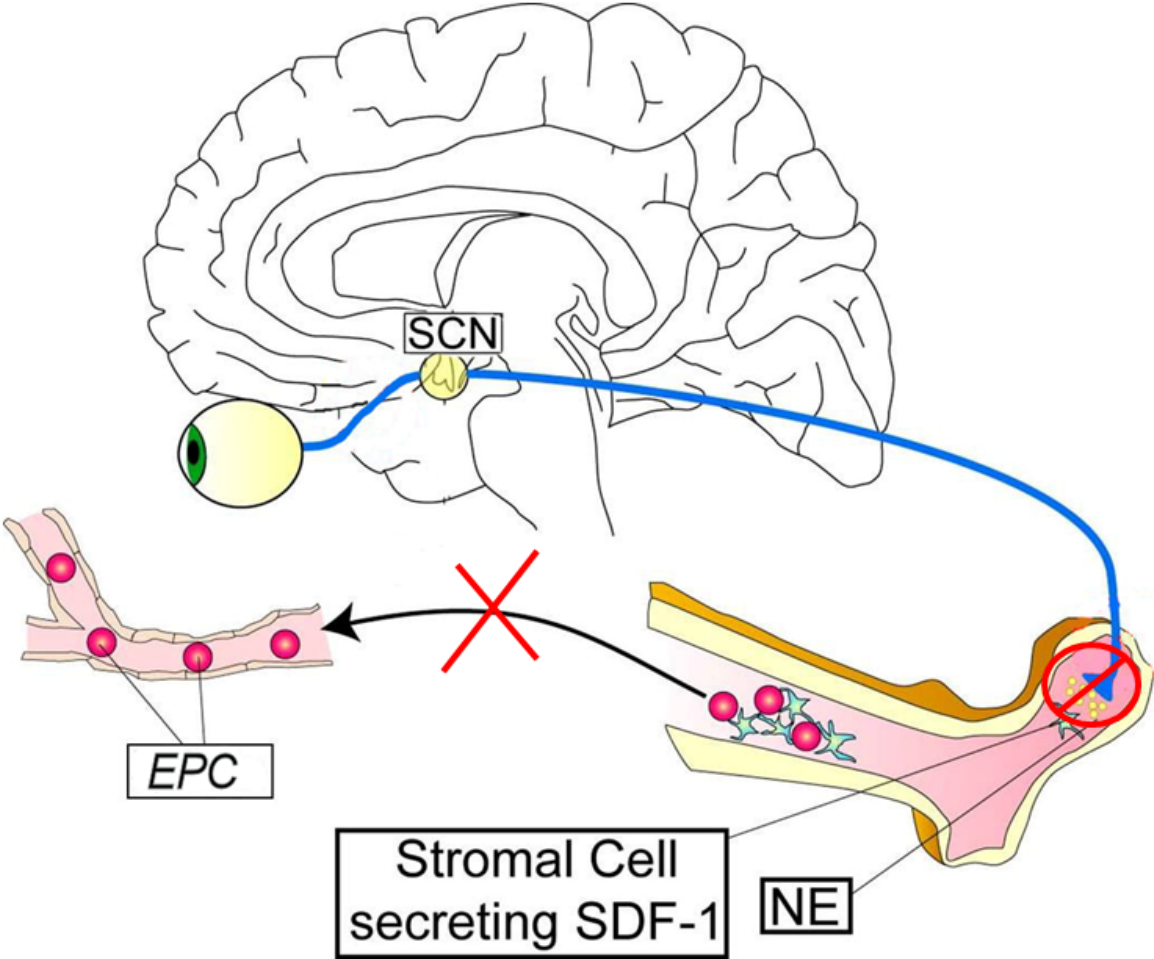


Figure 22: Schematic representation of the proposed mechanism. EPC release from bone marrow is regulated via local adrenergic signals: norepinephrine binds adrenergic receptor, reduces SDF-1 and stimulates entry of EPC into the circulation. In diabetes, number of nerve fibers in bone marrow is decreased, signal about the circadian time does not reach the bone marrow and as a result EPC are trapped within the bone marrow and unable to repair damaged vasculature.

Figure 22 (cont'd)



3.4 Methods

Rat model of type 2 diabetes. The BBZDR/Wor rat was specifically developed as a model of type 2 diabetes that develops diabetic complications. To produce this strain, classical genetic methods were used to remove the recessive gene responsible for spontaneous autoimmunity towards beta-cells from BBZDP strain. Islets from BBZDR/Wor rats are enlarged, with beta-cell hyperplasia and hyperinsulinemia, commonly seen in patients with type 2 diabetes.

Male obese BBZDR/Wor rats spontaneously develop diabetes that mimics human type 2 diabetes at 2 months of age. They demonstrate hyperglycemia and dyslipidemia, which are typical of type 2 diabetes, with increased levels of cholesterol, triglycerides, and nonesterified fatty acids [185]. The BBZDR/Wor rat develops retinopathy, neuropathy, nephropathy, and macrovascular complications typical of human type 2 diabetes and is emerging as the most applicable model of type 2 diabetic complications [185]. BBZDR/Wor animals demonstrate increased VEGF production and increased VEGF receptor expression [29], as well as increased NADPH oxidase activity [29] and hydrogen peroxide production [29] in the retinal vasculature as early as 2 weeks after diabetes onset. BBZDR/Wor rats also progress to early preproliferative DR with the development of acellular capillaries, pericyte ghosts, and capillary basement membrane thickening after 4 months of diabetes [185].

Rat models of type 1 diabetes. For histological evaluation of the BM STZ-induced model of type 1 diabetes was used. Male Sprague-Dawley rats weighing were made diabetic with a single intraperitoneal injection of STZ as described in the methods section of Chapter II.

For EPC counts in the peripheral blood, spontaneous auto-immune BBDP/Wor (biobreeding diabetes-prone rat) model of type 1 diabetes was used in this study. The BBDP/Wor rats develop all major diabetic complications, including retinopathy, nephropathy, and neuropathy [186]. As a spontaneous autoimmune model, the BBDP/Wor rat closely resembles the development of human type 1 diabetes and is free of any of the potential side effects of drug-induced diabetes models.

Femoral arterial catheterization. The protocols for the rat studies were approved by the Institutional Animal Care and Use Committee at Michigan State University, The University of Florida, and Biomedical Research Models, Inc. Multiple blood draws were performed by direct catheter placement into the femoral artery and vein. Animals were anesthetized with isoflurane (2%). The surgical approach for the femoral arterial catheters was through the ventral aspect of the leg. The catheters were tunneled subcutaneously to the nape of the neck and secured with sutures for later access while the animals were conscious. Blood draws were initiated after complete recovery of the animal, as determined by healing of the incision sites, usually 3–4 d after surgery. Blood draws (100 μ l each) were performed every 2 h for 24 h using an Automatic Blood Sampler (DiLab).

Isolation of thy-1⁺ cells from bone marrow. Rats were euthanized by exsanguination after anesthesia. Rat hind limb bones were dislocated and the skin removed. Bones were flushed with ice cold PBS and the cells pelleted. The cells were then treated with ammonium chloride (STEMCELL Technologies Inc.) to remove any contaminating red blood cells and resuspended in PBS (Mediatech, Inc.) containing 2% FBS and 1 mM EDTA. A custom rat negative selection kit (STEMCELL Technologies

Inc.) was used to deplete CD4, CD5, CD8a, and OX-43 cells of the rat. The cells were then further enriched for CD90 (thy-1)-positive cells using a positive selection kit (STEMCELL Technologies Inc.) tagged with a CD90/thy-1 antibody (Abcam).

Flow cytometry analysis. A flow cytometer (LSR II; BD) equipped with FACSDiva software (BD) was used for thy-1⁺CD3⁻CD4⁻CD8⁻ cell enumeration. PerCP-Cy5.5- (eBioscience), FITC-, RPE-, and Alexa Fluor 647-conjugated mouse anti-rat antibodies (AbD Serotec) were used to stain thy-1, CD3, CD4, and CD8 surface markers, respectively, in concentrations according to the manufacturer's instructions. PerCP-Cy5.5, FITC, and RPE were excited at 488 nm and their respective fluorescent emission was detected at 695, 530, and 576 nm. Alexa Fluor 647 was excited at 633 nm and its emission detected at 660 nm. Isotype-negative samples for all antibodies were used to determine the background fluorescence for each fluorochrome. Single-stained samples were used to set color compensation between fluorochromes. A gate was drawn around the white blood cell population in a forward versus side scatter histogram to exclude red blood cells debris.

NE ELISA. A competitive ELISA kit (ALPCO Diagnostics) was used to determine NE levels in 10 µl of rat plasma according to the manufacturer's instructions. In summary, NE was first extracted with a cis-diol-specific affinity gel and then acylated and converted enzymatically. After transfer on antiserum-covered microtiter plates, derivatized samples competed with solid phase-bound analytes for a fixed number of binding sites. After free analytes were removed by washing, the antibody bound to the solid phase was detected by peroxidase conjugation and read at 450 nm. Absorbance

reading of the standards (linear) was plotted against known standard concentrations (logarithmic) and a standard curve was drawn to quantify unknown samples.

Immunohistochemistry. Decalcified rat humerus bones were embedded in paraffin, sectioned on a rotary microtome at 4 μm , and then dried and deparaffinized. Enzymatic epitope retrieval was performed. After pretreatments, standard Avidin–Biotin complex staining steps were performed at room temperature on an Autostainer (Dako). After blocking nonspecific protein with nonimmune goat serum (Vector Laboratories), sections were incubated with an Avidin (Vector Laboratories)/Biotin (Sigma-Aldrich) blocking system. Polyclonal rabbit anti-NF200 (Sigma-Aldrich) at 1:100 or polyclonal rabbit anti-TH (Millipore) at 1:100 in normal antibody diluent (ScyTek Laboratories) was used for staining. Biotinylated secondary goat anti–rabbit IgG (Vector Laboratories) in normal antibody diluent diluted 1:400, followed by R.T.U. Elite Peroxidase reagent (Vector Laboratories), was applied for visualization. The slides were developed using Nova red (Vector Laboratories), counterstained using Gill (Lerner) 2 Hematoxylin (Thermo Fisher Scientific), dehydrated, cleared, and mounted using Permount (Thermo Fisher Scientific).

Retinal vasculature preparation. The sensory retina was isolated by gently separating it from pigment epithelium and choroid using a #00 paint brush under a dissecting microscope, prepared using trypsin digestion, and stained with hematoxylin and periodic acid–Schiff [9]. Acellular capillaries were quantified in a masked manner by three independent examiners.

gfp bone marrow chimeric mice. 10–12-week-old female C57BL6/J mice were lethally irradiated and then their BM was reconstituted with lineage-negative Sca1⁺ c-

kit⁺ HSCs from donor bone marrow of transgenic mice homozygous for gfp, according to methods published previously [106]. At selected times (ZT-5 and ZT-13) mice were euthanized and blood was collected for enumeration of thy-1⁺gfp⁺ circulating cells. The eyes were enucleated and preserved, retinas dissected, and mounted flat and image captures made using a fluorescent microscope (Eclipse TE200; Nikon) equipped with a digital camera (SPOT0.60XHRD06-NIK; Diagnostic Instruments, Inc.).

Real-time quantitative RT-PCR. Rat retinas and BM or blood EPCs were homogenized in Trizol reagent (Invitrogen), and RNA was isolated according to the manufacturer's instructions. First-strand complementary DNA was synthesized from isolated RNA using SuperScript II reverse transcription (Invitrogen). Prepared complementary DNA was mixed with 2× SYBR Green PCR Master Mix (Applied Biosystems) and various sets of gene-specific (Table 5) forward and reverse primers and subjected to real-time PCR quantification using the ABI PRISM 7700 Sequence Detection System (Applied Biosystems). All reactions were performed in triplicate. The relative amounts of mRNAs were calculated using the comparative threshold cycle method. Cyclophilin was used as a control, and all results were normalized to the abundance of cyclophilin.

Thymidine proliferation assay. 30,000 EPCs were plated per well using a 24-well plate and then treated with cytokine mix (Stem Cell Technologies) for 12 h. Thymidine was diluted 1:10 in PBS and added to the wells directly. The cells were then placed in the CO₂ incubator for 2 h. Then cells were removed, spun at 5,000 rpm for 5 min, and washed with ice cold 10% TCA (×2). 0.2 M NaOH was added to the cells and the plates were shaken gently for 10 min at room temperature. 100 µl of cell

homogenate was then added to 4 ml Cytoscint (Thermo Fisher Scientific). CPM was counted using thymidine settings.

Reendothelialization of diabetic mouse retina with control or diabetic EPC. STZ diabetic (≥ 6 months of diabetes) and age- and sex-matched normal control mice were administered 10,000 peripheral blood CD34+ cells from either diabetic or non-diabetic human blood donors by intravitreal injection. The eyes were harvested 48 h later and preserved for 1 h in freshly prepared buffered 4% paraformaldehyde. Retinas were dissected after preservation, permeabilized by overnight incubation in 10 mM HEPES + 150 mM NaCl buffer with 0.1% Tween 20, reacted with rhodamine-conjugated *R. communis agglutinin I* (red) and monoclonal anti-human nuclear antigen in PBS with 1% normal goat serum, and, finally, with FITC-conjugated goat anti-mouse IgG (green). The retinas were then radially sliced and mounted flat for epifluorescence microscopy image capture.

Table 5. Real-time qPCR primers

Gene name	Forward	Reverse
Clock rat	5'-TCTCTTCCAAACCAGACGCC-3'	5'-TGCGGCATACTGGATGGAAT-3'
Bmal-1 rat	5'-CCGATGACGAACTGAAACACCT-3'	5'-TGCAGTGTCCGAGGAAGATAGC-3'
Per-1 rat	5'-ACACCCAGAAGGAAGAGCAA-3'	5'-GCGAGAACGCTTTGCTTTAG-3'
Per-2 rat	5'-GAGAGAGGAACAGGGCTTCC-3'	5'-TTGACACGCTTGACTTCAG-3'
CRY-1 rat	5'-TGCTCCTGGAGAGAATGTCC-3'	5'-TGA CTCTCCCACTTCA-3'
CRY-2 rat	5'-CTGTGGCAGAGCCTGGTT-3'	5'-TCGCTGTCTGTTGGTGAC-3'
Rev-Erb rat	5'-ACAGCTGACACCACCCAGATC-3'	5'-CATGGGCATAGGTGAAGATTCT-3'
RORA rat	5'-CCCGATGTCTTCAAATCCTTAGG-3'	5'-TCAGTCAGATGCATAGAACAACA-3'
Cyclophilin rat	5'-CTTCTTGCTGGTCTTGCCATTCCT-3'	5'-TGGATGGCAAGCATGTGGTCTTTG-3'
Clock human	5'-TAAGGGCAACAGTGGATTTG-3'	5'-CAGCCCTA ACTTCTGCATAACTT-3'
Bmal-1 human	5'-GAGCAGCTCTCCTCCTCTGA-3'	5'-GGCCAGGGGTATATCTGT-3'
Per-1 human	5'-AGTGTCACCTCCACCTTTG-3'	5'-ACTTCAGCAGCTTGTCAGCA-3'
Per-2 human	5'-CTCCAGTGGCTACGGGAGT-3'	5'-TGGGGGATTAGTTTGCATTTCTG-3'
CRY-1 human	5'-GATACAGATGGCTTATCCTCTGC-3'	5'-CGCATTATTGAGGTCTTTCA-3'
CRY-2 human	5'-AAGTGCATCATTGGTGTGGA-3'	5'-GCGAAAGCTGCTGGTAAATC-3'
Rev-Erb human	5'-TGGACTCCAACAACAACACAG-3'	5'-GTGGGAAGTAGGTGGGACAG-3'
RORA human	5'-GGAGCCAGAAGGGATGAACTT-3'	5'-GGAACAACAGACGCCAGTAAG-3'
Cyclophilin human	5'-CAAGACTGAGTGGTTGGATGG-3'	5'-TGGTGATCTTCTGCTGGTCT-3'

Chapter IV

N3 fatty acids prevent diabetic retinopathy by inhibition of retinal vascular damage and enhanced endothelial progenitor cell reparative function.

This chapter is the edited version of a research article that was submitted to Diabetes.

Authors: Tikhonenko, M., Lydic, T. A., Opreanu, M., Li Calzi, S., Bozack, S.N., McSorley, K. M., Sochacki, A.L., Hazra, S., Grant, M. B., and Busik, J.V.

4.1 Abstract

The vasodegenerative phase of DR is characterized by not only retinal vascular degeneration but also inadequate vascular repair due to compromised BM derived EPCs. We propose that n3 PUFA deficiency in diabetes results in activation of the central enzyme of sphingolipid metabolism, acid sphingomyelinase (ASM) and that ASM represents a molecular metabolic link connecting the initial damage in the retina and the dysfunction of EPCs.

Type 2 diabetic rats on a control or DHA-rich diet were studied. The number of acellular capillaries in the retinas was assessed by trypsin digestion. mRNA levels of IL-1 β , IL-6, ICAM-1 in the retinas from diabetic animals were compared to controls and ASM protein was assessed by western blot analysis. EPCs were isolated from blood and BM and their numbers and ability to form colonies *in vitro* were measured.

We found that a DHA-rich diet prevented diabetes-induced increase in the number of retinal acellular capillaries and significantly enhanced the life span of type 2 diabetic animals. The DHA-rich diet prevented the upregulation of ASM and other inflammatory markers in diabetic retina. The diet also prevented the increase in ASM activity in EPCs, normalizing the numbers of circulating EPCs and improving EPC colony formation.

In summary, the DHA-rich significantly improved retinal vascular pathology in a type 2 diabetes animal model through inhibition of ASM in both retina and EPCs, leading to concomitant suppression of retinal inflammation and correction of EPC number and function in type 2 diabetes.

4.2 Introduction

Type 2 diabetic patients comprise over 85% of all cases of diabetes, more than half develop DR after 10 years of the disease [3]. DR is a microvascular complication of diabetes that can lead to vision loss. In diabetes, dysfunction of the endothelium is a key factor in the development of vascular complications [187-189], although nonvascular retinal tissue also plays an important role in the development of retinal pathology [8]. During the vasodegenerative stage of DR, capillary components such as pericytes and endothelial cells die prematurely [9]. This diabetes-induced injury of the retinal microvessels leads to increased vascular permeability, acellular capillary formation, non-perfusion and subsequent ischemia, ultimately leading to the proliferative stage of DR [9].

To counteract diabetes-induced endothelial cell injury and to replace injured endothelium, several endogenous repair mechanisms are available. Traditionally, microvascular repair was considered to be a result of proliferation of the resident vasculature [190]. However, there is a significant body of evidence that advocates that EPCs are a subpopulation of progenitor cells that play a critical role in endothelial repair and maintenance [106-108]. EPCs derived from the BM are released and recruited in areas of vascular repair, where EPC incorporate into injured vessels and differentiate into endothelial cells to restore the compromised endothelium [106]. Accumulating evidence suggests that diabetic EPCs lose the ability to aid in vascular repair which contributes to the development of the degenerative stage of DR [125]. Our recent report revealed that diabetic BM neuropathy affects EPC release and function and precedes retinal vascular degeneration in diabetes [191], thus providing additional evidence for the critical role of these cells in the disease's pathogenesis. Increased damage in the early stage of retinopathy followed by the reduction of EPC reparative function is likely to lead to the loss of viable vascular endothelial cells and increased acellular capillary formation in the retina.

We and others have shown that activated ASM participates in inflammatory cytokine signaling [192, 193], especially in endothelial cells [194]. ASM is a critical enzyme that catalyzes the hydrolysis of sphingomyelin to ceramide, and is rapidly activated in conditions of inflammation or stress [195]. Upon activation, ASM localizes to the caveolae of plasma membranes [196] and stimulates formation of ceramide-rich membrane microdomains. Ceramide has profound effects on a range of cellular functions such as apoptosis, phagocytosis, inflammation and cellular adhesion [192,

197, 198]. Enrichment of membrane microdomains by ceramide stimulates microdomain fusion [199, 200] which leads to cytokine receptor clustering and enhanced downstream signaling [201]. Several cytokine signaling pathways (such as TNF α and IL-1 β) that mediate inflammatory signaling in DR involve microdomains clustering [200].

N3 PUFAs and especially DHA have a unique ability to modulate endothelial integrity, neovascularization and inflammation in the retina [68, 76, 77]. DHA is decreased in the diabetic retina [202, 203] and plasma [58]. We and others demonstrated that increased dietary intake of n3 PUFAs reverses retinopathy in both type 1 diabetes [204] and retinopathy of prematurity [68]. There are, however, no studies addressing the role of n3 PUFAs in type 2 diabetes. Recently, we demonstrated that DHA acts through inhibition of the ASM pathway to prevent retinal endothelial cell activation by inflammatory cytokines [194]. However, EPCs are endothelial lineage cells and may be affected by the same mechanism that affects retinal endothelial cells. Despite the well-recognized EPC dysfunction in diabetes that prevents vascular repair and regeneration, there is a dearth of information on the effects of fatty acids on EPCs and particularly on the effects of n3 PUFAs of EPC function. In this study of type 2 diabetes, we propose that n3 PUFA-mediated ASM downregulation improves DR outcomes through both inhibition of retinal vascular damage and enhanced EPC function and subsequent retinal vascular repair.

4.3 Results

Effect of DHA rich diet on formation of acellular capillaries in type 2 diabetic rats. To determine whether a DHA enriched diet has a protective effect against the development of retinal vascular pathology in type 2 diabetes, BBZDR/Wor and their age-matched non-diabetic BBDR littermates were used. Retinal vasculature was isolated from diabetic rats subjected to either DHA enriched diet or standard rodent diet with soybean as a source of fat for 5-7 months. In agreement with previous reports, the number of acellular capillaries was dramatically increased in retinas from these type 2 diabetic rats fed the control diet. However, the number of acellular capillaries in the retinas from diabetic rats fed a DHA enriched diet was not significantly different from control retinas (Fig.23).

Effect of DHA rich diet on retinal inflammatory markers in control and diabetic rats. Vascular pathology in diabetes requires both retinal vascular damage and coinciding lack of vascular repair [125, 205]. Thus, to achieve the vasoprotective effects shown in Fig. 23, DHA could have a direct effect on retinal damage, the reparative function of EPCs, or both. Retinal damage in diabetes is known to be associated with an increase in pro-inflammatory and pro-angiogenic mediators. Indeed, we found that mRNA levels of IL-1 β , IL-6, and ICAM-1 were increased in the retinas from type 2 diabetic animals in this study. Importantly, the DHA-rich diet prevented the increases in IL-1 β , IL-6, and ICAM-1 expression (Fig. 24). TNF α levels showed a trend towards an increase in diabetic animals fed control diet, but this was not statistically significant.

We have previously identified ASM as an important modulator of the inflammatory response of the retinal vasculature in a model of type 1 diabetes and in

human retinal endothelial cell cultures [194]. To determine if ASM plays a role in the observed vasoprotective effect of DHA in this type 2 diabetes model, we measured the ASM expression level in the retinas isolated from control animals, diabetic animals on a control diet and diabetic animals on DHA rich diet. We observed a dramatic over 5 fold increase in ASM protein levels in the retinas from diabetic animals on control diet; this was completely prevented in the retinas from the animals on the DHA rich diet (Fig. 25).

Effect of DHA rich diet on EPC repair function in control and diabetic animals. To assess the effect of the DHA-rich diet on EPC reparative function, we first measured the number of EPCs in the circulation in control animals, and diabetic animals fed the a control or DHA supplemented diets. After 2 months of diabetes, the rats fed the control diet had significantly reduced number of EPCs in the peripheral blood (Fig. 26 A). The number of EPCs in diabetic animals fed a DHA-rich diet was significantly higher compared to diabetic animals fed the control diet.

To test whether the reduced EPC numbers in the circulation could be due to a loss of proliferation capacity, we extracted EPCs from the BM of control and type 2 diabetic rats following 2 months of diabetes. The diabetic animals were maintained on either the control diet or the DHA-rich diet. EPCs from diabetic animals fed the control diet demonstrated decreased colony formation *in vitro* which was prevented in EPCs from the diabetic animals on DHA-rich diet (Fig. 26 B).

ASM specific activity in bone marrow derived EPCs. Previously, we demonstrated that the protective effect of DHA in endothelial cells is due largely to inhibition of ASM activity. As EPCs are endothelial lineage cells, we next determined ASM activity in EPCs isolated from the BM of control and type 2 diabetic rats (Fig. 27).

EPCs from diabetic rats demonstrated more than 3 times increased ASM activity as compared to non-diabetic rats. Importantly, dietary supplementation with DHA reduced this elevation to control levels. These results suggest that ASM activation is involved in the EPC loss of function seen in diabetes and that DHA supplementation could reverse that pathology in an ASM-dependent manner.

Human diabetic CD34+ cells treated with DHA *in vitro*. To support our data from the diabetic animal model, we obtained CD34⁺ EPCs from peripheral blood of diabetic patients and evaluated the effect of *in vitro* DHA treatment on EPC function. One progenitor population, CD34+ cells, represent a cell population with marked clinical utility [206, 207]. Circulating CD34+ cell numbers predict cardiovascular risk and dysfunction and better than CD34+VEGFR2+ and CD133+-based populations [208, 209]. Recently, Fadini et al. [210] reported that circulating CD34+cell number was an independent risk biomarker of cardiovascular events and significantly correlated with outcomes in metabolic syndrome. These studies, taken together, suggest that CD34+ alone is sufficient as a marker for EPCs. DHA pretreatment dramatically improved EPC migration compared to vehicle control (Fig. 28).

Life span in diabetic animals fed DHA or control diet. In agreement with previous studies, diabetic animals exhibited a decreased survival rate compared to control. The DHA-rich fish oil diet, however, significantly increased the survival rate in diabetic animals (Fig. 29). The protective effect of DHA is most evident within the first 50 days of the diet. After 50 days, the slopes of the survival curves were similar between diabetic animals on control or DHA-rich oil diet. We suggest that the effect of DHA on survival rate in diabetic animals could be through a generalized improvement of

vascular function due to decreased vascular inflammation and enhanced vascular repair by EPCs, as observed for retinal vasculature.

Fig. 23: DHA-enriched fish oil diet prevents the formation of acellular capillaries in type 2 diabetes model.

A) Trypsin-digests of rat retinas stained with hematoxylin and periodic acid–Schiff. Representative regions around the mid-retina used for counting are shown. Bars, 10 μ m. Significantly increased numbers of acellular capillaries (black arrows) were observed in retinal vasculature isolated from diabetic animals as compared to control vasculature. No significant difference was found between diabetic animals fed DHA diet and control animals.

(B) Quantification of acellular capillaries in n=9 in control and n=9 in diabetes soybean diet group, n=4 in diabetes DHA diet group.

*** =P < 0.001 compared to control animals group

=P < 0.001 compared to diabetic animals fed with soybean oil diet.

Figure 24: DHA-enriched fish oil diet prevents increase in IL-1 β , IL-6, TNF α and ICAM gene expression in type 2 diabetes model. Gene expression of pro-inflammatory and pro-angiogenic mediators was assessed by real-time qPCR using the whole retina. A significant increase in IL-1 β , IL-6, TNF α and ICAM levels was observed in diabetic rats fed a standard diet compared to control rats. The DHA-enriched diet prevented these levels from reaching significant increase as compared to control. n=10 controls, n=4 diabetes soybean oil, n=8 diabetes fish oil. Data are expressed as the mean \pm SE.

*= P<0.05 compared to control animals group.

Figure24 (cont'd)

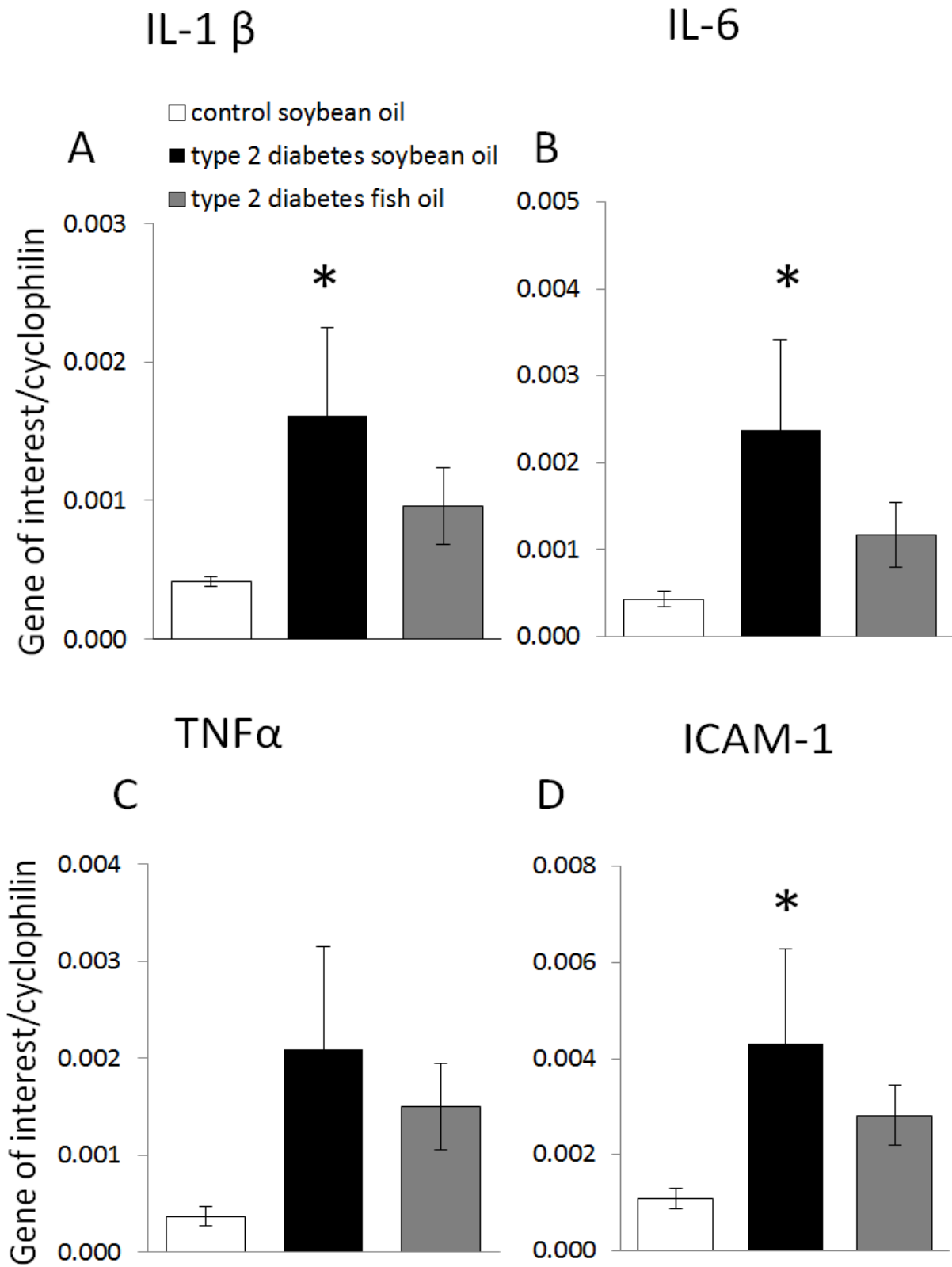


Figure 25: DHA-enriched fish oil diet normalizes the ASM protein levels in the whole retinas of type 2 diabetic rats.

(A) Retinal acid sphingomyelinase protein levels were assessed by Western blot analysis.

(B) Quantification of 4 rats / condition is shown in and normalized by tubulin (loading control).

***= $P < 0.001$ compared to control animals group.

###= $P < 0.001$ compared to diabetic animals fed with soybean oil diet.

Figure 25 (cont'd)

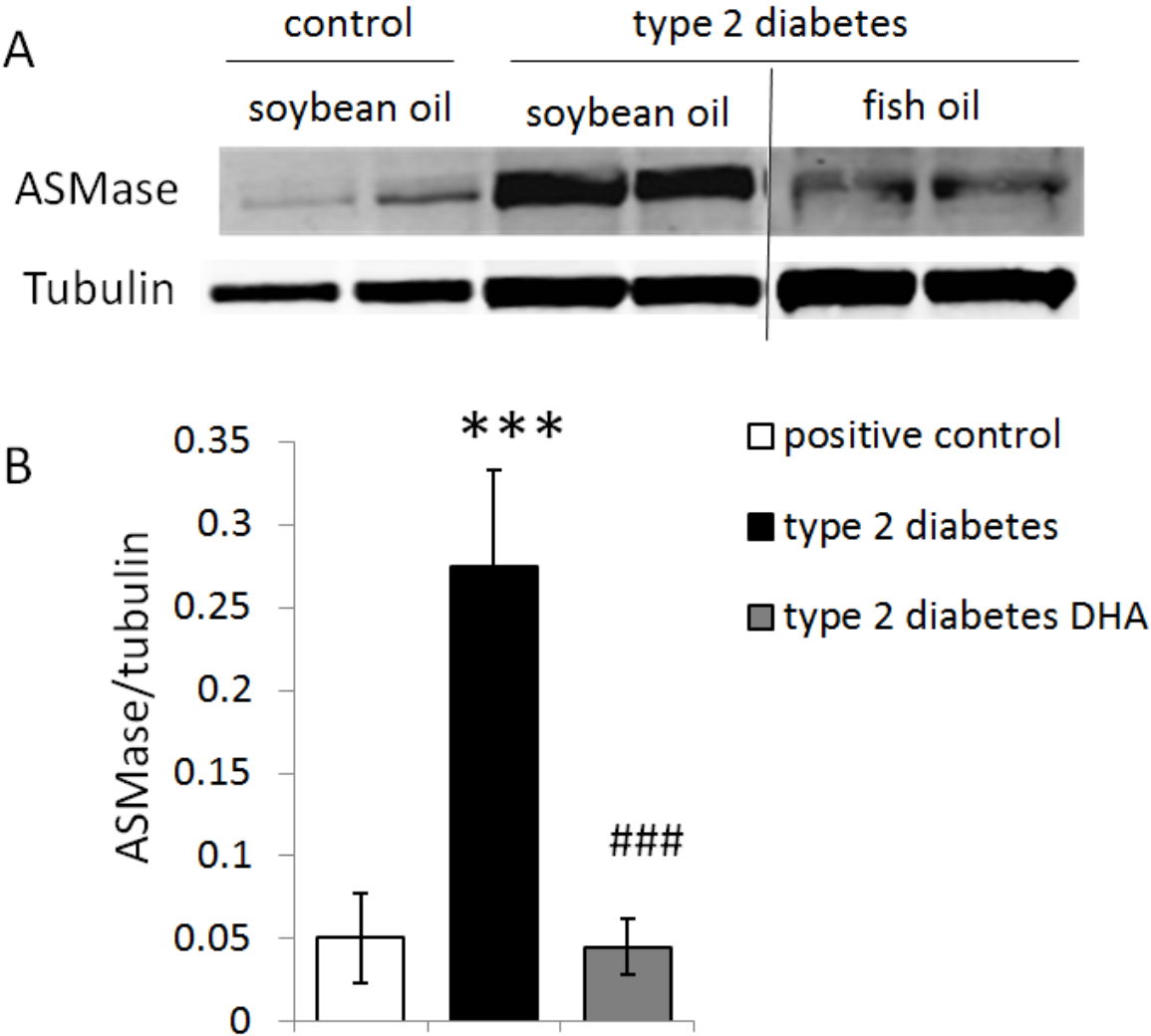


Fig. 26: A) DHA-rich fish oil diet attenuates a decrease in the number of circulating EPCs in type 2 diabetes model. EPCs were extracted by magnetic beads method from total peripheral blood. After 2 months of diabetes and feeding with the experimental diet, the control and diabetic animals were used. n=8 controls, n=5 in diabetes soybean oil diet, n=7 in diabetes fish oil diet.

* = $P < 0.05$ compared to control animals group.

= $P < 0.05$ compared to diabetic animals fed with soybean oil diet.

B) The DHA-rich fish oil diet improves EPC colony formation in type 2 diabetes model. EPCs were extracted by magnetic beads method from bone marrow. Bone marrow EPC proliferation was assessed by colony formation assay. EPC colony formation was significantly decreased in diabetic rats compared to controls but corrected by DHA-enriched fish oil diet. n=4 in each group.

* = $P < 0.05$, ** = $P < 0.01$ compared to control animals group,

= $P < 0.001$ compared to diabetic animals fed with soybean oil diet.

Figure 26 (cont'd)

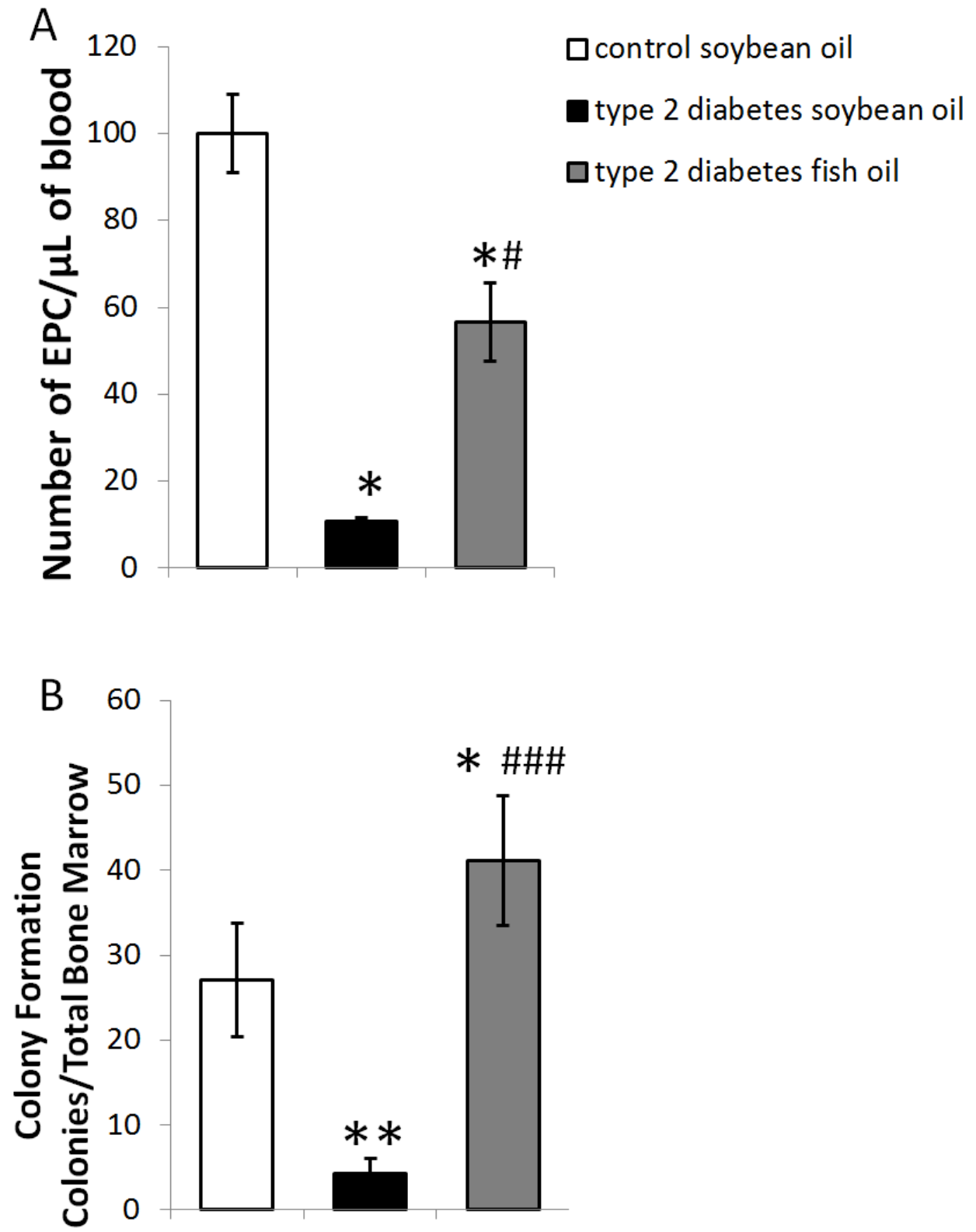


Figure 27: The increase in ASM activity observed in diabetic EPCs is prevented by DHA-rich fish oil diet. Diabetic bone marrow EPC showed a significant increase in ASM activity. However, the EPCs derived from diabetic animals fed DHA-rich fish oil diet showed reduced ASM activity that was similar to that observed in control rats.

n=8 controls, n=3 in diabetes soybean oil diet, n=5 in diabetes fish oil diet.

*** = $P < 0.001$ compared to control animals group

= $P < 0.001$ compared to diabetic animals fed with soybean oil diet.

Figure 27 (cont'd)

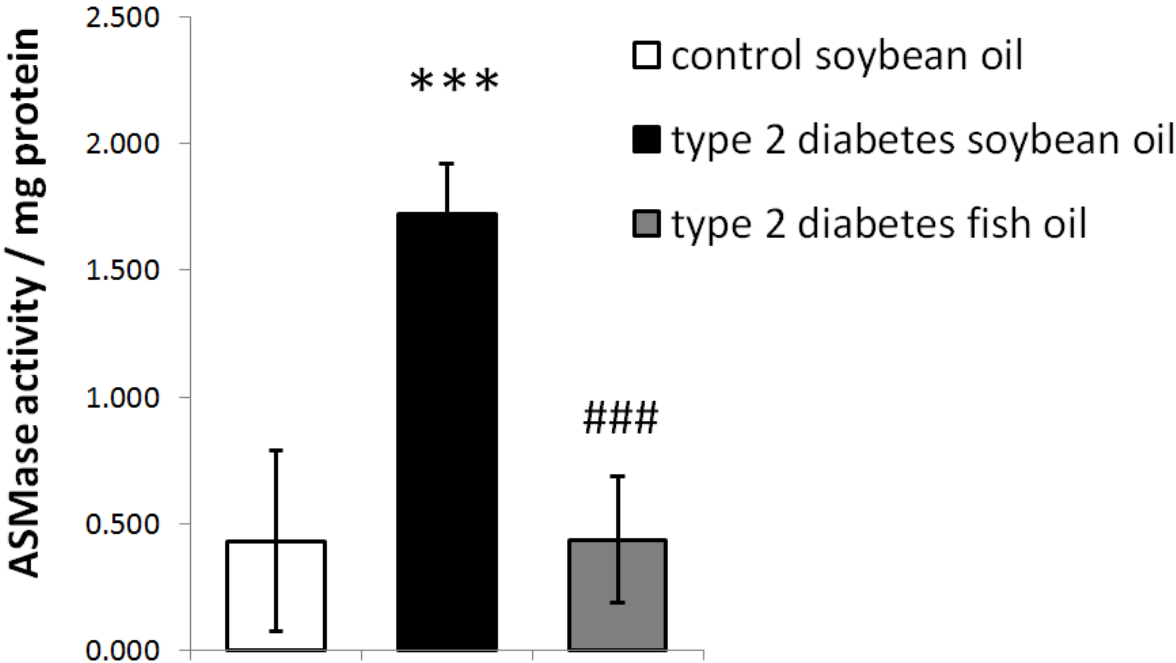


Figure 28: *In vitro* DHA pretreatment improves human CD34⁺ cell migration. EPCs were extracted by magnetic beads method from blood of diabetic patients. Cells were pretreated with BSA vehicle (untreated) or 100 μ M DHA and then placed in Boyden chamber for migration assay. Migration towards FBS was used as positive control.

n=4 in each group.

**= P<0.01 compared to positive control group

###= P<0.001 compared to untreated diabetic group.

Figure 28 (cont'd)

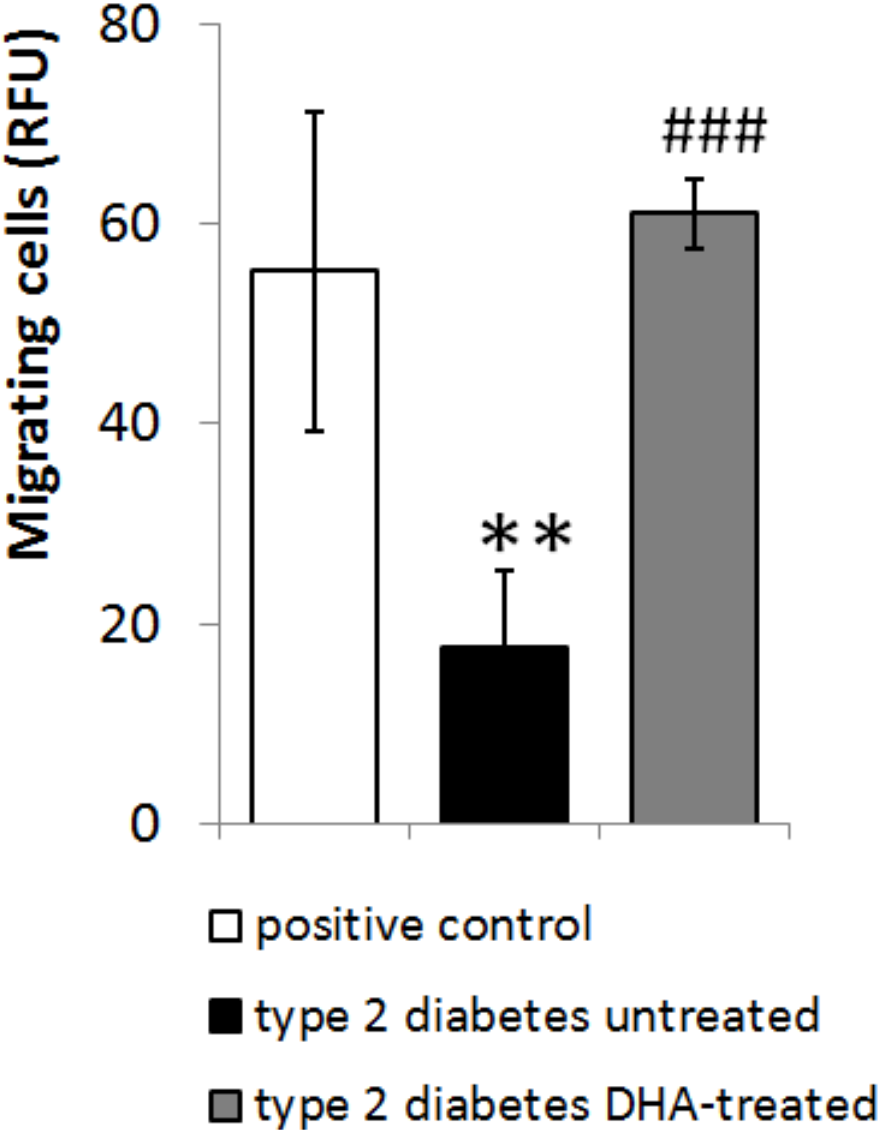


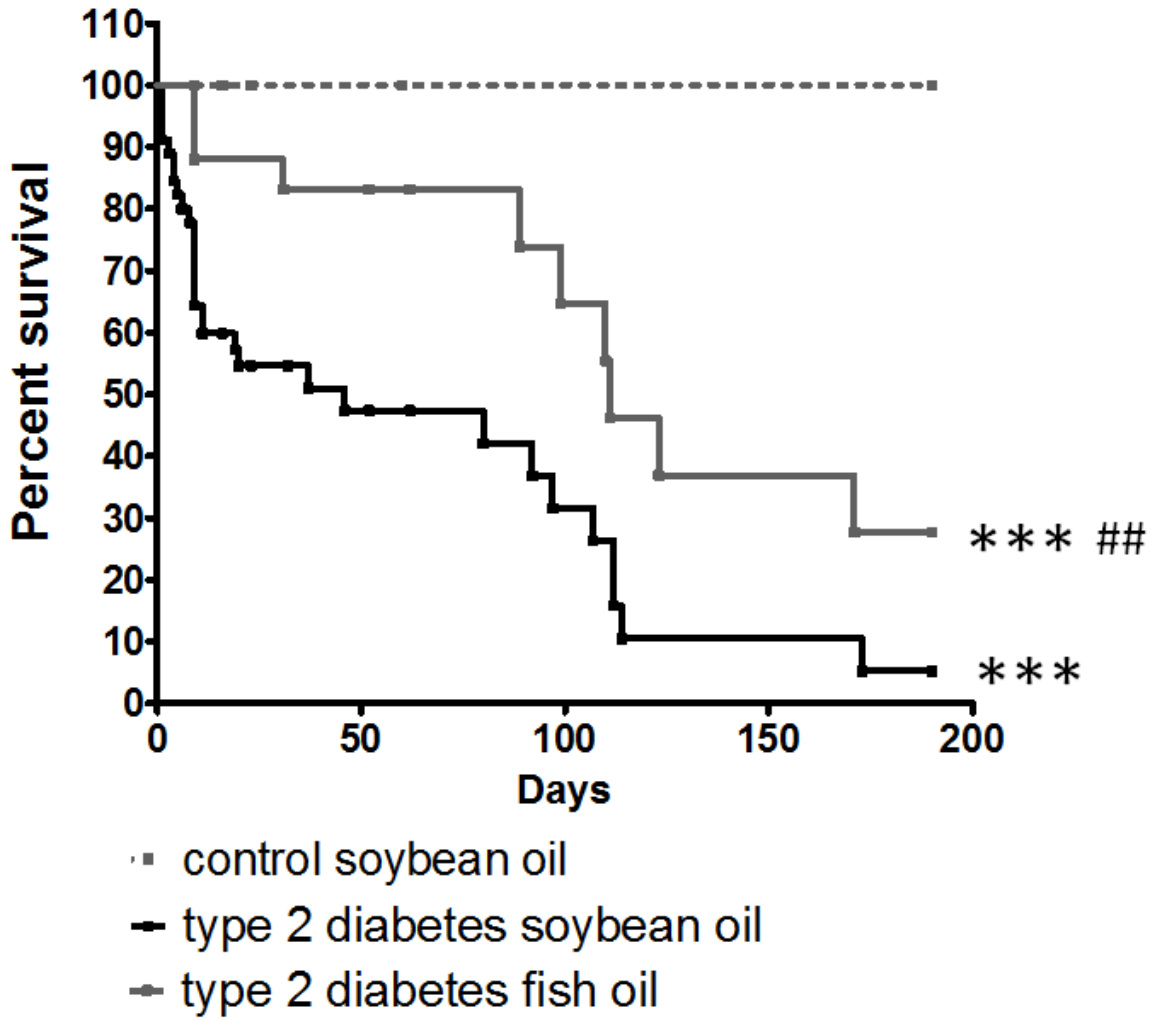
Figure 29: DHA-rich fish oil diet improves life span in type 2 diabetic rats. After induction of diabetes, rats were randomly assigned to soybean (black line) or DHA-rich fish oil diet (gray line) shown as day 0. Control animals (dashed line) were fed soybean oil diet. Survival was then assessed for 190 days. Diabetic rats fed DHA-rich fish oil diet had statistically improved survival as compared to the soybean oil diet.

n=45 of control animals group, n=45 of diabetic animals fed soybean oil group, n=25 of diabetic animals fed fish oil group.

***= $P < 0.001$ compared to control animals group

###= $P < 0.001$ compared to diabetic animals fed with soybean oil diet.

Figure 29 (cont'd)



4.4 Discussion

The vascular degeneration in diabetes is believed to initially involve endothelial cell damage due to low-grade chronic inflammation, with inadequate vascular repair due to compromised BM-derived EPCs. EPCs participate in retinal vascular repair by migrating to the site of injury and by providing paracrine support to the vasculature. In diabetes, we and others have shown that BM pathology with subsequent EPC dysfunction precedes and is necessary for the development of retinal vascular degeneration [125, 191].

In this study we show that the metabolic link connecting both the initial inflammation in the retina and the dysfunctional EPCs involves the activation of the central enzyme of sphingolipid metabolism, ASM.

Our previous studies of rat model of type 1 diabetes demonstrated a significant decrease in total n3 PUFAs, especially DHA, which was tightly coupled to increased inflammatory changes in the retina [91]. A recent study by Connor *et. al.* which used the rodent model of retinopathy of prematurity demonstrated that increasing n3 PUFAs levels by either dietary or genetic means decreases retinal TNF α levels and lessens microvessel pathology [68]. However, to our knowledge, this is the first study to examine the effect of increased dietary n3 PUFA such as DHA on the development of retinopathy in a type 2 diabetes model. The ultimate result of the DHA-rich dietary supplementation in this study is that it prevented retinal vessel loss as evidenced by the decreased number of acellular capillaries in retinas of type 2 diabetic animals.

In addition to improved retinal health, diabetic animals on the DHA-rich diet lived significantly longer than diabetic animals fed the control diet, suggesting that DHA

improved vascular health in diabetes. Our data is in agreement with a previously published study concerning the beneficial effects of dietary n3 PUFAs on life expectancy [211] in people. Vascular complications are the main cause of death in type 2 diabetes [212] and EPCs play a critical role in vascular regeneration [213].

Here we demonstrate that DHA supplementation improves the outcomes of DR by preventing endothelial cell loss and subsequent retinal damage through correction of BM derived EPC function. We demonstrate that the beneficial effects of DHA are due, at least in part, to inhibition of ASM activity in retinal endothelial cells and BM derived EPCs.

ASM-mediated production of pro-inflammatory and pro-apoptotic ceramide was shown to be an integral component of inflammatory signaling. Ceramide enrichment of microdomains stimulates their ability to fuse [199, 200] which results in the clustering of cytokine receptors and enhanced inflammatory signal transduction [192-194, 201].

In this study, we tested whether the inflammatory status associated with type 2 diabetes leads to increased ASM levels in whole retina. Indeed, protein analysis demonstrated a more than 5-fold increase in ASM levels in diabetic retina as compared to control animals. Importantly, in diabetic animals fed the DHA-rich diet, levels of ASM were not elevated (Fig. 25). An increase in ASM leads to enhanced conversion of sphingomyelin to ceramide, followed by the activation of the key pro-inflammatory signaling pathways, including the NF- κ B pathway [214]. The NF- κ B transcription factor controls the expression of a wide range of genes, such as ICAM-1. Indeed, we found that the pattern of ICAM-1 expression follows that of ASM. Retinal ICAM-1 mRNA was increased in diabetes compared to control, but was not increased in diabetic rats fed the

DHA-rich diet, highlighting the important role of ASM in diabetes-induced retinopathy. We previously observed anti-inflammatory effect of DHA through attenuating NF- κ B signaling in early steps of inflammation in retinal vascular cells [77]. Based on this finding and previous observations in other models of retinopathy [68], we hypothesized that the protective effect of DHA on retinal vasculature in diabetes is mediated, at least in part, by inhibition of retinal inflammation and cytokine signaling.

In this study, mRNA levels of IL-1 β , IL-6 and ICAM-1 were increased in the retinas of type 2 diabetic rats after 2 months of diabetes. However, the DHA-rich diet normalized inflammatory markers to control levels, thereby supporting the notion that chronic inflammation underlies the vascular pathology in type 2 diabetes and that a DHA-rich diet exhibits anti-inflammatory properties, which prevent endothelial cell loss.

EPCs arise from the BM, migrate into the bloodstream and home to peripheral vascular beds such as skin [215], kidney [216] or retina [106]. The EPCs can repair injured vasculature by maturing into endothelial cells and incorporating directly into vessels and by providing paracrine support to the resident vasculature [213]. Number of circulating EPC is decreased in diabetic patients [122, 123] and EPCs in diabetic individuals are not effective in vascular regeneration due to their impaired migration and proliferation abilities [125, 137, 191, 217].

Our findings confirmed that in a rat model of type 2 diabetes, the total number of EPCs in the blood was decreased. Moreover, diabetic BM derived EPCs did not form colonies as well as control EPCs. Importantly, in the animals exposed to the DHA-rich diet, the number of EPCs in the peripheral blood was significantly elevated and colony formation abilities were restored (Fig. 26). This suggests that DHA stimulated EPCs

proliferation and/or migratory capacity from the BM into the circulation, thus increasing EPC potential to repair vasculature.

For oriented migration toward a chemotactic signal, a spatial redistribution of membrane components occurs [218]. Recent studies have highlighted the importance of compartmentalized lipids within the membrane for generating this rearrangement [218, 219]. In particular, sphingolipid-enriched microdomains play a role in membrane compartmentalization [220] and cell migration [221, 222]. ASM converts sphingomyelin to ceramide [223]. Since using *in vitro* model of diabetes we previously found the cellular ASM levels to be increased [194], we hypothesized ASM could also be activated in EPCs in diabetes, altering sphingolipid content of EPC plasma membranes and resulting in decreased EPC migration ability. We have described the inhibitory function of DHA on ASM activity in cultured human retinal endothelial cell [194] and thus proposed that the protective effect of DHA may occur in another endothelial lineage cell, the EPC. We showed that in diabetic rats, the elevation in ASM activity in EPC was prevented by a DHA-rich diet (Fig. 27), supporting our hypothesis.

Current treatments for DR are highly invasive and do not completely prevent the pathology. This study has demonstrated that dietary supplementation with the n3 fatty acid DHA represents a safe, non-invasive, and effective strategy for prevention of DR. We demonstrate for the first time that in a rat model of type 2 diabetes, DHA inhibits ASM activity, reducing inflammatory mediators and improving EPC function. The combined actions of DHA lead to a pronounced protective effect on retinopathy and increased life expectancy in type 2 diabetic animals.

4.5 Methods

Rat model of type 2 diabetic retinopathy. Bio-Breeding Zucker diabetic rat (BBZDR/Wor) rats and their age-matched non-diabetic BBDR littermates were purchased from Biomedical Research Models Inc. The BBZDR/Wor strain was specifically developed as a model of type 2 diabetes. The rats spontaneously develop diabetes and diabetic complications including retinopathy, neuropathy, nephropathy, and macrovascular complications typical for type 2 diabetes in humans. BBZDR/Wor animals also demonstrate an early vasodegenerative stage of DR with acellular capillary development [185], thus making this model of type 2 diabetes highly applicable to human disease. All procedures involving the animal models adhered to the ARVO statement for the Use of Animals in Ophthalmic and Vision research. The protocols for the animal studies were approved by the Institutional Animal Care and Use Committee at Michigan State University.

Experimental diet. Within 1 month of diabetes onset, diabetic animals were randomly assigned to a soybean or fish oil diet. Control diet was made of AIN-93M purified rodent diet with 10% caloric intake as soybean oil (a standard rodent diet ingredient that contains 50.8% linoleic acid) from Dyets Inc. (Bethlehem, PA). In DHA-rich fish oil diet half of the soybean oil, or 5% caloric intake, was replaced with Menhaden oil (oil from a small plankton eating fish containing 10.26% DHA and 14.16% EPA).

Sphingomyelinase Assay. EPCs were lysed in acid lysis buffer (50 mM Sodium Acetate, pH=5; 1% TritonX-100; 1 mM EDTA) with freshly added protease inhibitor cocktail (Sigma, St. Louis, MO). Sphingomyelinase activity was measured using the

Amplex Red Sphingomyelinase Assay Kit (Molecular Probes, Eugene, OR) as described in the manufacturer's protocol.

Quantitative real time-polymerase chain reaction (qRT-PCR). Total RNA was extracted from rat retinas as previously described [224]. Specific primers for each gene were designed using IDT DNA PrimerQuest software (Coralville, IA). Rat gene-specific primers used in this study: IL-1 β (CAAGGAGAGACAAGCAACGA and GTTTGGGATCCACACTCTCC), IL-6 (CCAGGAAATTTGCCTATTGA and GCTCTGAATGACTCTGGCTTT), TNF α (GGTCCCAACAAGGAGGAGA and GCTTGGTGGTTTGCTACGA), ICAM-1 (CCACCATCACTGTGTATTCGTT and ACGGAGCAGCACTACTGAGA). First strand cDNA was synthesized using the SuperScript II RNase H-Reverse Transcriptase (Invitrogen Carlsbad, CA). Synthesized cDNA was mixed with 2x SYBR Green PCR Master Mix (Invitrogen Carlsbad, CA) and the different sets of gene-specific forward and reverse primers and subjected to real-time PCR quantification using the ABI PRISM 7900 (Applied Biosystems, Carlsbad, CA). All reactions were performed in triplicates. The relative amount of mRNAs was calculated using the comparative CT method (User Bulletin #2, Applied Biosystems). Cyclophilin was used as a control and all results were normalized to the abundance of cyclophilin mRNA.

Human CD 34⁺ cell isolation. The study protocol was approved by the institutional review board at the University of Florida IRB #2010-411, and written informed consent was obtained from each patient. Circulating CD 34⁺ cells were isolated from peripheral blood of diabetic or healthy human donors as previously described [137]. Briefly, for each patient 150 ml of blood were collected into Sodium

Citrate-containing CPT™ glass vacuum tubes (BD, Franklin Lakes, NJ) and then reacted with magnetic bead-conjugated anti-CD34 antibodies. For each assay a minimum of three patient's blood was pooled and separated according to manufacturer's directions (Stem Cell Technologies, Vancouver, BC, Canada).

Isolation of EPC from Rat: The Rat EPCs were isolated as previously described [191]. Mononuclear cells were separated with Ficoll-Plaque Plus (GE Healthcare) gradient and resuspended in PBS containing 2% FBS and 1mM EDTA. A custom rat negative selection kit (Stemcell Technologies Inc.) was used to deplete CD4, CD5, CD8a and OX-43 cells. Thy-1 positive cells were further extracted using the positive selection kit (Stemcell Technologies Inc.) tagged with CD90/thy-1 antibody (Abcam). The endothelial nature of isolated Thy-1 positive cells was confirmed by co-expression of CD-133, the presence of endothelial nitric oxide synthase, incorporation of Dil-acLDL and participation in capillary tube formation with human retinal endothelial cells. Countess automatic counter (Invitrogen) was used for the evaluation of EPC numbers.

Cell Migration. To test the effect of n3 PUFA on EPC cell migration, 20,000 human CD34⁺ cells per condition were incubated in 2% fetal bovine serum-supplemented medium in the presence of either 20 mM bovine serum albumin (vehicle control), 100 μM DHA or 100 μM palmitic acid (16:0) in 5% CO₂ at 37°C for 18 hours. After incubation, the cells were maintained overnight in StemSpan® H3000 with StemSpan® CC100 added (Stem Cell Technologies) overnight to allow the cells to recover from the isolation process. The following morning, cells were stained with Calcein-AM (Molecular Probes, Carlsbad, CA), loaded onto the upper compartment of a Boyden migration chamber (Neuro Probe, Inc. Gaithersburg, MD) and induced to

migrate through a 5 μm pore-size membrane towards either 100 nM SDF-1, PBS (negative control), or 10% FBS (positive control). After 4 h, the number of cells that migrated was determined by measuring the fluorescence emitted at 550 nm when the cells were exposed to light at an excitation frequency of 485 ± 20 nm. Each sample was run in triplicate and results expressed as a percentage of migrating cells relative to positive control \pm SEM.

DHA treatment. DHA stock was prepared by dissolving fatty acid (NuCheck Prep, Inc., Elysian, MN) in ethanol to a final concentration of 100 mM. DHA was added to EPC in serum-free medium to a concentration of 100 μM fatty acid, with 20 μM charcoal-treated, solvent extracted, fatty-acid-free bovine serum albumin (BSA; Serologica Inc., Norcross, GA) which served as the fatty acid carrier. The fatty acid/albumin molar ratio was maintained at 5:1. The final concentration of ethanol in the media was less than 0.1%. Cells were incubated with DHA for 18 hours at 37°C prior to SDF-1 treatment. Equivalent amounts of BSA (carrier control) and ethanol were added to the control plates. 16:0 (palmitic acid), and BSA was used as an additional control.

Western blot. Proteins were extracted from rat retinas using a simultaneous extraction of proteins and RNA method as previously described [224]. Protein concentration was measured by Qubit fluorometer (Invitrogen, Eugene, OR) as described in the manufacturer protocol. Proteins were resolved on NuPAGE Novex 10% Bis-Tris gels, transferred to nitrocellulose membrane and immunoblotted using anti-ASM antibody followed by secondary IRDye infrared secondary antibodies (Invitrogen, Molecular probes, Eugene, OR). Immunoreactive bands were visualized and quantified by Odyssey infrared imaging system (LI-COR Biosciences, Lincoln, NE).

Histological assessment of retinal capillaries. Rat retinal vascular beds were isolated by trypsin digestion [225] and acellular capillaries were systemically counted in the mid-retina by two independent investigators as previously described [225].

Statistical analysis. Data is expressed as the mean \pm SD for all parameters unless specified. Factorial ANOVA with post hoc Tukey's test (GraphPad Prism5, GraphPad Software, San Diego, CA) was used for comparing the data obtained from independent samples. Survival curves were compared by proc life test with Sidac multiple comparisons (SAS software, SAS Institute, Carry, NC). Significance was established at $P < 0.05$.

Chapter V

Direct Link between Retinopathy and Bone Marrow Neuropathy

5.1 Introduction

DR is a sight-threatening disease with no effective therapeutic options. Endothelial cell dysfunction due to diabetes is a key factor in the development of DR. The initial non-proliferative stage of DR is characterized by ischemia-induced pericyte and endothelial cell loss which leads to increased vascular permeability, non-perfusion and subsequent hypoxia of the retinal tissue [9]. The non-proliferative stage may advance into proliferative stage leading to blood vessels covering the field of view.

There is strong evidence that the endothelial loss of function in diabetes may be due to the failed attempts of EPCs at repairing injured capillaries [106-108, 127]. EPCs arise from the BM and are recruited to areas requiring vascular repair where they incorporate into the blood vessels to replace damaged endothelium [106, 107]. Previous studies have shown that diabetic patients have decreased numbers of circulating EPCs [122, 123]. EPC mobilization occurs as a result of activation of sympathetic nerve fibers in the BM and a subsequent decrease in local levels of SDF- 1 [112-114].

In Chapter III, we demonstrated that type 2 diabetes caused the loss of nerve fibers in the BM resulting in the loss of the circadian regulation of EPC release [191]. We found that the early signs of denervation in the BM preceded development of DR allowing us to propose that diabetic animals have a decreased ability to repair retinal vasculature due to a lack of sympathetic innervations which immobilizes EPCs within the BM.

Diabetes is a complex disease with multiple pathologies involved. To separate the defect in BM denervation from the other metabolic pathologies of diabetes, we examined the effects of surgical BM denervation in non-diabetic rats on their ability to repair damaged retinal vasculature.

5.2 Results

Effect of surgical bone marrow denervation on vascular permeability in intact retina. Male Wistar rats underwent a denervation surgery and were subjected to permeability assay 7 days later. We did not find any difference in vascular permeability in intact retinas between rats with denervated BM and control rats (Fig.30 A and C). That result suggests that lack of regulated EPC release does not affect healthy vasculature, at least short-term.

Effect of surgical bone marrow denervation on vascular permeability in ischemia-damaged retina. Male Wistar rats underwent a denervation surgery and were allowed to heal for 4-5 days before the ischemia-reperfusion (I/R) procedure. First, we confirmed that I/R caused damage and stimulated permeability (Fig. 30 A and B). I/R caused 58% increase in permeability in the ischemic retina compared to collateral intact retina.

Most importantly, when BM denervation was followed by retinal ischemia, we observed 47% significant increase in retinal vascular permeability in the ischemic retinas of animals that underwent surgical denervation as compared to ischemic retinas of sham controls (Fig. 30 B and D). This data demonstrates that to fully mimic the pathology occurring in diabetes, both initial damage and the lack of repair are required.

Figure 30: Bone marrow denervation coupled with retina ischemia leads to increased vascular permeability. Vascular permeability was determined in the retinas by intravenous injection of FITC-labeled bovine albumin (100mg/kg body weight). Animals were sacrificed after two hours and retinas were either fixed with formaldehyde for confocal microscopy (A-D) or homogenized for permeability quantitation (E).

Representative images show albumin extravasation out of capillaries in the retina.

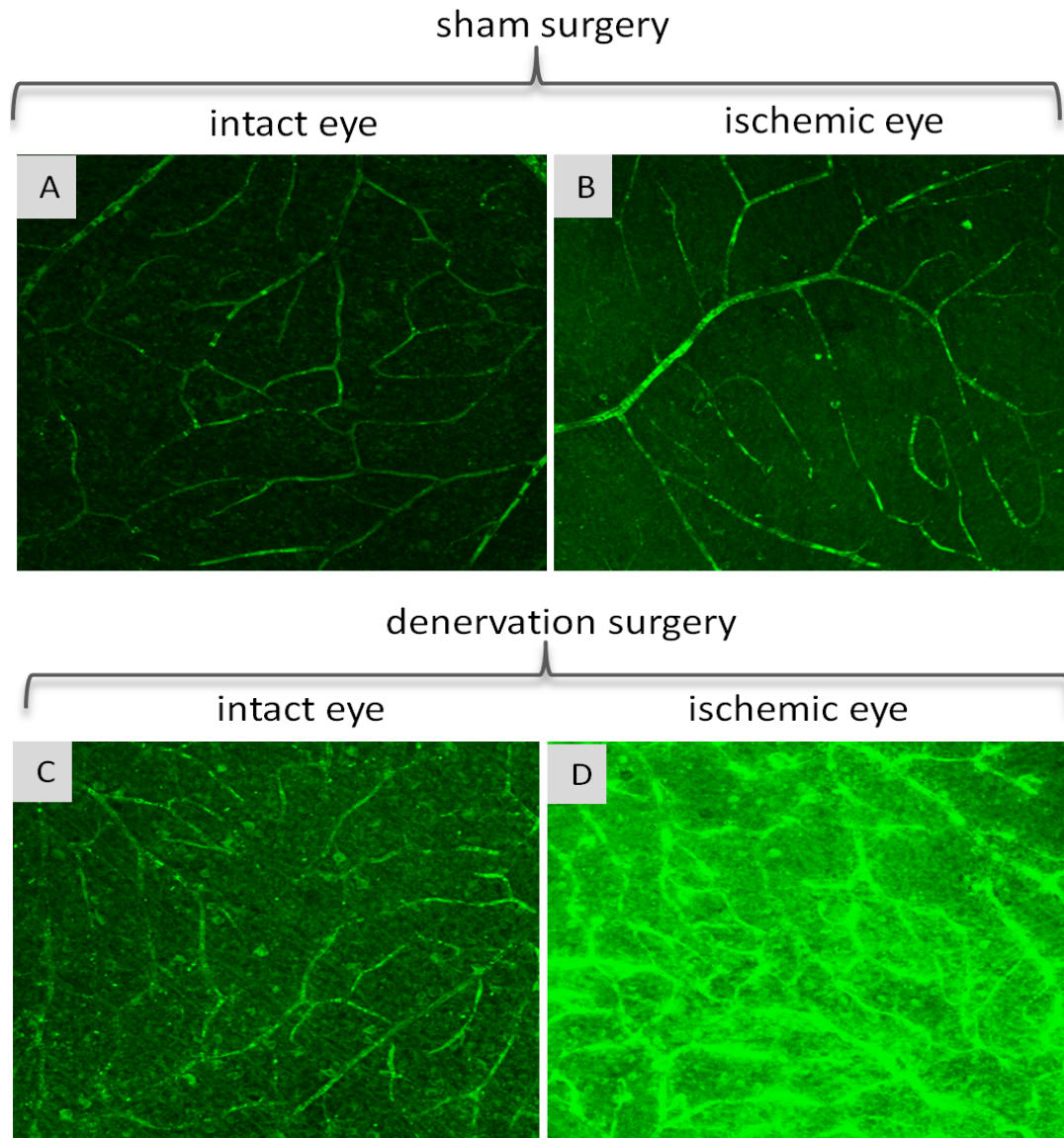
(A and C) There was no significant difference in permeability of intact eyes in animals with sham surgery (A) compared with animals with denervated bone marrow (C).

(B and D) However, in ischemia - injured retinas, lack of bone marrow innervation led to significant increase in permeability (D) compare to sham controls (B), confirming inability to repair damaged vasculature.

(E) Data shown is the mean \pm SD, n=4 rats with sham surgery and n=5 rats with denervation surgery.

* =P < 0.05

Figure 30 (cont'd)



5.3 Discussion

In Chapter III, we demonstrated that the loss of nerve fibers in diabetic BM preceded vascular pathology. We then postulated that the loss of nerve fibers in the diabetic BM leads to EPCs being trapped within the BM preventing efficient mobilization and recruitment to sites of injury. If true, the surgical denervation of the BM will result in an inability to repair damaged vasculature.

However, there are discrepancies between studies describing the effects of sympathectomy on cell release from the BM: it was shown to affect cell mobilization [115], or have no clear effect at all [116]. The first work published in 1997 by Afan *et al.* [115] has demonstrated that mechanical denervation of murine BM resulted in changes in both BM and blood cellularity, arguing for control of mobilization by the nervous system. However, later in 1998, Benestad *et al.* [116] found no clear indication that BM innervation influences cell production and release. Although the reason for this discrepancy is not clear, authors of the first paper argued that in the study by Benestad *et al.*, the sciatic nerve was cut at the level of the sciatic notch, while to produce complete denervation it has to be cut at the exit from the spine.

To study the effect of surgical BM denervation on EPC reparative function in the retina, we used vascular permeability as a measure of retinal microvascular health. Vascular permeability increase in the retina is a well-documented parameter of the vascular damage in DR [13, 226-230] and it has been shown to increase after only one week of diabetes [12-14]. Leaky endothelial junctions are associated with endothelial cell death and an inability to replace dead cells in diabetic vasculature.

Non-diabetic control rats were used in this experiment, allowing us to study the direct effect of the denervation without the other pathologies associated with diabetes. We found no difference in the retinal vascular permeability of animals subjected to surgical BM denervation compared to sham control (Fig. 30 A and C). We reasoned that the lack of repair is not detectable unless the vasculature has been previously damaged by diabetes-related pathology such as ischemia. To support this concept, we used a well-established model of accelerated ischemia/reperfusion injury that causes capillary degeneration analogous to DR [231]. Indeed, when BM denervation was coupled with retinal ischemia, we observed a significant increase in retinal vascular permeability in animals that underwent surgical denervation as compared to controls (Fig. 30 B and D). This study is the first direct demonstration of the role of the BM in the endothelial repair in the retina. Our data strongly support the hypothesis that BM neuropathy plays an important role in the diminished repair of retinal blood vessel in diabetes. This study provides novel insights into the potential therapeutic use of EPCs.

We conclude that understanding BM pathology in diabetes can lead to the development of new therapeutic strategies for DR.

5.4 Methods

Surgical denervation. All procedures involving the animal models adhered to the ARVO statement for the Use of animals in Ophthalmic and Vision research. Under isofluorane anesthesia, the femoral nerves were sectioned close to their exit from the spinal cord as described earlier [112, 115]. Sham surgery (the nerves are exposed, but not sectioned) was performed on a control group.

Retinal ischemia-reperfusion (I/R). We used ischemia-reperfusion (I/R) as accelerated model of non-proliferative DR. In this model, inflammatory changes and increased permeability in the retina can be seen as early as 2 days after the injury. Retinal ischemia-reperfusion (I/R) was created in one eye of each rat by increase in intraocular pressure to 90 mm Hg for 90 min as previously described [231, 232]. Retina from the opposite eye was used as a control. Blood-retinal permeability was measured 48 hours after I/R using a modification of method described by Xu *et al* [14]. Under anesthesia, rats received a tail vein injection of 100mg/kg body weight of FITC-conjugated BSA (Sigma) in PBS. Two hours later, animals were anesthetized again and 1ml of blood was drawn from tail artery for plasma FITC measurement. Chest cavity was open and the heart was perfused with 1% formaldehyde in warm saline.

Retinal permeability. Retinas were collected, weighted and homogenized in 1% Triton X (Sigma) in PBS. The homogenate was centrifuged and the supernatant used fluorescence measurement with infinite M1000 plate reader (Tecan). The retina permeability was calculated as intraretinal dye accumulation using the equation [retinal FITC-albumin concentration/ (retinal weight × blood FITC-albumin concentration × circulation time)]. The confocal fluorescent images were collected on an Olympus

FluoView FV1000 Confocal Laser Scanning Microscope (Olympus America, Inc., Center Valley, PA) configured on a fully automated Olympus IX81 inverted microscope using the 20x dry UPFLN (NA 0.7) objective. The green FITC fluorescence was excited using the 488nm Argon laser line and the emission was collected using a 505nm long pass filter. Brightfield transmitted laser light images were also collected using the 488nm Argon laser line. Maximum Intensity Projection images were generated from a series of confocal images collected through a 15 micron thickness using 3 micron step size.

Chapter VI

Summary and future perspectives

In summary, this study is the first to describe the fundamental dual mechanism of DR development with the key steps being premature death of endothelial cells due to inflammation and decreased ability to repair the injured vasculature due to reduced numbers and function of EPCs.

Diabetes is characterized by a systemic low-grade inflammatory state. Here, we are the first to demonstrate that in a type 1 model of diabetes that the expression of fatty acid elongases involved in n3 PUFA biosynthesis are decreased. This decrease in the expression of elongases results in a significant decrease in DHA, the major anti-inflammatory n3 PUFA in the retina as well as in decreased incorporation of VLCPUFA, particularly 32:6n3, into retinal phosphatidylcholine. Furthermore, the decrease in n3 PUFAs was associated with a pro-inflammatory cytokine profile in the retina.

Our study provides an important mechanistic understanding of the origin of n3 PUFA deficiency in the diabetic retina. Normalization of retinal fatty acid levels by modulating the expression of elongases and/or dietary supplementation with n3 PUFAs represents a potential target for the treatment of diabetes-induced inflammation.

In fact, we have established that dietary supplementation with DHA reduced the markers of retinal inflammation and prevented diabetic retinal capillary loss in both type 1 diabetes [105] and type 2 diabetes (Chapter IV) models. We have found that the beneficial effect of n3 PUFA could be due to inhibition of ASM in the retina.

Diabetes-induced vascular injury can be repaired by EPCs, a minor subpopulation of the mononuclear cells that are recruited from the BM, migrate to the sites of vascular damage and contribute to the viability of the retinal vasculature. Importantly, we demonstrated that the amplitude of EPC release from the BM into the circulation is significantly reduced in diabetes. Although peripheral and autonomic neuropathy is well described in diabetes, we are the first to demonstrate pronounced neuropathy in diabetic BM. Moreover, early changes in the BM preceded the development of DR, which suggests that the lack of sympathetic BM innervation is a causative factor in the deficiency of EPC-mediated vascular repair. In patients, this loss of EPC release may have a far-reaching impact on their ability to repair vasculature.

Despite the recognized EPC dysfunction in diabetes, there is no information on the influence of diabetic dyslipidemia on EPCs, particularly on the effect of n3 PUFAs on EPC function. In a type 2 diabetes model, we found that animals on a DHA-rich diet had increased numbers of EPCs in the circulation with improved colony formation capability. Taken together, this data suggests that DHA plays a distinct dual role, positively affecting both the local retinal and EPCs health. Dietary n3 PUFAs are a promising therapeutic target for stimulating EPC-mediated repair of retinal vasculature.

Furthermore, we have demonstrated that a DHA-rich diet prevents the increase of ASM activity in diabetic EPCs, suggesting that improvement of diabetic EPC function is through the inhibitory effect of DHA on ASM. Even though the physiologic mechanism by which the inhibition of ASM in EPCs could promote migration and proliferation is not known, participation of sphingolipids in membrane compartmentalization may play a

role. Future studies will shed light on the role of activated sphingolipid metabolism in EPCs in DR.

Our study provides important *in vitro* data describing the beneficial effects of DHA on EPC migration and function. However, continued investigation is required to test whether the inhibition of ASM is a central mechanism in the DHA-induced improvement of diabetic EPC function. Further studies will have to confirm that DHA pretreatment affects EPC incorporation in the retina *in vivo*. For example, a study may determine and compare the effect of ASM inhibition by DHA, pharmacological inhibitors or siRNA on migration and proliferation of diabetic EPC. Although these are important questions, they are beyond the scope of this dissertation.

To establish a direct link between BM pathology and DR, we examined the effect of surgical BM denervation on the ability to repair damaged vasculature in the retina. As expected, animals with denervated BM could not restore vascular integrity in ischemia-damaged retina and had increased vascular permeability compared to animals with intact BM. This data strengthens the importance of EPC dysfunction in the development of DR, highlighting that the combination of endothelial damage and lack of EPC repair is required for the development of DR. We concluded that BM pathology represents an underlying mechanism and potential therapeutic target for DR.

We leave our reader with the view that both endothelial damage and EPC dysfunction are critical for the development of the vasodegenerative phase of DR. We conclude that preventing the initial inflammation-induced injury, stimulating EPC-mediated repair, or combining both approaches would lead to effective therapy for DR.

REFERENCES

REFERENCES

1. King, H., R.E. Aubert, and W.H. Herman, *Global burden of diabetes, 1995-2025: prevalence, numerical estimates, and projections*. *Diabetes Care*, 1998. **21**(9): p. 1414-31.
2. *Estimated Diabetes Costs in the United States in 2007*. 2007; Available from: <http://diabetes.niddk.nih.gov/dm/pubs/statistics/index.htm#costs>.
3. Klein, R., et al., *The Wisconsin Epidemiologic Study of diabetic retinopathy. XIV. Ten-year incidence and progression of diabetic retinopathy*. *Arch Ophthalmol*, 1994. **112**(9): p. 1217-28.
4. Aiello, L.P., et al., *Diabetic retinopathy*. *Diabetes Care*, 1998. **21**(1): p. 143-56.
5. *Retinopathy and nephropathy in patients with type 1 diabetes four years after a trial of intensive therapy. The Diabetes Control and Complications Trial/Epidemiology of Diabetes Interventions and Complications Research Group*. *N Engl J Med*, 2000. **342**(6): p. 381-9.
6. Tumosa, N., *Eye disease and the older diabetic*. *Clinics in geriatric medicine*, 2008. **24**(3): p. 515-27, vii.
7. Brownlee, M., *Biochemistry and molecular cell biology of diabetic complications*. *Nature*, 2001. **414**(6865): p. 813-20.
8. Barber, A.J., *A new view of diabetic retinopathy: a neurodegenerative disease of the eye*. *Prog Neuropsychopharmacol Biol Psychiatry*, 2003. **27**(2): p. 283-90.
9. Mizutani, M., T.S. Kern, and M. Lorenzi, *Accelerated death of retinal microvascular cells in human and experimental diabetic retinopathy*. *J Clin Invest*, 1996. **97**(12): p. 2883-90.
10. Jousen, A.M., et al., *Leukocyte-mediated endothelial cell injury and death in the diabetic retina*. *Am J Pathol*, 2001. **158**(1): p. 147-52.
11. Antonetti, D.A., et al., *Molecular mechanisms of vascular permeability in diabetic retinopathy*. *Semin Ophthalmol*, 1999. **14**(4): p. 240-8.
12. Qaum, T., et al., *VEGF-initiated blood-retinal barrier breakdown in early diabetes*. *Invest Ophthalmol Vis Sci*, 2001. **42**(10): p. 2408-13.
13. Williamson, J.R., et al., *Increased vascular permeability in spontaneously diabetic BB/W rats and in rats with mild versus severe streptozocin-induced diabetes. Prevention by aldose reductase inhibitors and castration*. *Diabetes*, 1987. **36**(7): p. 813-21.
14. Xu, Q., T. Qaum, and A.P. Adamis, *Sensitive blood-retinal barrier breakdown quantitation using Evans blue*. *Invest Ophthalmol Vis Sci*, 2001. **42**(3): p. 789-94.
15. Frey, T.A. and D.A. Antonetti, *Alterations to the Blood-Retinal Barrier in Diabetes: Cytokines and Reactive Oxygen Species*. *Antioxid Redox Signal*.

16. Antonetti, D.A., et al., *Vascular permeability in experimental diabetes is associated with reduced endothelial occludin content: vascular endothelial growth factor decreases occludin in retinal endothelial cells*. Penn State Retina Research Group. *Diabetes*, 1998. **47**(12): p. 1953-9.
17. Frank, R.N., *Diabetic retinopathy*. *N Engl J Med*, 2004. **350**(1): p. 48-58.
18. Powell, E.D. and R.A. Field, *Diabetic Retinopathy and Rheumatoid Arthritis*. *Lancet*, 1964. **41**: p. 17-8.
19. Kern, T.S. and R.L. Engerman, *Pharmacological inhibition of diabetic retinopathy: aminoguanidine and aspirin*. *Diabetes*, 2001. **50**(7): p. 1636-42.
20. Adamis, A.P., *Is diabetic retinopathy an inflammatory disease?* *Br J Ophthalmol*, 2002. **86**(4): p. 363-5.
21. Miyamoto, K., et al., *Prevention of leukostasis and vascular leakage in streptozotocin-induced diabetic retinopathy via intercellular adhesion molecule-1 inhibition*. *Proc Natl Acad Sci U S A*, 1999. **96**(19): p. 10836-41.
22. MacKinnon, J.R., R.M. Knott, and J.V. Forrester, *Altered L-selectin expression in lymphocytes and increased adhesion to endothelium in patients with diabetic retinopathy*. *Br J Ophthalmol*, 2004. **88**(9): p. 1137-41.
23. Adamis, A.P., et al., *Increased vascular endothelial growth factor levels in the vitreous of eyes with proliferative diabetic retinopathy*. *Am J Ophthalmol*, 1994. **118**(4): p. 445-50.
24. Murata, T., et al., *The relation between expression of vascular endothelial growth factor and breakdown of the blood-retinal barrier in diabetic rat retinas*. *Lab Invest*, 1996. **74**(4): p. 819-25.
25. Aiello, L.P., et al., *Suppression of retinal neovascularization in vivo by inhibition of vascular endothelial growth factor (VEGF) using soluble VEGF-receptor chimeric proteins*. *Proc Natl Acad Sci U S A*, 1995. **92**(23): p. 10457-61.
26. Aiello, L.P., et al., *Hypoxic regulation of vascular endothelial growth factor in retinal cells*. *Arch Ophthalmol*, 1995. **113**(12): p. 1538-44.
27. Busik, J.V., S. Mohr, and M.B. Grant, *Hyperglycemia-induced reactive oxygen species toxicity to endothelial cells is dependent on paracrine mediators*. *Diabetes*, 2008. **57**(7): p. 1952-65.
28. Famiglietti, E.V., et al., *Immunocytochemical localization of vascular endothelial growth factor in neurons and glial cells of human retina*. *Brain Res*, 2003. **969**(1-2): p. 195-204.
29. Ellis, E.A., et al., *Increased H₂O₂, vascular endothelial growth factor and receptors in the retina of the BBZ/Wor diabetic rat*. *Free Radic Biol Med*, 2000. **28**(1): p. 91-101.
30. Jousseaume, A.M., et al., *Retinal vascular endothelial growth factor induces intercellular adhesion molecule-1 and endothelial nitric oxide synthase expression and initiates early diabetic retinal leukocyte adhesion in vivo*. *Am J Pathol*, 2002. **160**(2): p. 501-9.

31. Adamis, A.P., et al., *Changes in retinal neovascularization after pegaptanib (Macugen) therapy in diabetic individuals*. *Ophthalmology*, 2006. **113**(1): p. 23-8.
32. Arevalo, J.F., et al., *Primary intravitreal bevacizumab for the management of pseudophakic cystoid macular edema: pilot study of the Pan-American Collaborative Retina Study Group*. *J Cataract Refract Surg*, 2007. **33**(12): p. 2098-105.
33. Ng, E.W. and A.P. Adamis, *Anti-VEGF aptamer (pegaptanib) therapy for ocular vascular diseases*. *Ann N Y Acad Sci*, 2006. **1082**: p. 151-71.
34. Navarro, J.F. and C. Mora-Fernandez, *The role of TNF-alpha in diabetic nephropathy: pathogenic and therapeutic implications*. *Cytokine Growth Factor Rev*, 2006. **17**(6): p. 441-50.
35. Jousseaume, A.M., et al., *Nonsteroidal anti-inflammatory drugs prevent early diabetic retinopathy via TNF-alpha suppression*. *FASEB J*, 2002. **16**(3): p. 438-40.
36. Jousseaume, A.M., et al., *TNF-alpha mediated apoptosis plays an important role in the development of early diabetic retinopathy and long-term histopathological alterations*. *Mol Vis*, 2009. **15**: p. 1418-28.
37. Kowluru, R.A. and S. Odenbach, *Role of interleukin-1beta in the pathogenesis of diabetic retinopathy*. *Br J Ophthalmol*, 2004. **88**(10): p. 1343-7.
38. Vincent, J.A. and S. Mohr, *Inhibition of caspase-1/interleukin-1beta signaling prevents degeneration of retinal capillaries in diabetes and galactosemia*. *Diabetes*, 2007. **56**(1): p. 224-30.
39. Hong, D.S., L.S. Angelo, and R. Kurzrock, *Interleukin-6 and its receptor in cancer: implications for translational therapeutics*. *Cancer*, 2007. **110**(9): p. 1911-28.
40. Huber, S.A., et al., *Interleukin-6 exacerbates early atherosclerosis in mice*. *Arterioscler Thromb Vasc Biol*, 1999. **19**(10): p. 2364-7.
41. Mocan, M.C., S. Kadayifcilar, and B. Eldem, *Elevated intravitreal interleukin-6 levels in patients with proliferative diabetic retinopathy*. *Can J Ophthalmol*, 2006. **41**(6): p. 747-52.
42. Funatsu, H., et al., *Relationship between vascular endothelial growth factor and interleukin-6 in diabetic retinopathy*. *Retina*, 2001. **21**(5): p. 469-77.
43. Izumi-Nagai, K., et al., *Interleukin-6 receptor-mediated activation of signal transducer and activator of transcription-3 (STAT3) promotes choroidal neovascularization*. *Am J Pathol*, 2007. **170**(6): p. 2149-58.
44. Rojas, M., et al., *Role of IL-6 in angiotensin II-induced retinal vascular inflammation*. *Invest Ophthalmol Vis Sci*, 2010. **51**(3): p. 1709-18.
45. Kreisberg, R.A., *Diabetic dyslipidemia*. *Am J Cardiol*, 1998. **82**(12A): p. 67U-73U; discussion 85U-86U.

46. *The effect of intensive treatment of diabetes on the development and progression of long-term complications in insulin-dependent diabetes mellitus. The Diabetes Control and Complications Trial Research Group.* N Engl J Med, 1993. **329**(14): p. 977-86.
47. Vijan, S. and R.A. Hayward, *Pharmacologic lipid-lowering therapy in type 2 diabetes mellitus: background paper for the American College of Physicians.* Ann Intern Med, 2004. **140**(8): p. 650-8.
48. Kearney, P.M., et al., *Efficacy of cholesterol-lowering therapy in 18,686 people with diabetes in 14 randomised trials of statins: a meta-analysis.* Lancet, 2008. **371**(9607): p. 117-25.
49. Natarajan, R. and J.L. Nadler, *Lipid inflammatory mediators in diabetic vascular disease.* Arterioscler Thromb Vasc Biol, 2004. **24**(9): p. 1542-8.
50. Ferris, F.L., 3rd, E.Y. Chew, and B.J. Hoogwerf, *Serum lipids and diabetic retinopathy. Early Treatment Diabetic Retinopathy Study Research Group.* Diabetes Care, 1996. **19**(11): p. 1291-3.
51. Coppack, S.W., et al., *Adipose tissue metabolism in obesity: lipase action in vivo before and after a mixed meal.* Metabolism, 1992. **41**(3): p. 264-72.
52. Wang, Y., et al., *Regulation of hepatic fatty acid elongase and desaturase expression in diabetes and obesity.* J Lipid Res, 2006. **47**(9): p. 2028-41.
53. Poisson, J.P., *Essential fatty acid metabolism in diabetes.* Nutrition, 1989. **5**(4): p. 263-6.
54. Brenner, R.R., A.M. Bernasconi, and H.A. Garda, *Effect of experimental diabetes on the fatty acid composition, molecular species of phosphatidyl-choline and physical properties of hepatic microsomal membranes.* Prostaglandins Leukot Essent Fatty Acids, 2000. **63**(3): p. 167-76.
55. Weinstock, P.H., et al., *Lipoprotein lipase controls fatty acid entry into adipose tissue, but fat mass is preserved by endogenous synthesis in mice deficient in adipose tissue lipoprotein lipase.* Proc Natl Acad Sci U S A, 1997. **94**(19): p. 10261-6.
56. Mohamed, Q., M.C. Gillies, and T.Y. Wong, *Management of diabetic retinopathy: a systematic review.* JAMA, 2007. **298**(8): p. 902-16.
57. Roden, M., et al., *Mechanism of free fatty acid-induced insulin resistance in humans.* J Clin Invest, 1996. **97**(12): p. 2859-65.
58. Decsi, T., et al., *Polyunsaturated fatty acids in plasma and erythrocyte membrane lipids of diabetic children.* Prostaglandins Leukot Essent Fatty Acids, 2002. **67**(4): p. 203-10.
59. Dullaart, R.P., *Plasma lipoprotein abnormalities in type 1 (insulin-dependent) diabetes mellitus.* Neth J Med, 1995. **46**(1): p. 44-54.
60. Seigneur, M., et al., *Serum fatty acid profiles in type I and type II diabetes: metabolic alterations of fatty acids of the main serum lipids.* Diabetes Res Clin Pract, 1994. **23**(3): p. 169-77.

61. Ruiz-Gutierrez, V., et al., *Cell membrane fatty acid composition in type 1 (insulin-dependent) diabetic patients: relationship with sodium transport abnormalities and metabolic control*. Diabetologia, 1993. **36**(9): p. 850-6.
62. Lyons, T.J., et al., *Diabetic retinopathy and serum lipoprotein subclasses in the DCCT/EDIC cohort*. Invest Ophthalmol Vis Sci, 2004. **45**(3): p. 910-8.
63. Chew, E.Y., et al., *Association of elevated serum lipid levels with retinal hard exudate in diabetic retinopathy. Early Treatment Diabetic Retinopathy Study (ETDRS) Report 22*. Arch Ophthalmol, 1996. **114**(9): p. 1079-84.
64. Van Eck, W.F., *The effect of a low fat diet on the serum lipids in diabetes and its significance in diabetic retinopathy*. Am J Med, 1959. **27**: p. 196-211.
65. Duncan, L.J., et al., *A three-year trial of atromid therapy in exudative diabetic retinopathy*. Diabetes, 1968. **17**(7): p. 458-67.
66. Chew, E.Y., et al., *Effects of medical therapies on retinopathy progression in type 2 diabetes*. The New England journal of medicine, 2010. **363**(3): p. 233-44.
67. Houtsmuller, A.J., K.J. Zahn, and H.E. Henkes, *Unsaturated fats and progression of diabetic retinopathy*. Doc Ophthalmol, 1980. **48**(2): p. 363-71.
68. Connor, K.M., et al., *Increased dietary intake of omega-3-polyunsaturated fatty acids reduces pathological retinal angiogenesis*. Nat Med, 2007. **13**(7): p. 868-73.
69. Sprecher, H. and Q. Chen, *Polyunsaturated fatty acid biosynthesis: a microsomal-peroxisomal process*. Prostaglandins Leukot Essent Fatty Acids, 1999. **60**(5-6): p. 317-21.
70. Hillgartner, F.B., L.M. Salati, and A.G. Goodridge, *Physiological and molecular mechanisms involved in nutritional regulation of fatty acid synthesis*. Physiol Rev, 1995. **75**(1): p. 47-76.
71. Brown, J.E., R.M. Lindsay, and R.A. Riemersma, *Linoleic acid metabolism in the spontaneously diabetic rat: delta6-desaturase activity vs. product/precursor ratios*. Lipids, 2000. **35**(12): p. 1319-23.
72. Brenner, R.R., *Hormonal modulation of delta6 and delta5 desaturases: case of diabetes*. Prostaglandins Leukot Essent Fatty Acids, 2003. **68**(2): p. 151-62.
73. Vessby, B., *Dietary fat and insulin action in humans*. Br J Nutr, 2000. **83 Suppl 1**: p. S91-6.
74. Wang, Y., et al., *Elevated hepatic fatty acid elongase-5 activity affects multiple pathways controlling hepatic lipid and carbohydrate composition*. J Lipid Res, 2008. **49**(7): p. 1538-52.
75. Wang, Y., et al., *Tissue-specific, nutritional, and developmental regulation of rat fatty acid elongases*. J Lipid Res, 2005. **46**(4): p. 706-15.

76. SanGiovanni, J.P. and E.Y. Chew, *The role of omega-3 long-chain polyunsaturated fatty acids in health and disease of the retina*. Prog Retin Eye Res, 2005. **24**(1): p. 87-138.
77. Chen, W., et al., *Anti-inflammatory effect of docosahexaenoic acid on cytokine-induced adhesion molecule expression in human retinal vascular endothelial cells*. Invest Ophthalmol Vis Sci, 2005. **46**(11): p. 4342-7.
78. Chaudhary, R., J.O. Lee, and K. Muralidhar, *Simultaneous isolation of prolactin and growth hormone from "discarded acid pellet" obtained from buffalo pituitaries*. Prep Biochem Biotechnol, 2004. **34**(4): p. 331-43.
79. Calder, P.C., *N-3 polyunsaturated fatty acids and inflammation: from molecular biology to the clinic*. Lipids, 2003. **38**(4): p. 343-52.
80. McLennan, P., et al., *The cardiovascular protective role of docosahexaenoic acid*. Eur J Pharmacol, 1996. **300**(1-2): p. 83-9.
81. Kremer, J.M., et al., *Dietary fish oil and olive oil supplementation in patients with rheumatoid arthritis. Clinical and immunologic effects*. Arthritis Rheum, 1990. **33**(6): p. 810-20.
82. Yokoyama, A., et al., *Effect of aerosolized docosahexaenoic acid in a mouse model of atopic asthma*. Int Arch Allergy Immunol, 2000. **123**(4): p. 327-32.
83. Calder, P.C., *n-3 polyunsaturated fatty acids, inflammation, and inflammatory diseases*. Am J Clin Nutr, 2006. **83**(6 Suppl): p. 1505S-1519S.
84. Chen, W., et al., *Inhibition of cytokine signaling in human retinal endothelial cells through modification of caveolae/lipid rafts by docosahexaenoic acid*. Invest Ophthalmol Vis Sci, 2007. **48**(1): p. 18-26.
85. Chen, W., et al., *Dyslipidemia, but not hyperglycemia, induces inflammatory adhesion molecules in human retinal vascular endothelial cells*. Invest Ophthalmol Vis Sci, 2003. **44**(11): p. 5016-22.
86. Tilvis, R.S. and T.A. Miettinen, *Fatty acid compositions of serum lipids, erythrocytes, and platelets in insulin-dependent diabetic women*. J Clin Endocrinol Metab, 1985. **61**(4): p. 741-5.
87. Simopoulos, A.P., *Importance of the ratio of omega-6/omega-3 essential fatty acids: evolutionary aspects*. World Rev Nutr Diet, 2003. **92**: p. 1-22.
88. Simopoulos, A.P., *Omega-6/omega-3 fatty acid ratio and trans fatty acids in non-insulin-dependent diabetes mellitus*. Ann N Y Acad Sci, 1997. **827**: p. 327-38.
89. Anderson, R.E., *Lipids of ocular tissues. IV. A comparison of the phospholipids from the retina of six mammalian species*. Exp Eye Res, 1970. **10**(2): p. 339-44.
90. Lecomte, M., et al., *Docosahexaenoic acid is a major n-3 polyunsaturated fatty acid in bovine retinal microvessels*. J Neurochem, 1996. **66**(5): p. 2160-7.

91. Tikhonenko, M., et al., *Remodeling of retinal Fatty acids in an animal model of diabetes: a decrease in long-chain polyunsaturated fatty acids is associated with a decrease in fatty acid elongases Elovl2 and Elovl4*. *Diabetes*, 2010. **59**(1): p. 219-27.
92. Goldberg, R.B. and D. Capuzzi, *Lipid disorders in type 1 and type 2 diabetes*. *Clin Lab Med*, 2001. **21**(1): p. 147-72, vii.
93. Jakobsson, A., R. Westerberg, and A. Jacobsson, *Fatty acid elongases in mammals: their regulation and roles in metabolism*. *Prog Lipid Res*, 2006. **45**(3): p. 237-49.
94. Leonard, A.E., et al., *Elongation of long-chain fatty acids*. *Prog Lipid Res*, 2004. **43**(1): p. 36-54.
95. Jump, D.B., *Mammalian fatty acid elongases*. *Methods Mol Biol*, 2009. **579**: p. 375-89.
96. Agbaga, M.P., et al., *Role of Stargardt-3 macular dystrophy protein (ELOVL4) in the biosynthesis of very long chain fatty acids*. *Proc Natl Acad Sci U S A*, 2008. **105**(35): p. 12843-8.
97. Edidin, M., *The state of lipid rafts: from model membranes to cells*. *Annu Rev Biophys Biomol Struct*, 2003. **32**: p. 257-83.
98. Miyawaki-Shimizu, K., et al., *siRNA-induced caveolin-1 knockdown in mice increases lung vascular permeability via the junctional pathway*. *Am J Physiol Lung Cell Mol Physiol*, 2006. **290**(2): p. L405-13.
99. Li, S., K.S. Song, and M.P. Lisanti, *Expression and characterization of recombinant caveolin. Purification by polyhistidine tagging and cholesterol-dependent incorporation into defined lipid membranes*. *J Biol Chem*, 1996. **271**(1): p. 568-73.
100. Lisanti, M.P., et al., *Caveolae, transmembrane signalling and cellular transformation*. *Mol Membr Biol*, 1995. **12**(1): p. 121-4.
101. Marchesini, N. and Y.A. Hannun, *Acid and neutral sphingomyelinases: roles and mechanisms of regulation*. *Biochem Cell Biol*, 2004. **82**(1): p. 27-44.
102. Liu, P. and R.G. Anderson, *Compartmentalized production of ceramide at the cell surface*. *J Biol Chem*, 1995. **270**(45): p. 27179-85.
103. Martin, M.U. and H. Wesche, *Summary and comparison of the signaling mechanisms of the Toll/interleukin-1 receptor family*. *Biochim Biophys Acta*, 2002. **1592**(3): p. 265-80.
104. Opreanu, M., et al., *Inhibition of cytokine signaling in human retinal endothelial cells through downregulation of sphingomyelinases by docosahexaenoic acid*. *Invest Ophthalmol Vis Sci*, 2010. **51**(6): p. 3253-63.
105. Opreanu, M., et al., *The unconventional role of acid sphingomyelinase in regulation of retinal microangiopathy in diabetic human and animal models*. *Diabetes*, 2011. **60**(9): p. 2370-8.
106. Grant, M.B., et al., *Adult hematopoietic stem cells provide functional hemangioblast activity during retinal neovascularization*. *Nat Med*, 2002. **8**(6): p. 607-12.

107. Asahara, T., et al., *Isolation of putative progenitor endothelial cells for angiogenesis*. Science, 1997. **275**(5302): p. 964-7.
108. Urbich, C. and S. Dimmeler, *Endothelial progenitor cells: characterization and role in vascular biology*. Circ Res, 2004. **95**(4): p. 343-53.
109. Hirschi, K.K., D.A. Ingram, and M.C. Yoder, *Assessing identity, phenotype, and fate of endothelial progenitor cells*. Arterioscler Thromb Vasc Biol, 2008. **28**(9): p. 1584-95.
110. Loomans, C.J., et al., *Angiogenic murine endothelial progenitor cells are derived from a myeloid bone marrow fraction and can be identified by endothelial NO synthase expression*. Arterioscler Thromb Vasc Biol, 2006. **26**(8): p. 1760-7.
111. Schatteman, G.C., M. Dunnwald, and C. Jiao, *Biology of bone marrow-derived endothelial cell precursors*. Am J Physiol Heart Circ Physiol, 2007. **292**(1): p. H1-18.
112. Mendez-Ferrer, S., et al., *Haematopoietic stem cell release is regulated by circadian oscillations*. Nature, 2008. **452**(7186): p. 442-7.
113. Lapidot, T., A. Dar, and O. Kollet, *How do stem cells find their way home?* Blood, 2005. **106**(6): p. 1901-10.
114. Yamaguchi, J., et al., *Stromal cell-derived factor-1 effects on ex vivo expanded endothelial progenitor cell recruitment for ischemic neovascularization*. Circulation, 2003. **107**(9): p. 1322-8.
115. Afan, A.M., et al., *Bone marrow innervation regulates cellular retention in the murine haematopoietic system*. Br J Haematol, 1997. **98**(3): p. 569-77.
116. Benestad, H.B., et al., *No neuronal regulation of murine bone marrow function*. Blood, 1998. **91**(4): p. 1280-7.
117. Grunewald, M., et al., *VEGF-induced adult neovascularization: recruitment, retention, and role of accessory cells*. Cell, 2006. **124**(1): p. 175-89.
118. Asahara, T., et al., *VEGF contributes to postnatal neovascularization by mobilizing bone marrow-derived endothelial progenitor cells*. The EMBO journal, 1999. **18**(14): p. 3964-72.
119. Aicher, A., A.M. Zeiher, and S. Dimmeler, *Mobilizing endothelial progenitor cells*. Hypertension, 2005. **45**(3): p. 321-5.
120. Heissig, B., et al., *Recruitment of stem and progenitor cells from the bone marrow niche requires MMP-9 mediated release of kit-ligand*. Cell, 2002. **109**(5): p. 625-37.
121. Gallagher, K.A., et al., *Diabetic impairments in NO-mediated endothelial progenitor cell mobilization and homing are reversed by hyperoxia and SDF-1 alpha*. J Clin Invest, 2007. **117**(5): p. 1249-59.

122. Loomans, C.J., et al., *Endothelial progenitor cell dysfunction: a novel concept in the pathogenesis of vascular complications of type 1 diabetes*. *Diabetes*, 2004. **53**(1): p. 195-9.
123. Fadini, G.P., et al., *Circulating endothelial progenitor cells are reduced in peripheral vascular complications of type 2 diabetes mellitus*. *J Am Coll Cardiol*, 2005. **45**(9): p. 1449-57.
124. Guthrie, S.M., et al., *The nitric oxide pathway modulates hemangioblast activity of adult hematopoietic stem cells*. *Blood*, 2005. **105**(5): p. 1916-22.
125. Caballero, S., et al., *Ischemic vascular damage can be repaired by healthy, but not diabetic, endothelial progenitor cells*. *Diabetes*, 2007. **56**(4): p. 960-7.
126. Guerin, E., et al., *SDF1-alpha is associated with VEGFR-2 in human choroidal neovascularisation*. *Microvasc Res*, 2008. **75**(3): p. 302-7.
127. Otani, A., et al., *Bone marrow-derived stem cells target retinal astrocytes and can promote or inhibit retinal angiogenesis*. *Nat Med*, 2002. **8**(9): p. 1004-10.
128. Badiu, C., *Genetic clock of biologic rhythms*. *J Cell Mol Med*, 2003. **7**(4): p. 408-16.
129. Panda, S. and J.B. Hogenesch, *It's all in the timing: many clocks, many outputs*. *J Biol Rhythms*, 2004. **19**(5): p. 374-87.
130. Hastings, M.H., A.B. Reddy, and E.S. Maywood, *A clockwork web: circadian timing in brain and periphery, in health and disease*. *Nat Rev Neurosci*, 2003. **4**(8): p. 649-61.
131. Ptitsyn, A.A., S. Zvonic, and J.M. Gimble, *Digital signal processing reveals circadian baseline oscillation in majority of mammalian genes*. *PLoS Comput Biol*, 2007. **3**(6): p. e120.
132. Shaw, P.J., et al., *Stress response genes protect against lethal effects of sleep deprivation in Drosophila*. *Nature*, 2002. **417**(6886): p. 287-91.
133. Weber, F., *Remodeling the clock: coactivators and signal transduction in the circadian clockworks*. *Naturwissenschaften*, 2009. **96**(3): p. 321-37.
134. Kohsaka, A., et al., *High-fat diet disrupts behavioral and molecular circadian rhythms in mice*. *Cell Metab*, 2007. **6**(5): p. 414-21.
135. Su, W., et al., *Hypertension and disrupted blood pressure circadian rhythm in type 2 diabetic db/db mice*. *Am J Physiol Heart Circ Physiol*, 2008. **295**(4): p. H1634-41.
136. Halberg, F. and M.B. Visscher, *Regular diurnal physiological variation in eosinophil levels in five stocks of mice*. *Proceedings of the Society for Experimental Biology and Medicine*. Society for Experimental Biology and Medicine, 1950. **75**(3): p. 846-7.
137. Segal, M.S., et al., *Nitric oxide cytoskeletal-induced alterations reverse the endothelial progenitor cell migratory defect associated with diabetes*. *Diabetes*, 2006. **55**(1): p. 102-9.

138. Tepper, O.M., et al., *Human endothelial progenitor cells from type II diabetics exhibit impaired proliferation, adhesion, and incorporation into vascular structures*. *Circulation*, 2002. **106**(22): p. 2781-6.
139. Sorrentino, S.A., et al., *Oxidant stress impairs in vivo reendothelialization capacity of endothelial progenitor cells from patients with type 2 diabetes mellitus: restoration by the peroxisome proliferator-activated receptor-gamma agonist rosiglitazone*. *Circulation*, 2007. **116**(2): p. 163-73.
140. Capla, J.M., et al., *Diabetes impairs endothelial progenitor cell-mediated blood vessel formation in response to hypoxia*. *Plast Reconstr Surg*, 2007. **119**(1): p. 59-70.
141. Ando, H., et al., *Rhythmic messenger ribonucleic acid expression of clock genes and adipocytokines in mouse visceral adipose tissue*. *Endocrinology*, 2005. **146**(12): p. 5631-6.
142. Schroder, S., W. Palinski, and G.W. Schmid-Schonbein, *Activated monocytes and granulocytes, capillary nonperfusion, and neovascularization in diabetic retinopathy*. *Am J Pathol*, 1991. **139**(1): p. 81-100.
143. Yang, L.P., et al., *Baicalein reduces inflammatory process in a rodent model of diabetic retinopathy*. *Invest Ophthalmol Vis Sci*, 2009. **50**(5): p. 2319-27.
144. Sone, H., et al., *Ocular vascular endothelial growth factor levels in diabetic rats are elevated before observable retinal proliferative changes*. *Diabetologia*, 1997. **40**(6): p. 726-30.
145. Nozaki, M., et al., *Enhanced expression of adhesion molecules of the retinal vascular endothelium in spontaneous diabetic rats*. *Ophthalmic research*, 2002. **34**(3): p. 158-64.
146. Al-Shabrawey, M., et al., *Role of NADPH oxidase in retinal vascular inflammation*. *Invest Ophthalmol Vis Sci*, 2008. **49**(7): p. 3239-44.
147. Gustavsson, C., et al., *Inflammatory markers in nondiabetic and diabetic rat retinas exposed to ischemia followed by reperfusion*. *Retina*, 2008. **28**(4): p. 645-52.
148. Julius, U., *Influence of plasma free fatty acids on lipoprotein synthesis and diabetic dyslipidemia*. *Experimental and clinical endocrinology & diabetes : official journal, German Society of Endocrinology [and] German Diabetes Association*, 2003. **111**(5): p. 246-50.
149. Lagali, P.S., et al., *Evolutionarily conserved ELOVL4 gene expression in the vertebrate retina*. *Invest Ophthalmol Vis Sci*, 2003. **44**(7): p. 2841-50.
150. Umeda, S., et al., *Molecular cloning of ELOVL4 gene from cynomolgus monkey (*Macaca fascicularis*)*. *Experimental animals / Japanese Association for Laboratory Animal Science*, 2003. **52**(2): p. 129-35.
151. Zhang, X.M., et al., *Elovl4 mRNA distribution in the developing mouse retina and phylogenetic conservation of Elovl4 genes*. *Molecular vision*, 2003. **9**: p. 301-7.

152. Grayson, C. and R.S. Molday, *Dominant negative mechanism underlies autosomal dominant Stargardt-like macular dystrophy linked to mutations in ELOVL4*. J Biol Chem, 2005. **280**(37): p. 32521-30.
153. Karan, G., et al., *Lipofuscin accumulation, abnormal electrophysiology, and photoreceptor degeneration in mutant ELOVL4 transgenic mice: a model for macular degeneration*. Proceedings of the National Academy of Sciences of the United States of America, 2005. **102**(11): p. 4164-9.
154. Zhang, K., et al., *A 5-bp deletion in ELOVL4 is associated with two related forms of autosomal dominant macular dystrophy*. Nature genetics, 2001. **27**(1): p. 89-93.
155. Nakamura, M.T. and T.Y. Nara, *Gene regulation of mammalian desaturases*. Biochemical Society transactions, 2002. **30**(Pt 6): p. 1076-9.
156. Rimoldi, O.J., G.S. Finarelli, and R.R. Brenner, *Effects of diabetes and insulin on hepatic delta6 desaturase gene expression*. Biochemical and biophysical research communications, 2001. **283**(2): p. 323-6.
157. Meyer, A., et al., *Novel fatty acid elongases and their use for the reconstitution of docosahexaenoic acid biosynthesis*. Journal of lipid research, 2004. **45**(10): p. 1899-909.
158. Futterman, S., R. Sturtevant, and C. Kupfer, *Effect of alloxan diabetes on the fatty acid composition of the retina*. Investigative ophthalmology, 1969. **8**(5): p. 542-4.
159. Hegde, K.R. and S.D. Varma, *Electron impact mass spectroscopic studies on mouse retinal fatty acids: effect of diabetes*. Ophthalmic research, 2009. **42**(1): p. 9-14.
160. Harbige, L.S., *Fatty acids, the immune response, and autoimmunity: a question of n-6 essentiality and the balance between n-6 and n-3*. Lipids, 2003. **38**(4): p. 323-41.
161. Lu, M., et al., *VEGF increases retinal vascular ICAM-1 expression in vivo*. Invest Ophthalmol Vis Sci, 1999. **40**(8): p. 1808-12.
162. Fliesler, S.J. and R.E. Anderson, *Chemistry and metabolism of lipids in the vertebrate retina*. Prog Lipid Res, 1983. **22**(2): p. 79-131.
163. Delton-Vandenbroucke, I., P. Grammas, and R.E. Anderson, *Polyunsaturated fatty acid metabolism in retinal and cerebral microvascular endothelial cells*. Journal of lipid research, 1997. **38**(1): p. 147-59.
164. Moon, Y.A., et al., *Identification of a mammalian long chain fatty acyl elongase regulated by sterol regulatory element-binding proteins*. J Biol Chem, 2001. **276**(48): p. 45358-66.
165. Sunada, S., et al., *Effect of docosahexaenoic acid intake on lipid peroxidation in diabetic rat retina under oxidative stress*. Free radical research, 2006. **40**(8): p. 837-46.
166. Barber, A.J., et al., *Neural apoptosis in the retina during experimental and human diabetes. Early onset and effect of insulin*. J Clin Invest, 1998. **102**(4): p. 783-91.

167. Gardner, T.W., et al., *New insights into the pathophysiology of diabetic retinopathy: potential cell-specific therapeutic targets*. Diabetes technology & therapeutics, 2000. **2**(4): p. 601-8.
168. Lydic, T.A., et al., *Complementary precursor ion and neutral loss scan mode tandem mass spectrometry for the analysis of glycerophosphatidylethanolamine lipids from whole rat retina*. Analytical and bioanalytical chemistry, 2009. **394**(1): p. 267-75.
169. Murphy, E.J., et al., *Acidic hydrolysis of plasmalogens followed by high-performance liquid chromatography*. Lipids, 1993. **28**(6): p. 565-8.
170. Rose, H.G. and M. Oklander, *Improved Procedure for the Extraction of Lipids from Human Erythrocytes*. Journal of lipid research, 1965. **6**: p. 428-31.
171. Han, X. and R.W. Gross, *Shotgun lipidomics: electrospray ionization mass spectrometric analysis and quantitation of cellular lipidomes directly from crude extracts of biological samples*. Mass spectrometry reviews, 2005. **24**(3): p. 367-412.
172. Haimi, P., et al., *Software tools for analysis of mass spectrometric lipidome data*. Analytical chemistry, 2006. **78**(24): p. 8324-31.
173. Weston, P.J. and G.V. Gill, *Is undetected autonomic dysfunction responsible for sudden death in Type 1 diabetes mellitus? The 'dead in bed' syndrome revisited*. Diabet Med, 1999. **16**(8): p. 626-31.
174. Ruiten, M., R.M. Buijs, and A. Kalsbeek, *Hormones and the autonomic nervous system are involved in suprachiasmatic nucleus modulation of glucose homeostasis*. Curr Diabetes Rev, 2006. **2**(2): p. 213-26.
175. Ikeda, H., et al., *Clock gene defect disrupts light-dependency of autonomic nerve activity*. Biochem Biophys Res Commun, 2007. **364**(3): p. 457-63.
176. Peschke, E., *Melatonin, endocrine pancreas and diabetes*. J Pineal Res, 2008. **44**(1): p. 26-40.
177. Thomas, H.E., et al., *Circulating endothelial progenitor cells exhibit diurnal variation*. Arterioscler Thromb Vasc Biol, 2008. **28**(3): p. e21-2.
178. Serre, C.M., et al., *Evidence for a dense and intimate innervation of the bone tissue, including glutamate-containing fibers*. Bone, 1999. **25**(6): p. 623-9.
179. Katayama, Y., et al., *Signals from the sympathetic nervous system regulate hematopoietic stem cell egress from bone marrow*. Cell, 2006. **124**(2): p. 407-21.
180. Said, G., *Focal and multifocal diabetic neuropathies*. Arquivos de neuro-psiquiatria, 2007. **65**(4B): p. 1272-8.
181. *Standards of medical care in diabetes--2010*. Diabetes Care, 2010. **33 Suppl 1**: p. S11-61.

182. Peichev, M., et al., *Expression of VEGFR-2 and AC133 by circulating human CD34(+) cells identifies a population of functional endothelial precursors*. Blood, 2000. **95**(3): p. 952-8.
183. Schatteman, G.C., M. Dunnwald, and C. Jiao, *Biology of bone marrow-derived endothelial cell precursors*. American journal of physiology. Heart and circulatory physiology, 2007. **292**(1): p. H1-18.
184. Wang, C.Y., et al., *Increased vascular senescence and impaired endothelial progenitor cell function mediated by mutation of circadian gene Per2*. Circulation, 2008. **118**(21): p. 2166-73.
185. Tirabassi, R.S., et al., *The BBZDR/Wor rat model for investigating the complications of type 2 diabetes mellitus*. Ilar J, 2004. **45**(3): p. 292-302.
186. Mordes, J.P., et al., *Rat models of type 1 diabetes: genetics, environment, and autoimmunity*. ILAR journal / National Research Council, Institute of Laboratory Animal Resources, 2004. **45**(3): p. 278-91.
187. Clarkson, P., et al., *Impaired vascular reactivity in insulin-dependent diabetes mellitus is related to disease duration and low density lipoprotein cholesterol levels*. J Am Coll Cardiol, 1996. **28**(3): p. 573-9.
188. Tooke, J.E. and K.L. Goh, *Vascular function in Type 2 diabetes mellitus and pre-diabetes: the case for intrinsic endotheiopathy*. Diabet Med, 1999. **16**(9): p. 710-5.
189. De Caterina, R., *Endothelial dysfunctions: common denominators in vascular disease*. Curr Opin Clin Nutr Metab Care, 2000. **3**(6): p. 453-67.
190. Folkman, J., *Angiogenesis*. Annu Rev Med, 2006. **57**: p. 1-18.
191. Busik, J.V., et al., *Diabetic retinopathy is associated with bone marrow neuropathy and a depressed peripheral clock*. J Exp Med, 2009. **206**(13): p. 2897-906.
192. Mathias, S., L.A. Pena, and R.N. Kolesnick, *Signal transduction of stress via ceramide*. Biochem J, 1998. **335 (Pt 3)**: p. 465-80.
193. Mathias, S., et al., *Activation of the sphingomyelin signaling pathway in intact EL4 cells and in a cell-free system by IL-1 beta*. Science, 1993. **259**(5094): p. 519-22.
194. Opreanu, M., et al., *Docosahexaenoic Acid Inhibits Cytokine Signaling in Human Retinal Endothelial Cells by Downregulating Sphingomyelinases*. Invest Ophthalmol Vis Sci.
195. Zeidan, Y.H. and Y.A. Hannun, *The Acid sphingomyelinase/ceramide pathway: biomedical significance and mechanisms of regulation*. Curr Mol Med. **10**(5): p. 454-66.
196. Gulbins, E. and P.L. Li, *Physiological and pathophysiological aspects of ceramide*. Am J Physiol Regul Integr Comp Physiol, 2006. **290**(1): p. R11-26.
197. Ruvolo, P.P., *Intracellular signal transduction pathways activated by ceramide and its metabolites*. Pharmacol Res, 2003. **47**(5): p. 383-92.
198. Seumois, G., et al., *De novo C16- and C24-ceramide generation contributes to spontaneous neutrophil apoptosis*. J Leukoc Biol, 2007. **81**(6): p. 1477-86.

199. Grassme, H., J. Riethmuller, and E. Gulbins, *Biological aspects of ceramide-enriched membrane domains*. Prog Lipid Res, 2007. **46**(3-4): p. 161-70.
200. Kolesnick, R.N., F.M. Goni, and A. Alonso, *Compartmentalization of ceramide signaling: physical foundations and biological effects*. J Cell Physiol, 2000. **184**(3): p. 285-300.
201. Monks, C.R., et al., *Three-dimensional segregation of supramolecular activation clusters in T cells*. Nature, 1998. **395**(6697): p. 82-6.
202. Futterman, S. and C. Kupfer, *The fatty acid composition of the retinal vasculature of normal and diabetic human eyes*. Invest Ophthalmol, 1968. **7**(1): p. 105-8.
203. Tikhonenko, M., et al., *Remodeling of retinal Fatty acids in an animal model of diabetes: a decrease in long-chain polyunsaturated fatty acids is associated with a decrease in fatty acid elongases Elovl2 and Elovl4*. Diabetes. **59**(1): p. 219-27.
204. Opreanu, M., et al., *The unconventional role of acid sphingomyelinase in regulation of retinal microangiopathy in diabetic human and animal models*. Diabetes, 2011.
205. Cubbon, R.M., A. Rajwani, and S.B. Wheatcroft, *The impact of insulin resistance on endothelial function, progenitor cells and repair*. Diab Vasc Dis Res, 2007. **4**(2): p. 103-11.
206. Kerzic, P.J., et al., *Inhibition of NF-kappaB by hydroquinone sensitizes human bone marrow progenitor cells to TNF-alpha-induced apoptosis*. Toxicology, 2003. **187**(2-3): p. 127-37.
207. Koizumi, K., et al., *Contribution of TNF-alpha to leukocyte adhesion, vascular leakage, and apoptotic cell death in endotoxin-induced uveitis in vivo*. Invest Ophthalmol Vis Sci, 2003. **44**(5): p. 2184-91.
208. Fadini, G.P., et al., *Number and function of endothelial progenitor cells as a marker of severity for diabetic vasculopathy*. Arterioscler Thromb Vasc Biol, 2006. **26**(9): p. 2140-6.
209. Yamakawa, M., et al., *Age-related alterations in IL-1beta, TNF-alpha, and IL-6 concentrations in parotid acinar cells from BALB/c and non-obese diabetic mice*. J Histochem Cytochem, 2000. **48**(8): p. 1033-42.
210. Mendel, D.B., et al., *Development of SU5416, a selective small molecule inhibitor of VEGF receptor tyrosine kinase activity, as an anti-angiogenesis agent*. Anticancer Drug Des, 2000. **15**(1): p. 29-41.
211. Hu, F.B., et al., *Fish and long-chain omega-3 fatty acid intake and risk of coronary heart disease and total mortality in diabetic women*. Circulation, 2003. **107**(14): p. 1852-7.
212. Morrish, N.J., et al., *Mortality and causes of death in the WHO Multinational Study of Vascular Disease in Diabetes*. Diabetologia, 2001. **44 Suppl 2**: p. S14-21.
213. Miller-Kasprzak, E. and P.P. Jagodzinski, *Endothelial progenitor cells as a new agent contributing to vascular repair*. Arch Immunol Ther Exp (Warsz), 2007. **55**(4): p. 247-59.

214. Yang, Z., et al., *Tumor necrosis factor activation of the sphingomyelin pathway signals nuclear factor kappa B translocation in intact HL-60 cells*. J Biol Chem, 1993. **268**(27): p. 20520-3.
215. Sivan-Loukianova, E., et al., *CD34+ blood cells accelerate vascularization and healing of diabetic mouse skin wounds*. J Vasc Res, 2003. **40**(4): p. 368-77.
216. Ikarashi, K., et al., *Bone marrow cells contribute to regeneration of damaged glomerular endothelial cells*. Kidney Int, 2005. **67**(5): p. 1925-33.
217. Churdchomjan, W., et al., *Comparison of endothelial progenitor cell function in type 2 diabetes with good and poor glycemic control*. BMC Endocr Disord. **10**: p. 5.
218. Gomez-Mouton, C., et al., *Dynamic redistribution of raft domains as an organizing platform for signaling during cell chemotaxis*. J Cell Biol, 2004. **164**(5): p. 759-68.
219. Kay, R.R., et al., *Changing directions in the study of chemotaxis*. Nat Rev Mol Cell Biol, 2008. **9**(6): p. 455-63.
220. Pike, L.J., *Lipid rafts: heterogeneity on the high seas*. Biochem J, 2004. **378**(Pt 2): p. 281-92.
221. Pierini, L.M., et al., *Membrane lipid organization is critical for human neutrophil polarization*. J Biol Chem, 2003. **278**(12): p. 10831-41.
222. Bodin, S. and M.D. Welch, *Plasma membrane organization is essential for balancing competing pseudopod- and uropod-promoting signals during neutrophil polarization and migration*. Mol Biol Cell, 2005. **16**(12): p. 5773-83.
223. Uhlig, S. and E. Gulbins, *Sphingolipids in the lungs*. Am J Respir Crit Care Med, 2008. **178**(11): p. 1100-14.
224. Agardh, E., et al., *Modifying a standard method allows simultaneous extraction of RNA and protein, enabling detection of enzymes in the rat retina with low expressions and protein levels*. Metabolism, 2006. **55**(2): p. 168-74.
225. Kern, T.S., et al., *Response of capillary cell death to aminoguanidine predicts the development of retinopathy: comparison of diabetes and galactosemia*. Invest Ophthalmol Vis Sci, 2000. **41**(12): p. 3972-8.
226. Parving, H.H., *Increased microvascular permeability to plasma proteins in short- and long-term juvenile diabetics*. Diabetes, 1976. **25**(2 SUPPL): p. 884-9.
227. Pugliese, G., R.G. Tilton, and J.R. Williamson, *Glucose-induced metabolic imbalances in the pathogenesis of diabetic vascular disease*. Diabetes Metab Rev, 1991. **7**(1): p. 35-59.
228. Tucker, B.J., *Early onset of increased transcapillary albumin escape in awake diabetic rats*. Diabetes, 1990. **39**(8): p. 919-23.
229. Pugliese, G., et al., *Effects of very mild versus overt diabetes on vascular haemodynamics and barrier function in rats*. Diabetologia, 1989. **32**(12): p. 845-57.

230. Kilzer, P., et al., *Albumin permeation of new vessels is increased in diabetic rats*. *Diabetes*, 1985. **34**(4): p. 333-6.
231. Zheng, L., et al., *Retinal ischemia and reperfusion causes capillary degeneration: similarities to diabetes*. *Invest Ophthalmol Vis Sci*, 2007. **48**(1): p. 361-7.
232. Abcouwer, S.F., et al., *Effects of ischemic preconditioning and bevacizumab on apoptosis and vascular permeability following retinal ischemia-reperfusion injury*. *Invest Ophthalmol Vis Sci*, 2010. **51**(11): p. 5920-33.